

GD-Rebound: Key Collisions on Reduced AES, Rijndael, and the Impact on AES-GCM (Full Version)

Lingyue Qin^{1,2,3}, Wenquan Bi², Liyuan Tang¹, Xiaoyang Dong^{1,2,3}, and Xiaoyun Wang^{1,2,3}

¹ Tsinghua University, Beijing, P.R.China
{qinly,xiaoyangdong,xiaoyunwang}@tsinghua.edu.cn

² Zhongguancun Laboratory, Beijing, P.R.China
biwq@mail.zgclab.edu.cn

³ State Key Laboratory of Cryptography and Digital Economy Security, Tsinghua University, Beijing, P.R.China

Abstract. This paper introduces the *guess-and-determine rebound* (GD-Rebound) attack that improves Dong *et al.*'s *triangulating rebound attack* in CRYPTO 2022 and Taiyama *et al.*'s key collision attack in ASIACRYPT 2024. The improvement comes from two aspects: The first improvement is to explore related-key differentials to suit for key collision attack, while Dong *et al.*'s *triangulating rebound attack* only considered single-key differentials on AES. To avoid the contradictions in the related-key differential, two tricks are proposed to identify valid trails for key collision attacks. The second improvement is to determine the range of Inbound phase flexibly with the guess-and-determine technique, to reduce the overall time complexity of the attack. By dividing the conflicts in the guess-and-determine steps into different types and handling them separately, the Inbound phase is significantly extended and ultimately leads to better or even practical key collision attacks.

As applications, we improve the time complexities of all the theoretical key collision attacks on AES proposed by Taiyama *et al.* into practical ones, *i.e.*, from 2^{49} to our 2^6 on 2-round AES-128, from 2^{61} to our 2^{21} for 5-round AES-192 and 6-round AES-256. Notably, a new 3-round practical key collision attack on AES-128 is given, which is assumed to be impossible by Taiyama *et al.* Besides, we propose the key collision attack on reduced Rijndael-256 (planned for standardization by NIST) and some quantum key/semi-free-start collision attacks on AES. Finally, based on the key collision attacks, we introduce the first key committing attacks on round-reduced AES-GCM with 128-bit padding fix. All the practical attacks are implemented and some example pairs were found instantly on a standard PC.

Keywords: Rebound Attack · Guess-and-Determine · Key Collision · Key Committing · Quantum Attack

Table of Contents

41	GD-Rebound: Key Collisions on Reduced AES, Rijndael, and the Impact	
42	on AES-GCM (Full Version)	1
43	<i>Lingyue Qin, Wenquan Bi, Liyuan Tang, Xiaoyang Dong, and</i>	
44	<i>Xiaoyun Wang</i>	
45	1 Introduction	3
46	1.1 Our Contributions	4
47	1.2 Comparison to the concurrent work by Ni <i>et al.</i> [49]	7
48	2 Preliminaries	10
49	2.1 AES and Rijndael	10
50	2.2 Key Collision Attacks and the Quantum Settings	10
51	2.3 The Rebound Attack	12
52	2.4 Triangulating Rebound Attack	12
53	3 Guess-and-Determine Rebound Attack	14
54	3.1 The Weaknesses of Dong <i>et al.</i> 's Triangulating Rebound	14
55	3.2 Guess-and-Determine Rebound Attack (GD rebound)	15
56	4 Key Collision Attacks on Reduced AES-128	20
57	4.1 The Invalid Key Collision on 2-round AES-128 in [53]	20
58	4.2 The Practical Key Collision Attack on 2-round AES-128	21
59	4.3 The Practical Key Collision Attack on 3-round AES-128	24
60	5 Key Collision Attacks on Reduced AES-192	27
61	5.1 The Practical Key Collision Attack on 5-round AES-192	27
62	5.2 The Quantum Key Collision Attack on 6-round AES-192	30
63	6 Key Collision Attacks on Reduced AES-256	36
64	6.1 The Invalid Key Collision on 6-round AES-256 in [53]	36
65	6.2 Practical Key Collision Attack on 6-round AES-256	38
66	6.3 Quantum Key Collision Attack on 7-round AES-256	43
67	6.4 Quantum Key Collision Attack on 8-round AES-256	48
68	7 Key Collision Attack on 3-round Rijndael-256	53
69	8 Semi-Free-Start Collisions on Reduced AES-DM and Rijndael-DM	56
70	8.1 The Practical SFS Collision Attack on 5-round AES-128-DM	57
71	8.2 The Practical SFS Collision Attack on 7-round AES-192-DM	61
72	8.3 The Practical SFS Collision Attack on 5-round Rijndael-256-DM	66
73	8.4 The SFS Collision Attack on 6-round Rijndael-256-DM	69
74	9 Impacting on the Padding Fix with AES-GCM	75
75	9.1 Preliminaries	75
76	9.2 Key Committing Attacks on Round-Reduced AES-GCM with a	
77	128-bit Padding Fix	77
78	9.3 The Practical Key Committing Attack on Padding fixed	
79	AES-GCM with 3-round AES-128	78
80	9.4 The Practical Key Committing Attack on Padding Fixed	
81	AES-GCM with 5-round AES-192	81

82	9.5 The Practical Key Committing Attack on Padding Fixed	
83	AES-GCM with 6-round AES-256	82
84	10 Discussion and Conclusion	82

85 1 Introduction

86 **Rebound attack** [44] introduced by Mendel, Rechberger, Schl  ffer and Thom-
87 sen at FSE 2009, is a generic cryptanalysis tool on AES-like hash functions.
88 The attack consists of an inbound phase and an outbound phase. In the in-
89 bound phase, the degrees of freedom are used to realize part of the differential
90 characteristic deterministically. The remainder of the characteristic in the out-
91 bound phase is fulfilled in a probabilistic manner. To penetrate more rounds,
92 at ASIACRYPT 2009, Lamberger *et al.* [39] proposed to connect two inbound
93 phases by leveraging the degrees of freedom of the key. Gilbert and Peyrin [27]
94 and Lamberger *et al.* [39] extended the inbound phase by treating two consec-
95 utive AES-like rounds as the Super-Sbox [12]. At ASIACRYPT 2010, Sasaki *et*
96 *al.* [51] reduced the memory cost by exploiting the differential property of the
97 non-full-active Super-Sbox. The memory cost of the rebound attack was further
98 improved sequentially by Naya-Plasencia’s advanced merging list algorithm [48]
99 and Dinur *et al.*’s dissection technique [16]. At CRYPTO 2022, Dong *et al.* [18]
100 introduced the triangulating rebound attack to penetrate more rounds in the
101 inbound phase with the help of the triangulation algorithm [37]. The rebound
102 attack has become a basic cryptanalysis tool to evaluate hash functions against
103 collision attacks or distinguishing attacks [33,34,45,15,38,21,42], as well as the
104 key collision attack on AES [53].

105 Quantum attacks has made significant progress in block ciphers [36,40,5,52]
106 and hash functions [8,31,24]. At EUROCRYPT 2020, Hosoyamada and Sasaki [31]
107 first converted the rebound attack [44] into a quantum one, and showed that,
108 under their respective bounds of generic algorithms, quantum attacks can pene-
109 trate more rounds than classical attacks. At ASIACRYPT 2020, Dong *et al.* [19]
110 reduced the requirement of qRAM in the quantum rebound attack by exploit-
111 ing the non-full-active Super-Sbox technique [51], and Fl  rez-Guti  rrez [23] ex-
112 plored quantum collision attacks on Gimli. At CRYPTO 2021, Hosoyamada and
113 Sasaki [32] introduced quantum collision attacks on reduced SHA-2. At ASI-
114 ACRYPT 2021, Dong *et al.* [20] studied quantum free-start collision attacks. At
115 ASIACRYPT 2022, Guo *et al.* [30] found quantum collision attacks on 6-round
116 SHA-3. At ToSC 2024, Chen *et al.* [10] proposed some chosen-prefix (quantum)
117 collisions on AES-like hashing.

118 **The Committing Attack and Key Collision.** Recently, there has been a
119 great deal of interest in the security of authenticated encryption with associated
120 data (AEAD) in the key commitment frameworks [22,47,14,55,11]. The secu-
121 rity in this framework ensures that a ciphertext chosen by an attacker does not
122 decrypt into two different sets of key, nonce, and associated data. In USENIX

Security 2022, Albertini *et al.* [1] revealed that the widely used AE schemes AES-GCM and ChaCha20-Poly1305 may suffer from the key committing attack. They introduced a simple countermeasure (named padding fix) by prepending a l -bit string of 0's, denoted as X , to the message M for each encryption, resulting in $\text{Enc}(K, N, A, X \| M)$, and checking for the presence of X at the start of the message after decryption; decryption fails if X is not present. This countermeasure leads to the following open problem [22]:

“In particular, the padding fix with AES-GCM assumes an ideal cipher, and therefore raises the following interesting problem: Is it possible to find two keys K_1 and K_2 such that $\text{AES}_{K_1}(0) = \text{AES}_{K_2}(0)$ in less than 2^{64} trials. If the key size is larger than the block size, then such a pair of keys must exist. While there has been some work on the chosen-key setting [25] or using AES in a hashing mode [50], we are not aware of any results on this specific problem.”

At ASIACRYPT 2024, Taiyama *et al.* [53] first answered this open question by introducing the key collision attack on AES based on the rebound attack. They found K_1 and K_2 such that $\text{AES}_{K_1}(0) = \text{AES}_{K_2}(0)$ for 2-round AES-128, 5-round AES-192, and 6-round AES-256 with 2^{49} , 2^{61} , and 2^{61} time complexities, respectively.

1.1 Our Contributions

In order to extend the attacked rounds by the rebound attack, Dong *et al.* introduced the triangulating rebound attack [18] and connected multiple inbound phases with the available degrees of freedom both from the key schedule and the encryption path. The core idea is to efficiently solve a nonlinear system of the byte equations of AES with the help of Khovratovich *et al.*'s triangulation algorithm [37] to fulfill the differential characteristics. However, the triangulation algorithm may fail to find good ways to solve the system when all variables appear in all or most equations simultaneously. Moreover, only single-key differentials of AES are explored in Dong *et al.*'s triangulating rebound attack [18], while the key collision attack should explore related-key differentials. As stated in [54, Section A.2], such techniques are not well-suited for solving key collision attacks:

“Besides, even when differential characteristics for key collision are identified, rebound attacks [44] and triangle attacks [37], which efficiently find the values which fulfill differential characteristics, are not well-suited for solving target-plaintext key collisions.”

We improve Dong *et al.*'s triangulating rebound attack [18] and Taiyama *et al.*'s key collision attack [53] with two strategies:

- First, we explore the related-key differential characteristics for our rebound attacks to adapt the key collision attacks on AES, while Dong *et al.*'s *triangulating rebound attack* only explored single-key differentials. The single-key differential characteristic allows to use all of degree of freedom of the

key, while related-key differential has already fixed some key values due to fixed input/output differences of the active Sboxes in the key schedule. The consumed degrees of freedom in the key schedule may lead to contradictions with the value deduced from the encryption data path. In fact, we find the related-key differential trails on 2-round AES-128 and 6-round AES-256 used in Taiyama *et al.* [53] are invalid when searching the key collision $\text{AES}_{K_1}(0) = \text{AES}_{K_2}(0)$ (details are given in Section 4.1 and 6.1).

To avoid the contradictions in the related-key differentials of the key collision attacks, we introduce two tricks in the search model. The first one is to avoid activating Sboxes in round 0 of the key schedule, so that the available degrees of freedom from the key can be leveraged to connect the fixed bytes from the active Sboxes in the encryption path and the fixed plaintext P . The second trick is to assign the same difference to the active Sboxes at the same positions of the key schedule (KS) and the encryption path (EN). In this case, the probability of the two active Sboxes from the EN and KS only needs to be calculated once. This is the key factor that we can give a 3-round key collision attack on AES-128. Note that it has been proved in Taiyama *et al.*'s [54, Section B] that the 3-round key collision attack on AES-128 can hardly work:

“...the probability drops below 2^{-128} after 3 rounds. It means that in the fixed-target-plaintext scenario, no key collision pairs are guaranteed after 3 rounds for a given target plaintext, even when considering the entire 128-bit key space.”

For our new related-key differential characteristic, if we use the same way of Taiyama *et al.* [54] to calculate its probability, it will be 2^{-131} , which is infeasible for a key collision attack. However, as the probability of two active Sboxes from the EN and KS only needs to be calculated once, the real probability is 2^{-125} , which is sufficient for a key collision attack.

- Second, we embed the guess-and-determine technique by Bouillaguet, Derbez, and Fouque [6] to solve the nonlinear system of the inbound phase to address problem that the triangulating rebound attack may not work. Moreover, we analyze the guess-and-determine (GD) steps in detail and find the conflicts (*e.g.* five conflicts marked by “?” in Table 11), which determine the complexity of the GD, could be divided into three types, *i.e.*, Type-I/II/III. Among them, Type-I conflicts could be moved to the outbound phase and Type-II conflicts could be solved with precomputation, which significantly reduces the complexity of the GD and thus the complexity of the inbound phase.

Compared to the key collision attacks in [54], our inbound phase covers more rounds including parts of both EN and KS, while the inbound phase in [54] only covers part of EN. For example, the inbound phase of the 6-round key collision attack on AES-256 in [54] only covers 2-round EN without KS (see Figure 19), while our inbound phase covers 4-round EN and 4-round KS (see Figure 20). Therefore, our attacks can achieve significant improvements than Taiyama *et al.*'s [54].

Based on the above two strategies, we build a heuristic method to find successful rebound attacks and key collision attacks, named the *guess-and-determine rebound attack* (GD-Rebound). The method includes two steps, the first step is to determine related-key differentials with restrictions on the degree of freedom and the tricks to avoid contradictions in the related-key differentials of the key collision attacks; the second step is to determine an efficient inbound phase via the GD and the methods to deal with the conflicts. Finally, a full rebound attack is determined.

Applications to Key Collision Attacks on Reduced AES and Rijndael.

We primarily focus on the key collision attacks, i.e., finding key pair (K_1, K_2) such that $\text{AES}_{K_1}(0) = \text{AES}_{K_2}(0)$, since this scenario has a practical impact on the key committing security of the widely used AES-GCM. We improve all the theoretical key collision attacks on AES proposed by Taiyama *et al.* [53] into practical ones. Besides, some the quantum key collision attacks and semi-free-start collision attacks are also given on reduced AES-DM and Rijndael-DM.

- We improve the key collision attack on 2-round AES-128 from Taiyama *et al.*'s 2^{49} into the practical 2^6 time complexity. Notably, we first propose a new key collision attack on 3-round AES-128 with a practical time complexity of 2^{35} , which is believed to be impossible by Taiyama *et al.*'s. Besides, the 5-round semi-free-start collision attack on AES-128-DM becomes practical.
- We improve the key collision attack on 5-round AES-192 from Taiyama *et al.*'s 2^{61} into the practical 2^{21} time complexity, and also propose a 6-round quantum key collision attack on AES-192. Besides, the 7-round semi-free-start collision attack on AES-192-DM becomes practical.
- We improve the key collision attack on 6-round AES-256 from Taiyama *et al.*'s 2^{61} into the practical 2^{21} time complexity, and also propose the 7-/8-round quantum key collision attacks on AES-256.
- Very recently, NIST proposes to standardize a wider variant of Rijndael⁴, i.e., Rijndael-256. Besides, at the NIST Workshop on Block Cipher Modes of Operation, Kampanakis *et al.* from AWS discussed the standardization Rijndael-256 and a new AEAD mode with key/context commitment resistance as an option [35]. Therefore, it is well-motivated to study the key collision attacks on Rijndael-256. In this paper, we propose the practical key collision attacks on 3-round Rijndael-256. Besides, the 5-/6-round semi-free-start collision attacks on Rijndael-256 in DM mode are given.

Key Committing Attacks on Reduced AES-GCM with Padding Fix.

Based on key committing attack on AES-GCM, practical attacks have been constructed on the upper-level applications and protocols. At CRYPTO 2017 and 2018, Grubbs *et al.* [29] and Dodis *et al.* [17] show how to exploit AE schemes which do not commit to the key in the context of abuse reporting in Facebook

⁴<https://csrc.nist.gov/news/2024/nist-proposes-to-standardize-wider-variant-of-aes>

250 Messenger. At USENIX Security 2021, Len *et al.* [41] proposed the partition-
 251 ing oracle attacks to recover passwords from Shadowsocks proxy servers due to
 252 incorrectly using non-committing AEAD.

253 At USENIX Security 2022, Albertini *et al.* [1] proposed two solutions against
 254 the key committing attacks on AES-GCM, named as padding fix solution and
 255 generic solution. The generic solution needs an additional primitive, *i.e.*, a col-
 256 lision resistance of hash function. While the padding fix solution does not need
 257 additional primitive, and it only prepends a l -bit string of 0's to the message M
 258 for encryption of AES-GCM. Obviously, AES-GCM with a padding fix maintains
 259 compatibility with the original AE and can be more efficient and easy to deploy
 260 in practice. Albertini *et al.* proved that l -bit padding leads to $l/2$ -bit key commit-
 261 ting security for AES-GCM by assuming AES as an ideal block cipher. **However,**
 262 **there lacks dedicated (round-reduced) key-committing cryptanalysis**
 263 **on padding fixed AES-GCM by taking the detailed operations of AES**
 264 **into account.**

265 In this paper, based on our key collision attacks on reduced AES, we introduce
 266 the first key committing attacks on reduced AES-GCM with 128-bit padding fix
 267 (suggested by Albertini *et al.* [1]). The key committing attacks on AES-GCM
 268 with 128-bit padding fixed need to find key pair (K_1, K_2) such that $\text{AES}_{K_1}(N \parallel$
 269 $0^{30}10) = \text{AES}_{K_2}(N \parallel 0^{30}10)$, where N is a 96-bit nonce. This is the main difference
 270 from the key collision attacks, where the plaintext of AES should be 128-bit
 271 0's. The differential characteristics used delicately for the key collision attacks
 272 may lead to contradictions when applied to key committing. For example, the
 273 differential path used in the 3-round key collision attack on AES-128 in Sect.
 274 4.3 can not be applied to the key committing attack, since the differential path
 275 requires the last byte of the plaintext to be $0x0$, while for key committing attack
 276 the last byte will be $0x2$. Therefore, new differential path and new contradictions
 277 should be handled in the key committing attacks. Finally, we find practical key
 278 committing attacks on 3-round AES-128-GCM, 5-round AES-192-GCM, and 6-
 279 round AES-256-GCM in Table 2.

280 All our practical key collision and key committing attacks have been im-
 281 plemented and some instances are found in Tables 3 and 4. All our results are
 282 summarized in Table 1 and 2. The verification codes for the practical attacks
 283 are given in

284 <https://github.com/biwenquan/Guess-and-determine-Rebound-2>

285 1.2 Comparison to the concurrent work by Ni *et al.* [49]

286 A related work recently appeared in eprint 2025/462 [49] that introduces key
 287 collision attacks on reduced AES and Kiasu-BC. In [49], the inbound phase covers
 288 2-round or 2.5-round AES. Our inbound phase covers up to 4-round AES and up
 289 to 6-round AES's key schedule. For AES-128, we get the first 3-round practical
 290 key collision, while Ni *et al.* [49] only get a 2-round one. We get a 5-round semi-
 291 free-start collision with time complexity 2^{39} , while Ni *et al.*'s time complexity is
 292 2^{54} ; For AES-192, we get a 7-round practical semi-free-start collision with time

complexity 2^{20} , while Ni *et al.*'s time complexity is 2^{56} ; For AES-256, we get a
6-round practical key collision with time complexity 2^{21} , while Ni *et al.*'s time
complexity is 2^{60} . They do not give the key committing attacks on AES-GCM
with padding fix. The comparison is given in Table 1.

Table 1: Key and semi-free-start collision attacks on AES and Rijndael

Target	Attack	Rounds	Time	C-Mem	qRAM	Setting	Ref.
AES-128	Key Collision	2/10	2^{49}	-	-	Classic	[53]
		2/10	- Practical	2^{22}	-	Classic	[49]
		2/10	2^6 Practical	-	-	Classic	Sect. 4.2
		3/10	2^{35} Practical	-	-	Classic	Sect. 4.3
	DM mode	5/10	2^{57}	-	-	Classic	[53]
	Semi-free-start	5/10	2^{54}	-	-	Classic	[49]
		5/10	2^{39} Practical	-	-	Classic	Sect. 8.1
AES-192	Key Collision	5/12	2^{61}	-	-	Classic	[53]
		5/12	- Practical	2^5	-	Classic	[49]
		5/12	2^{21} Practical	-	-	Classic	Sect. 5.1
		6/12	$2^{38.7}$	-	44	Quantum†	Sect. 5.2
	DM mode	7/12	2^{62}	-	-	Classic	[53]
	Semi-free-start	7/12	2^{56}	-	-	Classic	[49]
		7/12	2^{20} Practical	-	-	Classic	Sect. 8.2
AES-256	Key Collision	6/14	2^{61}	-	-	Classic	[53]
		6/14	2^{60}	-	-	Classic	[49]
		6/14	2^{21} Practical	-	-	Classic	Sect. 6.2
		7/14	$2^{36.7}$	-	60	Quantum†	Sect. 6.3
		8/14	$2^{50.2}$	-	44	Quantum†	Sect. 6.4
Rijndael-256	Key Collision	3/14	2^{32} Practical	-	-	Classic	Sect. 7
		5/14	2^{33} Practical	-	-	Classic	Sect. 8.3
	Semi-free-start	6/14	2^{87}	-	-	Classic	Sect. 8.4

†: The quantum attacks are better than quantum version of parallel rho's algorithm [56,3,31], which is 2^{64} in a single quantum computer.

Table 2: A summary of the results on AES-GCM with 128-bit Padding Fix

Target	Attack	Rounds	Time	C-Mem	Setting	Ref.
AES-128-GCM	Key Committing	3/10	2^{36} Practical	-	Classic	Sect. 9.3
AES-192-GCM	Key Committing	5/12	2^{21} Practical	-	Classic	Sect. 9.4
AES-256-GCM	Key Committing	6/14	2^{21} Practical	-	Classic	Sect. 9.5

Table 3: Practical instances for key collision and semi-free-start Collisions

Key Collisions on 2-round AES-128: $\text{AES}_{K_1}(0) = \text{AES}_{K_2}(0)$	
K_1	: 0x377008630096ccb134256ba749694717
K_2	: 0xeb700840dc4ad4b1340d738449694717
C	: 0xb6446d21185c641fb8919d7a9b317fa7
Key Collisions on 3-round AES-128: $\text{AES}_{K_1}(0) = \text{AES}_{K_2}(0)$	
K_1	: 0x0f6eef4eea138a1b60057a26d30bedfa
K_2	: 0xd76ec74dcc138ad460057a26d30bed36
C	: 0x87c494f5d33621b65ad032992b8f6def
Key Collisions on 5-round AES-192: $\text{AES}_{K_1}(0) = \text{AES}_{K_2}(0)$	
K_1	: 0x44d96d845d5312c8f19c3600814ba03196f3705625a24502
K_2	: 0x6bf638da727c4780deb3475eae64d17996f3704025a24502
C	: 0x4b49ed9c3ccc1a9dd3dcaa16f22165ce
Key Collisions on 6-round AES-256: $\text{AES}_{K_1}(0) = \text{AES}_{K_2}(0)$	
K_1	: 0xcc642ac6ef0e7385009b145cd43c0606997c122e7ec132621604eedc0013e201
K_2	: 0xe8722dd2ef0e7385009b145cd485060202ec2477c713660afd23eb50215e603
C	: 0x3dea345ea340d0a3e4dd1a7c28d6babc
Key Collisions on 3-round Rijndael-256-256: $\text{Rijndael}_{K_1}(0) = \text{Rijndael}_{K_2}(0)$	
K_1	: 0xa163a9977d458d8501544d25006800739044edc336abb5fe93651abb551d9ec6
K_2	: 0xaffba99773dd8d850ffcae250ec0e3739044edc336abb5fe9365e0e3551d9ec6
C	: 0x42a5054833fac9fd271f24181e7758f741ed5e4fddfc7b4d3c73bae4c998e05
Semi-free-start Collisions on 5-round AES-128-DM: $\text{AES}_{K_1}(P) = \text{AES}_{K_2}(P)$	
P	: 0xf7c68bc6a5845f062ff27ff65abcfe75
K_1	: 0x4a7a06e49c84b1762eeffeeab50d39d3
K_2	: 0x4b7b06e49c85b1762feffeeab50d39d3
C	: 0xf0b78c57afa2c7a5f45577f4b202a0fb
Semi-free-start Collisions on 7-round AES-192-DM: $\text{AES}_{K_1}(P) = \text{AES}_{K_2}(P)$	
P	: 0x64d66875c60b79e2e68073168f38cd68
K_1	: 0x70496db77bb5888702db85c405b090700753b5f50ff32437
K_2	: 0x70416db77bb57d8702db85c405b090700753b5f50ff3d137
C	: 0x909987f518b5eda72b0fd6912066b853
Semi-free-start Collisions on 5-round Rijndael-256-DM: $\text{Rijndael}_{K_1}(P) = \text{Rijndael}_{K_2}(P)$	
P	: 0x523be7e8dc57c8f6166da76593b5b43cdb31f7a62a73dc3a9e7cc6661cf7c30d
K_1	: 0x562b3f8f19fd1417ec7f4fd5a04a3e6600f1655d3be0b5a542ec558ac41fdc7d
K_2	: 0x567d3f8f19fd1417ec294fd5a04a3e6600f1415d3be091a542ec558ac41fdc7d
C	: 0x8f075ef13c5d67972cb42cb14b50a2875812e7176a2f1cd7f165bc05a4072d4c

Table 4: Practical key-committing attack on padding fixed AES-GCM with reduced AES. The plaintexts have a 128-bit zero padding before message.

Key-Committing Attack on Padding Fixed AES-GCM with 3-round AES-128	
N	: 00000000000000000000000000000001; AD : 00000000000000000000000000000001
P_1	: 00000000000000000000000000000000, 02fe47f51d0a8f0cedacd439ad623fe8, 33aa11e0a26b984d5d5808b631010d8f
P_2	: 00000000000000000000000000000000, 023fa93c158b8fbf39acd4b0ad62df6a, 3337cd72337b98264258086631018551
K_1	: 641ac462464cb9c81f4a430b3ab5d51e
K_2	: 64c0c7ef464c8a751f4a430b3ab5e51e
C	: 149ae51c9dfbc937d84491988b7bab89, dc25ef603fa0b9581c6a9d38eeba5646, 00000000000000000000000000000000
T	: d0bc7b73b16c00b0f37331cc76287684
Key-Committing Attack on Padding Fixed AES-GCM with 5-round AES-192	
N	: 010203040506070809101112; AD : 00000000000000000000000000000001
P_1	: 00000000000000000000000000000000, 485ba161b66c7987b048ed1e077a3cae, 057925e641fea30e003483232b067709
P_2	: 00000000000000000000000000000000, 42d3426e2baf4a5b8b9efa7b069e9f5c, 481f48565aab7523a6ff0d620531d6c
K_1	: 6af46ede587a4088f88c274c814ba0338223e9f065f71112
K_2	: 45db3b80775515c0d7a35612ae64d17b8223e9e665f71112
C	: 8a65dafa25e3a0f1a31cd8a17f901b1d, 8d2dbf690f882fa4579be014ceb816ce, 00000000000000000000000000000000
T	: 32583fc513e3f4b1c02dc9959cccb30d
Key-Committing Attack on Padding Fixed AES-GCM with 6-round AES-256	
N	: 000000010000000100000001; AD : 00000000000000000000000000000001
P_1	: 00000000000000000000000000000000, 4f618fe7e543c4b6509bd5b802148766, 83f4796bbce7452d657129e0158bee36
P_2	: 00000000000000000000000000000000, 5bb605eb9be830a1c29d70be90fe96e8, 423b4b41c3f86806c9ae001494dd9d42
K_1	: cc642ac7ef1473960081155dd43c171556bf13f9c94b0f6fa21bcfe20013e201
K_2	: e8722dd3ef1473960081155dd4851715efedc390cbfb0b6d1bcd1f8b0215e603
C	: 94a7f0fcd06e74090ca954cfe00d69ae, 76960e56dcae854e2f2dc0ea378dc6d6, 00000000000000000000000000000000
T	: 339382636355e731d830a3e954625b85

2 Preliminaries

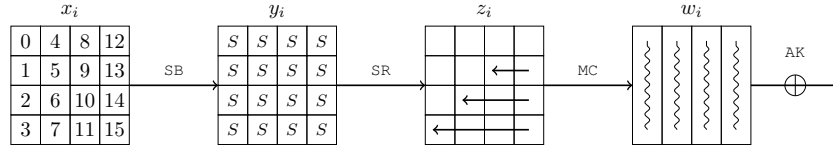
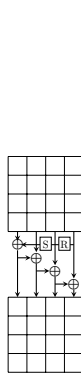
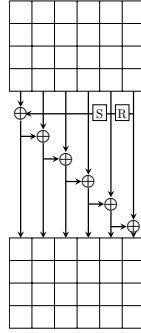
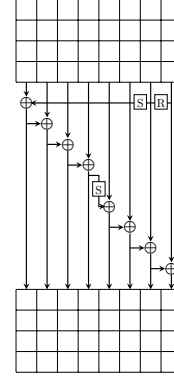
2.1 AES and Rijndael

AES-128/192/256 [13] is a 128-bit block cipher with a 128/192/256-bit key, respectively. In contrast, the block length of Rijndael [13] can be 128/192/256 bits. The state is treated as a $4 \times N_{col}$ ($N_{col} = 4, 6, 8$) two-dimensional array of bytes. The i -th round of Rijndael (Fig. 1) typically consists of the following operations:

- SubBytes (SB): Substitute each cell of x_i according to an S-box to get y_i .
- ShiftRows (SR): For $N_{col} = 4, 6$, rotate the j th row of y_i to the left by j bytes ($j = 0, 1, 2, 3$). For $N_{col} = 8$, rotate the 0, 1, 2, 3rd row to the left by 0, 1, 3, 4 bytes, respectively.
- MixColumns (MC): Update each column of z_i by left-multiplying an MDS matrix to get w_i .
- AddRoundKey (AK): XOR a round key into the state. The length of the master key can be chosen as $4 \times N_k$ bytes with $N_k = 4, 6, 8$. The key schedules for $N_k = 4, 6, 8$ are given in Fig. 2, 3, 4, respectively.

2.2 Key Collision Attacks and the Quantum Settings

At ASIACRYPT 2024, Taiyama *et al.* introduced three variants of key collisions as Fig. 5.


 Fig. 1: The round function of Rijndael (with $N_{col} = 4$)

 Fig. 2: $N_k = 4$

 Fig. 3: $N_k = 6$

 Fig. 4: $N_k = 8$

315 **Definition 1 (Key Collision [53]).** *It is two distinct keys that generate the*
 316 *same ciphertext for a single target plaintext.*

317 Identifying such a collision can be classified into two different problems de-
 318 pending on whether a single target plaintext is predetermined or not, illustrated
 319 in Fig. 5. *Obviously, the most important and difficult case is fixed-target-plaintext*
 320 *key collision, i.e., finding key pair (K_1, K_2) such that $\text{AES}_{K_1}(0) = \text{AES}_{K_2}(0)$.*
 321 *This scenario has a direct impact on the key commitment security of AES-GCM*
 322 *and its padding fix variant [1]. Therefore, this paper focuses on this important*
 323 *case. If the single target plaintext is free, i.e., the free-target-plaintext key col-*
 324 *lision in Fig. 5, it is also known as the semi-free-start collision attack on AES in*
 325 *the DM hashing mode.*

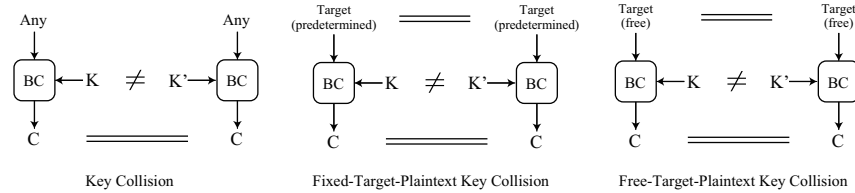


Fig. 5: Variants of key collisions

The time complexity for solving these problems by generic attack (assuming that an underlying block cipher is an ideal cipher) depends on the size of the ciphertext. Specifically, for an n -bit ciphertext, such pairs can be found within a time complexity of $2^{n/2}$ in classical setting, owing to the birthday paradox. In quantum setting, there are three generic quantum algorithms under different assumptions of the availability of quantum and classical memory resources:

- Condition 1: Exponentially large quantum random access memory (qRAM) is available. Brassard, Høyer, and Tapp [7] introduced the generic quantum collision attack with $2^{n/3}$ quantum time complexity and $2^{n/3}$ qRAM.
- Condition 2: Neither exponentially large qRAM nor classic RAM is available. The quantum version of parallel rho’s algorithm [56,3,31] achieves a time-space trade off of time $\frac{2^{n/2}}{S}$ with S computers.
- Condition 3: Exponentially large qRAM is not available but large classical RAM is. Chailloux, Naya-Plasencia, and Schrottenloher [8] introduced the CNS algorithm to find collision in time $2^{2n/5}$ with classical RAM of size $2^{n/5}$.

2.3 The Rebound Attack

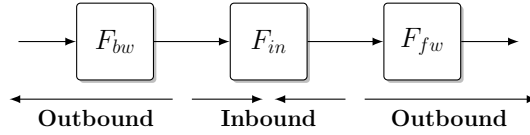


Fig. 6: The rebound attack

The rebound attack was first introduced by Mendel *et al.* in [44], which consists of an inbound phase and an outbound phase as shown in Fig. 6, where F is an internal block cipher or permutation which is split into three subparts, then $F = F_{fw} \circ F_{in} \circ F_{bw}$.

- **Inbound phase.** In the inbound phase, the attackers efficiently fulfill the low probability part in the middle of the differential trail with a meet-in-the-middle technique. The degree of freedom is the number of matched pairs in the inbound phase, which will act as the starting points for the outbound phase.
- **Outbound phase.** In the outbound phase, the matched values of the inbound phase, *i.e.*, starting points, are computed backward and forward through F_{bw} and F_{fw} to obtain a pair of values which satisfy the outbound differential trail in a brute-force fashion.

2.4 Triangulating Rebound Attack

At CRYPTO 2022, Dong *et al.* introduced the triangulating rebound attack [18]. The core idea is to connect multiple inbound phases by solving a nonlinear system of byte equations.

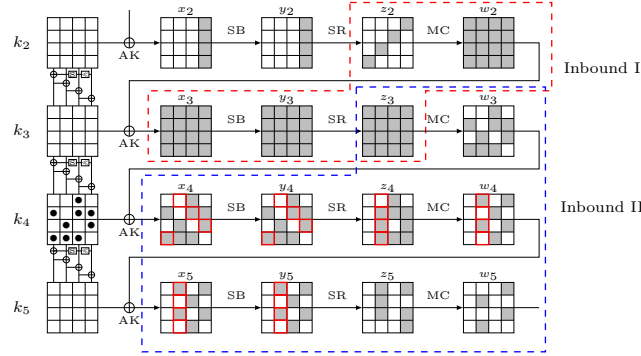


Fig. 7: Example of triangulating rebound attack in [18]

In Fig. 7, we take the inbound phase of Dong *et al.*'s 7-round rebound attack on AES-128 as an example (see [18, Section 4.1]) to describe the triangulating rebound attack. There are two inbound phases named 'Inbound I' and 'Inbound II'. The triangulating rebound attack begins with the given differences of $(\Delta z_2, \Delta w_3, \Delta w_4, \Delta w_5)$, so that the input-output differences for the three SB layers in Round 3, 4, and 5 are determined. Based on the differential property of AES's Sbox, one can expect one pair of values for active bytes $(x_3[\square], x_4[\square], x_5[\square])$. To connect these values, 9 bytes of $k_4[\bullet]$ are directly determined by $k_4 = x_4 \oplus w_3$. The other 7 bytes of k_4 act as variables. Together with the known state w_3 , we compute forward to get 6 nonlinear byte equations with the 6 known bytes $x_5[\square]$ for the 7 variables of k_4 . There expect 2^8 solutions for the nonlinear system. Trivially, we may solve the system by exhaustive search and check if the 6 equations are satisfied, which needs 2^{56} time complexity to find all the solutions. Dong *et al.* figure out that the system can be solved by a triangulation algorithm efficiently in 2^8 time.

The triangulation algorithm was introduced by Khovratovich, Biryukov, and Nikolic [37] at CT-RSA 2009. The heart of the triangulation algorithm is to search for free variables. The formal process can be described as follows:

1. Given the system of equations with predefined values fixed as constants.
2. Label all variables and equations as unprocessed. Initially, all variables and equations are marked as unprocessed, meaning they have not yet been simplified or solved.
3. Identify a variable that appears in only one unprocessed equation. Label both the variable and the corresponding equation as processed. If there is no such variable — exit.
4. Repeat Step 3 if there are still unprocessed equations.
5. If all equations have been processed or no further simplification can be made, mark all remaining unprocessed variables as free.
6. Assign random values to free variables and compute the remaining variables.

388 Assume we have 7 byte-variables $s, t, u, v, x, y, z \in \mathbb{F}_2^8$ which are involved in
 389 the following byte-equations:

$$\begin{cases} F(x \oplus s) \oplus v = 0, \\ G(x \oplus u) \oplus s \oplus L(y \oplus z) = 0, \\ v \oplus G(u \oplus s) = 0, \\ H(z \oplus s \oplus v) \oplus t = 0, \\ u \oplus H(t \oplus x) = 0, \end{cases} \quad (1)$$

390 where F, G, H , and L are the bijective functions. After processing with the tri-
 391 angulation algorithm, we get

$$\begin{cases} L(y \oplus z) \oplus G(u \oplus x \oplus s) = 0, \\ z \oplus H^{-1}(t \oplus v \oplus s) = 0, \\ t \oplus H^{-1}(u \oplus x) = 0, \\ u \oplus G^{-1}(v \oplus s) = 0, \\ v \oplus F(x \oplus s) = 0. \end{cases} \quad (2)$$

392 Evidently, $x, s \in \mathbb{F}_2^8$ can be assigned randomly and fully define the other vari-
 393 ables.

394 3 Guess-and-Determine Rebound Attack

395 3.1 The Weaknesses of Dong *et al.*'s Triangulating Rebound

396 **Weakness I: Triangulation algorithm failed.** The weakness of Dong *et al.*'s
 397 triangulating rebound [18] inherits from the triangulation algorithm [37]. The
 398 triangulation algorithm may fail to find good ways to solve the nonlinear sys-
 399 tem when all the variables appear in all or most equations simultaneously. For
 400 example, if the nonlinear system is the following Equation 3 (' S ' is the applica-
 401 tion of Sbox), the triangulation algorithm terminates immediately without any
 402 processing, and the system will be solved by exhaustive search.

$$\begin{cases} x \oplus y \oplus S(y) \oplus z \oplus S(z) \oplus t \oplus S(t) = 0, \\ S(x) \oplus y \oplus S(y) \oplus z \oplus S(z) \oplus t \oplus S(t) = 0, \\ x \oplus S(x) \oplus 2y \oplus S(y) \oplus 3z \oplus 3S(z) \oplus 2t \oplus 3S(t) = 0. \end{cases} \quad (3)$$

403 However, the system can be simplified by the Gaussian elimination to be

$$\begin{cases} z \oplus S(z) \oplus S(t) \oplus S(y) = 0, \\ t \oplus S(x) \oplus y \oplus 2S(y) = 0, \\ x \oplus S(x) \oplus 2S(y) = 0. \end{cases} \quad (4)$$

404 The simplified system can be solved easily in 2^8 time by exhausting $y \in \mathbb{F}_2^8$.
 405 In fact, at CRYPTO 2011, Bouillaguet, Derbez and Fouque [6] have already
 406 proposed an efficient guess-and-determine method to solve the nonlinear system
 407 of related-key AES, which adopted the Gaussian elimination method to process
 408 the system. Therefore, we apply Bouillaguet *et al.*'s guess-and-determine tool [6]
 409 to solve AES's nonlinear system and improve the rebound attack.

Weakness II: Related-key differential unexplored on AES for triangulation rebound. The other weakness is that Dong *et al.*'s triangulating rebound attack [18] on AES only explores the single-key differential. Note that single-key differential allows full use of degree of freedom of the key, while related-key differential characteristic has already fixed some key values (lost some degrees of freedom from the key schedule) due to the fixed input/output differences of the active Sboxes in the key schedule. In addition, using related-key differential may induce unexpected conflicts in the attacks [4]. In fact, we find that the related-key differential characteristics on 2-round AES-128 and 6-round AES-256 used in Taiyama *et al.* [53] are invalid when searching the key collision $\text{AES}_{K_1}(0) = \text{AES}_{K_2}(0)$. When P is fixed, the value deduced from the active Sbox in the encryption path may conflict with the value deduced from the active Sbox in the key schedule. The details are given in Section 4.1 and 6.1. Hence, considering related-key differential is not trivial, the consumed degrees of freedom in the key schedule may lead to the whole attack being invalid.

Those problems make Dong *et al.*'s triangulating rebound attack [18] not well-suited for the key-collision attack on AES, since this kind of attack is based on differences in the key schedule. This drawback has been spotted by Taiyama *et al.* [53] from ASIACRYPT 2024 that “rebound attacks and triangle attacks are not well-suited for solving target-plaintext key collisions” [54, Section A.2].

3.2 Guess-and-Determine Rebound Attack (GD rebound)

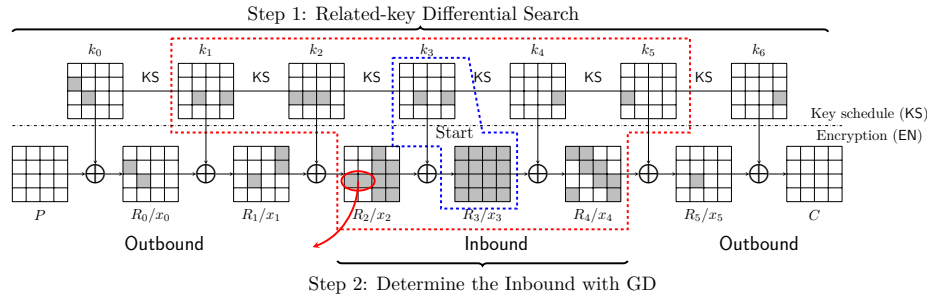


Fig. 8: Framework of guess-and-determine rebound

Our *guess-and-determine rebound attack* (abbreviated as “GD rebound”) investigates the related-key differentials of AES to suit key collision attacks. Fig. 8 shows the framework of our GD rebound, where the two critical steps are given as follows.

Step 1: Search for related-key differentials of AES by applying G rault *et al.*'s model [26]. This step involves two sub-steps, *i.e.*, searching for the

related-key truncated differential and searching for the instantiation of the truncated differential. The instantiation of the related-key differential characteristic (RKDC) should satisfy the following conditions:

- *Collision Condition*: There should be no active bytes in the states P and C for fixed or free-target-plaintext key collision.
- *Degree of Freedom (DoF)*: Similar to Taiyama *et al.* [53], the differential characteristic should be constrained by the maximum DoF in each attack. A fixed-target-plaintext key collision can utilize the DoF of the key K , while the free-target-plaintext key collision can utilize the DoF of both the key K and plaintext P . Thus, the differential characteristic with probability 2^{-p} should meet the condition $p < |K|$ for fixed-target-plaintext key collision, or condition $p < n + |K|$ for free-target-plaintext key collision, where $|K|$ and n are the bit-length of the key and the plaintext.
- *Restriction on Differential in Round 0*: For key collision, the differences are all introduced by the key. Especially, for state x_0 in the round 0, we have $\Delta x_0 = \Delta k_0$. For the fixed-target attack, the value deduced from the active Sbox in the encryption path may conflict with the value deduced from the active Sbox in the key schedule in the position of fixed P . We take the RKDC of 2-round AES-128 given in [53] as an example. As shown in Fig. 9, there are $(\Delta x_0[12], \Delta \text{SB}(x_0[12])) = (0\text{x}69, 0\text{x}\text{ef})$ and $(\Delta k_0[12], \Delta \text{SB}(k_0[12])) = (0\text{x}69, 0\text{x}08)$. To fulfill the differential, the values of $x_0[12]$ and $k_0[12]$ must be $x_0[12] \in \{0\text{x}1\text{b}, 0\text{x}72\}$ and $k_0[12] \in \{0\text{x}60, 0\text{x}08\}$. With fixed $P[12] = 0$ and $P[12] = k_0[12] \oplus x_0[12] = 0$, the values of $x_0[12]$ and $k_0[12]$ cannot satisfy the differential. For details please refer to Section 4.1.

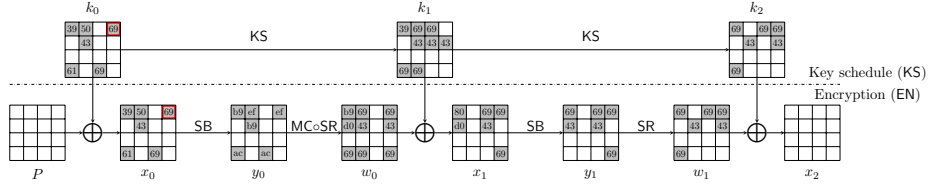


Fig. 9: The differential for 2-round AES-128 in [53]

460
461
462
463
464
465
466
467
468
469
470

We solve this incompatibility with two tricks:

1. The first way is to avoid activating Sbox in round 0 of the key schedule. For AES-128, the condition is satisfied by $\Delta k_0[j] = 0$ ($j \in [12, 13, 14, 15]$). One example is the new 2-round RKDC in Fig. 11 of Section 4.2, that leads to a practical key collision attack on 2-round AES-128.
2. The second way is to set the output differences in the corresponding active Sbox in KS and EN path to be same. Then fix the corresponding state byte and key byte to the same value to keep $P = 0$. For example, in Fig. 9, we can modify $\Delta \text{SB}(x_0[12]) = \Delta \text{SB}(k_0[12])$ and keep $x_0[12] = k_0[12]$.

However, the degree of freedom and probability of the RKDC should be reconsidered. Because when $x_0[12] = k_0[12]$, once the value of $x_0[12]$ satisfies the active Sbox in the SB operation in encryption path EN, this value will instantly satisfy the corresponding active Sbox in the key schedule KS with probability 1. For the two active Sboxes of $x_0[12]$ and $k_0[12]$, the probability only needs to be calculated once⁵. At the same time, the degree of freedom should take into account the choice of $x_0[12] = k_0[12]$. This is the key factor that we can give a 3-round practical key collision attack on AES-128 in Section 4.3, which is believed impossible by Taiyama *et al.* [54, Section B].

Step 2: Determine the Inbound phase with guess-and-determine. Given a related-key differential characteristic (RKDC), the key point of the GD rebound attack is to determine the Inbound phase. Fig. 8 shows a 6-round RKDC, where R_i represents the round i and only the state x_i before SB in round i is presented for short. Our strategy for determining the Inbound phase with guess-and-determine is as follows.

1. Select the starting round as the initial Inbound, *e.g.*, the starting round 3 in Fig. 8 including the key schedule path KS and the encryption path EN. There are different choices for the starting round. Since the differences of the active Sboxes of the RKDC are fixed, we then fix all the values of the active Sboxes in KS and EN path by accessing DDT in the initial Inbound. The remaining part of the RKDC is the initial Outbound, which will be satisfied in a brute-force fashion. Suppose that the probability of the initial Outbound part is $2^{-P_{out}}$. If $2^{P_{out}} \geq 2^{n/2}$ (the rebound attack is already weaker than the birthday attack), add more rounds (or a partial round) of the KS or EN into the initial Inbound to get the new Inbound⁶ marked by red dashed box in Fig. 8. For fixed target-plaintext key collision, the Inbound phase usually includes the state P . Otherwise, a complexity of 2^n should be added to the Outbound phase to meet the fixed P , which already invalidates the attack. Suppose that the current probability of the Outbound part is $2^{-P_{out}}$.
2. Feed the known bytes (deduced by DDT) and unknown bytes of the Inbound into Builaguet *et al.*'s guess-and-determine tool [6] to find an efficient GD for the Inbound. For example, Table 11 summarizes the steps of the GD for the Inbound on 7-round AES-256. However, in our cryptanalysis on AES, there exist *conflicts* during the GD, *e.g.*, five conflicts marked by “?” in Table 11. Trivially, these *conflicts* can be solved in a brute-force search. Suppose that the number of *conflicts* is c_{in} , the time complexity of the GD to find one starting point is $\mathcal{T}_{GD} = 2^{8c_{in}}$. If there are too many *conflicts*, the overall time complexity may exceed the upper bound of a valid attack. In our cryptanalysis, we find that there are

⁵Similar features are also spotted by Nageler *et al.* when studying the joint differential characteristics [46].

⁶Note that in [53], only part of EN is selected as Inbound without the KS.

three types of *conflict*, which should be treated in different ways to speed up the full attack.

- **Type I: Active sboxes falsely included in the Inbound.** In Fig. 8, all the active Sboxes in the Inbound should be specified as known bytes by DDT. When the known bytes in the boundary of the Inbound are deduced again from GD, they will lead to conflicts. For example, two active bytes $x_2[2, 6]$ included in the Inbound of Fig. 8 are deduced again by GD, which will result in a 2-byte conflict acting as a filter of 2^{-16} . However, if we put the two bytes in the Outbound, they will be satisfied with probability of at least $2^{-7 \times 2} = 2^{-14}$. Therefore, this type of conflicts should be solved in the Outbound phase to save time complexity.
- **Type II: Conflict between KS and EN path.** Fig. 10 shows the first 3 rounds of the Inbound in the 6-round attack on AES-256 in Section 6.2. After fixing the active bytes of $\{x_0, y_0, x_1, y_1, x_2, k_1\}$ (marked by V) by DDT, we deduce $k_2[2]$. Then with fixed $P = 0$ for key collision attack, $k_2[2]$ is again deduced through KS, *i.e.*, we get two equations about $k_2[2]$ in Equation 5.

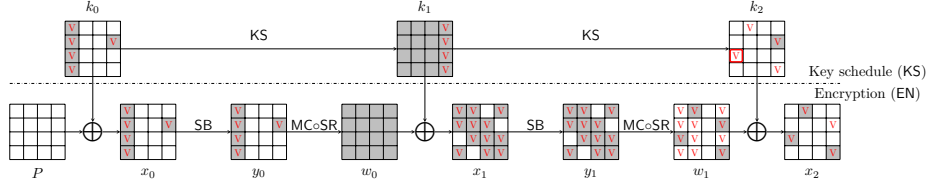


Fig. 10: Type II conflict between KS and EN path

$$\begin{cases} k_2[2] = y_1[0] \oplus y_1[5] \oplus 02 \cdot y_1[10] \oplus 03 \cdot y_1[15] \oplus x_2[2], \\ k_2[2] = x_0[2] \oplus P[2] \oplus SB(k_1[15]). \end{cases} \quad (5)$$

where the bytes marked by red are known. The conflict can be solved in the brute-force fashion with time complexity 2^8 . However, with a precomputation of Equation 6 as

$$y_1[0] \oplus y_1[5] \oplus 02 \cdot y_1[10] \oplus 03 \cdot y_1[15] \oplus x_2[2] \oplus x_0[2] \oplus P[2] \oplus SB(k_1[15]) = 0, \quad (6)$$

on the known bytes $y_1[0, 5, 10, 15]$, $x_2[2]$, $x_0[2]$ and $k_1[15]$, the 2^8 complexity can be saved. If any of the choices of the known bytes can not satisfy Equation 6, search a new differential characteristic. If satisfied, deduce the value of $k_2[2]$ without conflict. So this type of conflict does not affect the overall complexity.

Following the above example, we formalize the Type II conflict: Given the input/output differences of active Sboxes, one can derive a couple of input/output values by DDT of those active Sboxes. Given a differential characteristic, there are some constraints on those input/output values

of the active Sboxes, like Equation 6, which are the so-called Type II conflicts. The steps to handle the Type II conflicts are:

- (a) Given a differential characteristic, precompute all Type II conflicts, like Equation 6.
- (b) Select the input/output values of the active Sboxes to directly satisfy all Type II conflicts.
- (c) Perform the rebound attacks with these valid input/output values for those active Sboxes.
- (d) If any input/output value of the active Sboxes does not satisfy the constraints, search a new differential characteristic.

– **Type III: Internal Conflict.** Conflicts that cannot be moved to the Outbound phase (conflicts are not on the boundary of the Inbound phase) or resolved by precomputation are called internal conflicts. This type of conflicts can only be solved in a brute-force fashion. For example, the conflicts marked by the underline in step 13 of 7-round attack AES-256 in Section 6.3. The nonlinear equations about these conflicts are too complicated to be precomputed. The number of type III conflicts will greatly affect the complexity.

Let the numbers of Type I/II/III conflicts be c_1, c_2, c_3 , where $c_{in} = c_1 + c_2 + c_3$. Then, after addressing the conflicts in different ways, the time complexity of the GD to find one starting point is about $\mathcal{T}'_{GD} = \mathcal{T}_{GD} / 2^{8(c_1+c_2)} = 2^{8c_3}$. The probability of the Outbound decreases to $2^{-p_{out} - (7 \text{ or } 6) \cdot c_1}$. The overall time complexity of the GD rebound will be

$$\mathcal{T} = 2^{8c_3} \cdot 2^{p_{out} + (7 \text{ or } 6) \cdot c_1}.$$

If $\mathcal{T} > 2^{n/2}$, add one more round (or a partial round) of the KS or EN path into the Inbound and update the probability of the Outbound phase. Run Builaguet *et al.*'s guess-and-determine tool [6] to find a new GD for the new Inbound and analyze the conflicts. If $\mathcal{T} < 2^{n/2}$, we can still repeat the above steps to find a possible better attack.

Initially, with the short Inbound phase, the probability $2^{-p_{out}}$ of the Outbound phase is usually very low, leading to the complexity exceeding the birthday paradox. As the range of the Inbound phase increases, the probability of outbound will increase, but the number of conflicts could also increase. Our algorithm can find a balance between the time to solve the conflicts 2^{8c_3} and the time $2^{p_{out}}$ for the Outbound phase, leading to a better overall time complexity.

Summary of the GD Rebound Attack. After determining the related-key differential suitable for key collision (**Step 1**) and the Inbound phase (**Step 2**), we can conduct the full GD rebound attack as follows.

1. For the Inbound differential with s_1 active Sboxes of 2^{-7} probability and s_2 active Sboxes of 2^{-6} probability, we can determine $2^{(s_1+2s_2)-1}$ choices for the combinations of the known bytes in the Inbound.

2. In the GD steps of the **Inbound**, assuming that the number of guessed bytes is g , there are $2^{(s_1+2s_2)-1+8g}$ choices for the combinations of the known bytes and guessed bytes in the **Inbound**. Note that in the final **Inbound** phase, there are no Type I conflicts (removed to **Outbound**), only Type II and Type III conflicts, *i.e.*, $c_1 = 0$ and $c_{in} = c_2 + c_3$.
3. If $c_2 > 0$, precompute to solve the c_2 conflicts. Otherwise, skip this step.
4. Choosing $2^{8c_3+p_{out}}$ combinations of known and guessed bytes, run the GD steps to obtain $2^{p_{out}}$ starting points. Then, calculate whether the starting points satisfy the **Outbound** differential. One collision is expected. The time complexity of finding one starting point is $\mathcal{T}_{GD} = 2^{8c_3}$, and the overall time complexity of the GD rebound is $\mathcal{T} = 2^{8c_3} \cdot 2^{p_{out}}$. Note that in **Step 1** to choose a RKDC, the degrees of freedom are already taken into account and there should be some key pairs that satisfy the full RKDC (thus leading to collisions). In the concrete attack, the total degree of freedom of the **Inbound** is $2^{(s_1+2s_2)-1+8g}$, and the consumed degree of freedom to precompute the c_2 Type II conflicts is 2^{8c_2} . Since the total probability of finding the final collision is $2^{-(8c_3+p_{out})}$, it is expected that $2^{(s_1+2s_2)-1+8g-8c_2} \geq 2^{(8c_3+p_{out})}$ according to the property of the RKDC.

4 Key Collision Attacks on Reduced AES-128

This section discusses the fixed-target-plaintext key collision on 2-round AES-128 in [53], and then gives practical key collision attacks on 2-/3-round AES-128.

4.1 The Invalid Key Collision on 2-round AES-128 in [53]

In [53], Taiyama *et al.* gave a fixed-target-plaintext key collision attack on 2-round AES-128. Their underlying differential characteristic is shown in Fig. 9, which has a probability of 2^{-98} . In their attack, the round 0 in the EN path is the inbound phase with a probability of 2^{-42} , and the remaining parts including the key schedule are the outbound phase with a probability of 2^{-56} .

At the beginning of their attack, 2^{14} values of 4-byte $x_0[12, 13, 14, 15]$ are chosen. Then with fixed plaintext P , compute 2^{14} values of $k_0[12, 13, 14, 15]$. Since the input difference $\Delta k_0[12]$ and the output difference of $\Delta SB(k_0[12])$ are fixed with a probability of 2^{-7} , the authors hope that there are $2^{7=(14-7)}$ values remaining. Focusing on the value of $x_0[12]$, since $\Delta x_0[12] = 0x69$ and $\Delta SB(x_0[12]) = 0xef$, there are only two possible values of $x_0[12]$, *i.e.*, $0x1b$ and $0x72$. For $k_0[12]$, since $\Delta k_0[12] = 0x69$ and $\Delta SB(k_0[12]) = 0x08$, there are also only two possible values of $k_0[12]$, *i.e.*, $0x02$ and $0x6b$. So $P[12]$ is fixed according to $k_0[12] = P[12] \oplus x_0[12]$ for this differential.

- CASE-1: When $x_0[12]$ is fixed to $0x1b$ or $0x72$ in all 2^{14} values of $x_0[12, 13, 14, 15]$, $P[12]$ should be fixed to corresponding values to satisfy the differential, *i.e.*,

$$(x_0[12], P[12]) \in \{(0x1b, 0x19), (0x1b, 0x70), (0x72, 0x70), (0x72, 0x19)\}.$$

In this case, all the 2^{14} values will remain.

613 – CASE-2: When $x_0[12]$ varies and $(x_0[12], P[12])$ is not among the value pairs
 614 in CASE-1, all the 2^{14} values of $x_0[12, 13, 14, 15]$ do not satisfy the differences
 615 in $\Delta k_0[12]$ and $\Delta SB(k_0[12])$. No collision can be found.

616 As in the discussion above, the key collision attack for 2-round AES-128 in [53]
 617 is only valid for some plaintexts with fixed values in $P[12]$, and requires careful
 618 selection of $x_0[12]$. For other plaintexts, including $P = 0$, one cannot find a key
 619 pair that generates the same ciphertext.

620 4.2 The Practical Key Collision Attack on 2-round AES-128

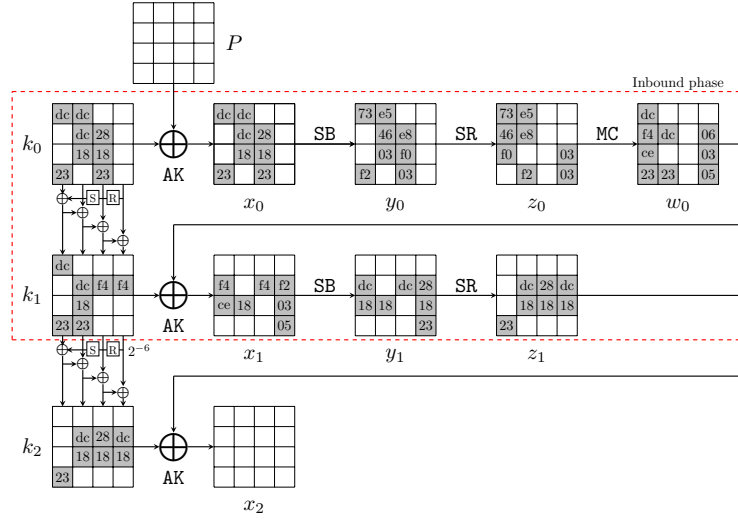


Fig. 11: The new related-key differential characteristic on 2-round AES-128

621 We give a new key collision attack on 2-round AES-128 based on a new
 622 related-key differential characteristic as shown in Fig. 11, whose probability is
 623 2^{-107} . We choose the differential with $\Delta k_0[j] = 0$ ($j \in [12, 13, 14, 15]$) to avoid
 624 the restriction on the plaintext as in Section 4.1. Only the last round of the key
 625 schedule is the outbound phase. Since $\Delta k_1[13] = 0xf4$ and $\Delta SB(k_1[13]) = 0xdc$,
 626 the probability is $2^{-p_{out}} = 2^{-6}$. The remaining parts are the inbound phase. The
 627 steps of the GD for the inbound phase are marked in Fig. 12 and the detailed
 628 equations are listed in Table 5.

629 Guess-and-determine procedures of the inbound phase.

- 630 1. With the fixed differences in $\Delta x_0[0, 3 - 6, 9 - 11]$ and $\Delta y_0[0, 3 - 6, 9 - 11]$,
 631 we can deduce $x_0[0, 3 - 6, 9 - 11]$ and $y_0[0, 3 - 6, 9 - 11]$ (marked by 1 in

- Fig. 12) by accessing the DDT. Similarly, deduce $x_1[1, 2, 6, 9, 13, 14, 15]$ and $y_1[1, 2, 6, 9, 13, 14, 15]$ (marked by $\boxed{1}$).
- (a) In round 0, compute $k_0[0, 3, 4, 5, 6, 9, 10, 11] = (x_0 \oplus P)[0, 3, 4, 5, 6, 9, 10, 11]$ (marked by $\overleftarrow{1}$).
- (b) Compute forward to get $z_0[0, 1, 2, 4, 5, 7, 14, 15]$ and $z_1[3, 5, 6, 9, 10, 13, 14]$ (marked by $\overrightarrow{1}$).
2. Guess $k_0[15]$ (marked by $\boxed{2}$), and compute forward to get $x_0[15]$, $y_0[15]$ and $z_0[3]$ (marked by $\overrightarrow{2}$). Then compute $w_0[0, 1, 2, 3] = \text{MC}(z_0[0, 1, 2, 3])$. Since $x_1[1, 2]$ are known, compute $k_1[1, 2] = x_1[1, 2] \oplus w_0[1, 2]$ (marked by $\overrightarrow{2}$).
3. According to the key relations, we can deduce $k_1[5, 6, 9, 10]$ and $k_0[2]$ (marked by $\boxed{3}$) with equations given in Table 5.
- (a) Compute forward to get $x_0[2]$, $y_0[2]$ and $z_0[10]$ (marked by $\overrightarrow{3}$).
- (b) Compute backward to get $w_0[6, 9] = x_1[6, 9] \oplus k_1[6, 9]$ (marked by $\overleftarrow{3}$).
4. For column 1 over the MC operation in round 0, four values in the inputs and outputs are known, and we can deduce the other four values. That is, deduce $z_0[6]$ and $w_0[4, 5, 7]$ (marked by $\boxed{4}$) from $z_0[4, 5, 7]$ and $w_0[6]$.
- (a) Compute backward to get $k_0[14] = P[14] \oplus \text{SB}^{-1}(z_0[6])$ (marked by $\overleftarrow{4}$).
- (b) Compute forward to get $x_1[5]$, $y_1[5]$ and $z_1[1]$ (marked by $\overrightarrow{4}$).
5. According to the key relations, deduce $k_0[1]$ and $k_1[14]$ (marked by $\boxed{5}$). Compute forward to get $z_0[13]$ (marked by $\overrightarrow{5}$) and compute backward to get $w_0[14]$ (marked by $\overleftarrow{5}$).
6. For column 3 of round 0, deduce $w_0[12, 13, 15]$ and $z_0[12]$ (marked by $\boxed{6}$) from $z_0[13, 14, 15]$ and $w_0[14]$.
- (a) Compute backward to get $k_0[12]$ (marked by $\overleftarrow{6}$).
- (b) Compute forward to get $k_1[13, 15]$ (marked by $\overrightarrow{6}$).
7. According to the key relations, deduce $k_1[0, 3, 4, 7, 11]$ and $k_0[7, 13]$ (marked by $\boxed{7}$). Compute forward to get $z_0[9, 11]$ and $z_1[0, 4, 7, 11]$ (marked by $\overrightarrow{7}$).
8. For column 2 over the MC operation in round 0, deduce $z_0[8]$ and $w_0[8, 10, 11]$ (marked by $\boxed{8}$) from $z_0[9, 10, 11]$ and $w_0[9]$.
- (a) Compute backward to get $k_0[8]$ (marked by $\overleftarrow{8}$).
- (b) Compute forward to get $z_1[2, 15]$ (marked by $\overrightarrow{8}$).
9. According to the key relations, deduce $k_1[8, 12]$ (marked by $\boxed{9}$). Then we get all the states of the starting point.

Degree of freedom and complexity.

- In step 1 of the above procedures, we deduce the values for active bytes from the input/output differences in the inbound phase. There are 15 active Sboxes with a total probability 2^{-101} , including $s_1 = 11$ active Sboxes with probability 2^{-7} and $s_2 = 4$ active Sboxes with probability 2^{-6} . Therefore, there are $2^{11+8}/2 = 2^{18}$ combinations for the 15 active bytes, *i.e.*, there are 2^{18} choices for the bytes marked by $\boxed{1}$ with a green border in Fig. 12.

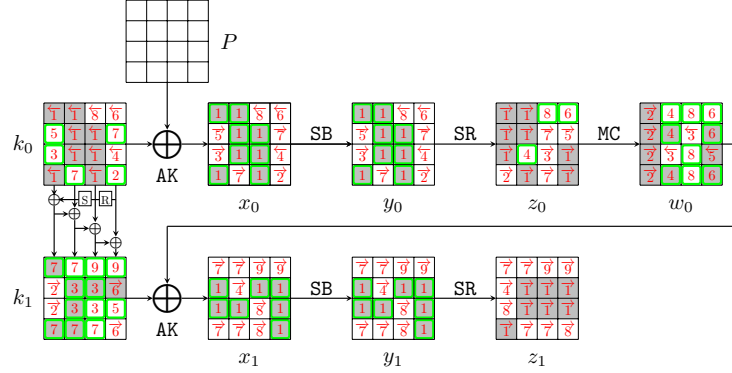


Fig. 12: Steps of the GD in the inbound phase for 2-round AES-128. The green border bytes are the known or guessed bytes at the beginning of each step, which are used to deduce other bytes. E.g., in step 2, $k_0[15]$ marked by **2** with a green border is guessed at the beginning of step 2, then it is used to deduce $x_0[15]$, $y_0[15]$ and $z_0[3]$, etc.

1.	$k_0[0, 3, 4, 5, 6, 9, 10, 11] = (x_0 \oplus P)[0, 3, 4, 5, 6, 9, 10, 11]$	
2.	$z_0[3] = \text{SB}(P[15] \oplus \underline{k_0[15]})$	$w_0[0, 1, 2, 3] = \text{MC}(z_0[0, 1, 2, 3])$
	$k_1[1, 2] = x_1[1, 2] \oplus w_0[1, 2]$	
3.	$k_1[5] = k_0[5] \oplus k_1[1]$	$k_1[6] = k_0[6] \oplus k_1[2]$
	$k_1[9] = k_0[9] \oplus k_1[5]$	$k_1[10] = k_0[10] \oplus k_1[6]$
	$k_0[2] = k_1[2] \oplus \text{SB}(k_0[15])$	
4.	$w_0[4, 5, 7], z_0[6] = \text{MC}(z_0[4, 5, 7], w_0[6])$	$k_0[14] = P[14] \oplus \text{SB}^{-1}(z_0[6])$
5.	$k_0[1] = k_1[1] \oplus \text{SB}(k_0[14])$	$k_1[14] = k_1[10] \oplus k_0[14]$
6.	$w_0[12, 13, 15], z_0[12] = \text{MC}(z_0[13, 14, 15], w_0[14])$	$k_0[12] = P[12] \oplus \text{SB}^{-1}(z_0[12])$
	$k_1[13] = w_0[13] \oplus x_1[13]$	$k_1[15] = w_0[15] \oplus x_1[15]$
7.	$k_1[3] = k_0[3] \oplus \text{SB}(k_0[12])$	$k_1[11] = k_0[15] \oplus k_1[15]$
	$k_1[7] = k_1[11] \oplus k_0[11]$	$k_0[7] = k_1[7] \oplus k_1[3]$
	$k_0[13] = k_1[13] \oplus k_1[9]$	$k_1[0] = k_0[0] \oplus \text{SB}(k_0[13]) \oplus \text{const}$
	$k_1[4] = k_0[4] \oplus k_1[0]$	
8.	$w_0[8, 10, 11], z_0[8] = \text{MC}(z_0[9, 10, 11], w_0[9])$	$k_0[8] = P[8] \oplus \text{SB}^{-1}z_0[8]$
9.	$k_1[8] = k_0[8] \oplus k_1[4]$	$k_1[12] = k_0[12] \oplus k_1[8]$

Table 5: Equations in the guess-and-determine steps for 2-round AES-128. The blue byte is guessed.

- Given one out of 2^{18} choices marked by **1**, one byte $k_0[15]$ (marked by a wavy line) is guessed in step 2. Therefore, there expect $2^{18+8} = 2^{26}$ states satisfying the inbound trial in total, which act as the starting points for the outbound phase.
- Since there is no conflict in the inbound phase, i.e., $c_{in} = 0$, the time of the GD to find one starting point is $\mathcal{T}_{\text{GD}} = 1$. Since the probability of the outbound phase is $2^{-p_{out}} = 2^{-6}$, we need to collect 2^6 starting points to expect one collision. The overall time complexity is only $\mathcal{T} = 2^6$ and the

memory complexity is negligible. We could find the key collisions in seconds on a desktop equipped with Intel Core i7-13700F @2.1 GHz 396 and 16G RAM, and some examples are listed in Table 3.

4.3 The Practical Key Collision Attack on 3-round AES-128

We give a new key collision attack on 3-round AES-128 based on a new related-key differential characteristic as shown in Fig. 13. There is one active $k_0[15]$ in the first round key, *i.e.* $\Delta k_0[15] = 0\text{xcc}$, which brings the same difference to $x_0[15]$. Applying the observation in Section 3.2, to prevent the restriction on P , we set $\Delta\text{SB}(k_0[15]) = \Delta\text{SB}(x_0[15]) = 0\text{x28}$, and keep $x_0[15] = k_0[15]$ in the attack, which makes $P[15] = 0$. So when we choose the value of $x_0[15]$ satisfying the difference over the active Sbox in the EN path, the value of $k_0[15]$ satisfies the difference over the active Sbox in the KS with probability 1. Therefore, although there are 19 active Sboxes in the differential, we only count the probability of 18 of them, which is 2^{-125} . We choose the first two rounds of the EN and KS as the inbound phase, with a probability of 2^{-90} . The remaining parts are the outbound phase, with a probability of $2^{-p_{out}} = 2^{-35}$. The steps of the GD for the inbound phase are marked in Fig. 14 with equations listed in Table 6.

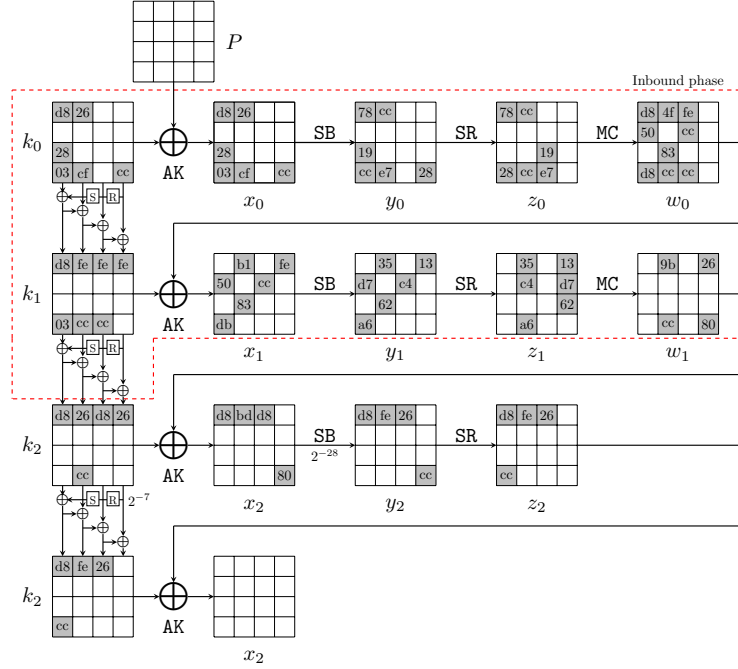


Fig. 13: The related-key differential characteristic on 3-round AES-128

697 **Guess-and-determine procedures of the inbound phase.**

- 698 1. With the fixed differences in $\Delta x_0[0, 2-4, 7, 15]$ and $\Delta y_0[0, 2-4, 7, 15]$, we
 699 can deduce $x_0[0, 2-4, 7, 15]$ and $y_0[0, 2-4, 7, 15]$ (marked by $\boxed{1}$ in Fig. 14) by
 700 accessing the DDT. Similarly, deduce $x_1[1, 3, 4, 6, 9, 12]$ and $y_1[1, 3, 4, 6, 9, 12]$
 701 (marked by $\boxed{1}$).
 702 (a) In round 0, deduce $k_0[0, 2, 3, 4, 7, 15] = (x_0 \oplus P)[0, 2, 3, 4, 7, 15]$ (marked
 703 by $\overleftarrow{1}$). Compute forward to $z_0[0, 3, 4, 7, 10, 11]$ (marked by $\overrightarrow{1}$).
 704 (b) In round 1, since the differences $\Delta k_1[12]$ and $\Delta SB(k_1[12])$ are known, de-
 705 duce $k_1[12]$ (marked by $\boxed{1}$) by accessing the DDT. Compute backward to
 706 get $w_0[12]$ (marked by $\overleftarrow{1}$) and compute forward to get $z_1[4, 5, 7, 12, 13, 14]$
 707 (marked by $\overrightarrow{1}$).
 708 2. Guess $k_0[5, 12]$ (marked by $\boxed{2}$). According to the key relations, deduce $k_1[2, 3, 7, 8]$
 709 (marked by $\boxed{2}$) as Table 6.
 710 (a) Compute forward to get $x_0[5, 12]$, $y_0[5, 12]$ and $z_0[1, 12]$ (marked by $\overrightarrow{2}$).
 711 (b) Compute backward to get $w_0[3] = k_1[3] \oplus x_1[3]$ (marked by $\overleftarrow{2}$).
 712 3. For column 0 over the MC operation of round 0, deduce $w_0[0, 1, 2]$ and $z_0[2]$
 713 (marked by $\boxed{3}$) from $z_0[0, 1, 3]$ and $w_0[3]$.
 714 (a) Compute backward to get $x_0[10]$ and $k_0[10]$ (marked by $\overleftarrow{3}$).
 715 (b) Compute forward to get $k_1[1] = w_0[1] \oplus x_1[1]$ and $z_1[10]$ (marked by $\overrightarrow{3}$).
 716 4. Guess $k_0[13]$ (marked by $\boxed{4}$). According to the key relations, deduce $k_0[8]$
 717 and $k_1[0, 4, 5]$ (marked by $\boxed{4}$) as Table 6.
 718 (a) Compute forward to get $z_0[8, 9]$ and $z_1[0]$ (marked by $\overrightarrow{4}$).
 719 (b) Compute backward to get $w_0[4]$ (marked by $\overleftarrow{4}$).
 720 5. For column 2 over the MC operation of round 0, deduce $w_0[8, 9, 10, 11]$
 721 (marked by $\boxed{5}$) from $z_0[8, 9, 10, 11]$. Compute forward to get $k_1[9] = w_0[9] \oplus$
 722 $x_1[9]$ and $z_1[8]$ (marked by $\overrightarrow{5}$).
 723 6. According to the key relations, deduce $k_0[9]$ and $k_1[13]$ (marked by $\boxed{6}$).
 724 Compute forward to get $z_0[5]$ (marked by $\overrightarrow{6}$).
 725 7. For column 1 over the MC operation of round 0, deduce $w_0[5, 6, 7]$ and $z_0[6]$
 726 (marked by $\boxed{7}$) from $z_0[4, 5, 7]$ and $w_0[4]$.
 727 (a) Compute backward to get $x_0[14]$ and $k_0[14]$ (marked by $\overleftarrow{7}$).
 728 (b) Compute forward to get $k_1[6]$ and $z_1[1, 11]$ (marked by $\overrightarrow{7}$).
 729 8. According to the key relations, deduce $k_0[1, 6]$ and $k_1[10, 14]$ (marked by $\boxed{8}$).
 730 Compute forward to get $z_0[13, 14]$ and $z_1[2]$ (marked by $\overrightarrow{8}$).
 731 9. For column 3 over the MC operation of round 0, deduce $w_0[13, 14, 15]$ and
 732 $z_0[15]$ (marked by $\boxed{9}$) from $z_0[12, 13, 14]$ and $w_0[12]$.
 733 (a) Compute backward to get $x_0[11]$ and $k_0[11]$ (marked by $\overleftarrow{9}$).
 734 (b) Compute forward to get $z_1[6, 9]$ and columns 1,2 of w_1 (marked by $\overrightarrow{9}$).
 735 10. According to the key relations, deduce $k_1[11, 15]$ (marked by $\boxed{10}$). Compute
 736 forward to get $z_1[3, 15]$ and columns 0,3 of w_1 (marked by $\overrightarrow{10}$). Then we get
 737 all the states of the starting point.

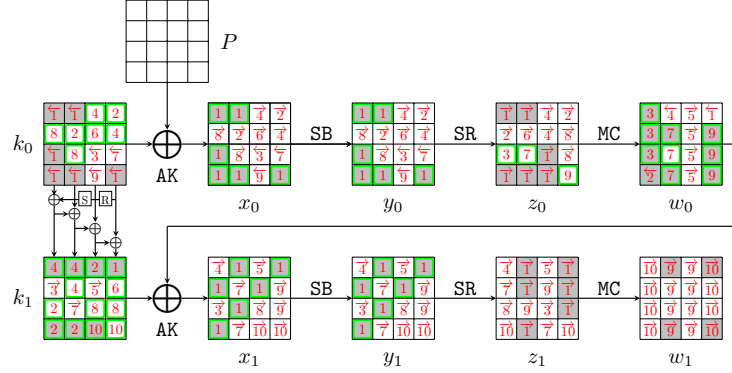


Fig. 14: Steps of the GD in the inbound phase for 3-round AES-128

1.	$k_0[0, 2, 3, 4, 7, 15] = (x_0 \oplus P)[0, 2, 3, 4, 7, 15]$	$w_0[12] = k_1[12] \oplus x_1[12]$
2.	$k_1[3] = k_0[3] \oplus \text{SB}(\underline{k_0[12]})$	$k_1[7] = k_0[7] \oplus k_1[3]$
	$k_1[8] = k_1[12] \oplus \underline{k_0[12]}$	$k_1[2] = k_0[2] \oplus \text{SB}(k_0[15])$
	$z_0[1] = \text{SB}(\underline{k_0[5]} \oplus P[5])$	
3.	$w_0[0, 1, 2], z_0[2] = \text{MC}(z_0[0, 1, 3], w_0[3])$	$k_0[10] = P[10] \oplus \text{SB}^{-1}(z_0[2])$
	$k_1[1] = w_0[1] \oplus x_1[1]$	
4.	$k_1[0] = k_0[0] \oplus \text{SB}(\underline{k_0[13]}) \oplus \text{const}$	$k_1[4] = k_0[4] \oplus k_1[0]$
	$k_0[8] = k_1[8] \oplus k_1[4]$	$k_1[5] = k_0[5] \oplus k_1[1]$
5.	$w_0[8, 9, 10, 11] = \text{MC}(z_0[8, 9, 10, 11])$	$k_1[9] = w_0[9] \oplus x_1[9]$
6.	$k_0[9] = k_1[9] \oplus k_1[5]$	$k_1[13] = k_1[9] \oplus k_0[13]$
7.	$w_0[5, 6, 7], z_0[6] = \text{MC}(z_0[4, 5, 7], w_0[4])$	$k_0[14] = P[14] \oplus \text{SB}^{-1}(z_0[6])$
	$k_1[6] = w_0[6] \oplus x_1[6]$	
8.	$k_0[1] = k_1[1] \oplus \text{SB}(k_0[14])$	$k_0[6] = k_1[6] \oplus k_1[2]$
	$k_1[10] = k_1[6] \oplus k_0[10]$	$k_1[14] = k_1[10] \oplus k_0[14]$
9.	$w_0[13, 14, 15], z_0[15] = \text{MC}(z_0[12, 13, 14], w_0[12])$	$k_0[11] = P[11] \oplus \text{SB}^{-1}(z_0[15])$
10.	$k_1[11] = k_0[11] \oplus k_1[7]$	$k_1[15] = k_1[11] \oplus k_0[15]$

Table 6: Equations in the GD steps for 3-round AES-128. The blue bytes are guessed.

738 Degree of freedom and complexity.

- 739 – In step 1, we deduce the values for active bytes from the input/output differ-
740 ences in the inbound phase. There are 13 active Sboxes with a total proba-
741 bility 2^{-90} , including $s_1 = 12$ active Sboxes with probability 2^{-7} and $s_2 = 1$
742 active Sboxes with probability 2^{-6} . Therefore, there are $2^{12+2}/2 = 2^{13}$ com-
743 binations for the 13 active bytes, *i.e.*, there are 2^{13} choices for the bytes
744 marked by 1 in Fig. 14.
- 745 – Given one out of 2^{13} choices marked by 1, three bytes $k_0[5, 12, 13]$ (marked
746 by a wavy line) are guessed in step 2 and 4. Therefore, there expect $2^{13+24} =$

747 2^{37} states satisfying the inbound trial in total, which act as the starting
 748 points for the outbound phase.
 749 – Since there is no conflict in the inbound phase, *i.e.*, $c_{in} = 0$, the time of
 750 the GD to find one starting point is $\mathcal{T}_{GD} = 1$. Since the probability of the
 751 outbound phase is $2^{-p_{out}} = 2^{-35}$, we need to collect 2^{35} starting points to
 752 expect one collision. The overall time complexity is $\mathcal{T} = 2^{35}$ and the memory
 753 complexity is negligible, which is practical. We find key collisions in several
 754 hours on a desktop equipped with Intel Core i7-13700F @2.1 GHz and 16G
 755 RAM using one CPU core, and some examples are listed in Table 3.

756 5 Key Collision Attacks on Reduced AES-192

757 In this section, we give a practical key collision attack on 5-round AES-192
 758 applying the differential characteristic in [53]. We also give the first quantum
 759 key collision attack on 6-round AES-192.

760 5.1 The Practical Key Collision Attack on 5-round AES-192

761 We reuse the differential characteristic for AES-192 with a probability of 2^{-186} in
 762 [53], which is shown in Fig. 15. Our inbound phase covers the first three rounds
 763 of the EN and KS, which has 24 active Sboxes with a probability of 2^{-165} ,
 764 including 1 active Sbox in the key schedule. The probability of the outbound
 765 phase is $2^{-p_{out}} = 2^{-21}$. The guess-and-determine steps of the GD are listed
 766 below, also in Fig. 16. The detailed equations are listed in Table 7.

767 Guess-and-determine procedure of the inbound phase.

- 768 1. Since all 16 bytes Δx_0 and Δy_0 are known, we can deduce the full state of
 769 x_0 and y_0 (marked by 1 in Fig. 16) by accessing the DDT. With fixed P , we
 770 can deduce the whole state of k_0 (marked by 1) from x_0 . Compute forward
 771 to $w_0 = MC \circ SR(y_0)$, marked by 1.
- 772 2. Similarly, deduce $x_1[2, 7, 8, 13, 15]$ and $y_1[2, 7, 8, 13, 15]$ (marked by 2) by
 773 accessing the DDT. Then compute $k_1[2, 7, 8, 13, 15] = (x_1 \oplus w_0)[2, 7, 8, 13, 15]$
 774 (marked by 2). We can also deduce $z_1[3, 8, 9, 10, 11]$ (marked by 2) from
 775 $y_1[2, 7, 8, 13, 15]$, and compute $w_1[8, 9, 10, 11] = MC(z_1[8, 9, 10, 11])$ (marked
 776 by 2).
- 777 3. Deduce $x_2[3, 15]$ and $y_2[3, 15]$ (marked by 3) by accessing the DDT. Since
 778 $\Delta k_2[15]$ and $\Delta SB(k_2[15])$ are known (see Figure 15), deduce $k_2[15]$ (marked
 779 by 3) by accessing the DDT. Compute backward to get $w_1[15] = k_2[15] \oplus x_2[15]$
 780 (marked by 3).
- 781 4. According to the key relations, we can deduce $k_1[3, 4, 5, 6, 9, 10, 11, 12, 14]$
 782 and $k_2[0, 1, 2, 3, 4, 5, 6, 7, 10, 11, 14]$ (marked by 4). The equations are given
 783 in Table 7.
 784 (a) Compute forward in round 1, we can deduce $z_1[1, 2, 4, 5, 6, 7, 12, 14, 15]$
 785 and compute $w_1[4, 5, 6, 7] = MC(z_1[4, 5, 6, 7])$ (marked by 4).

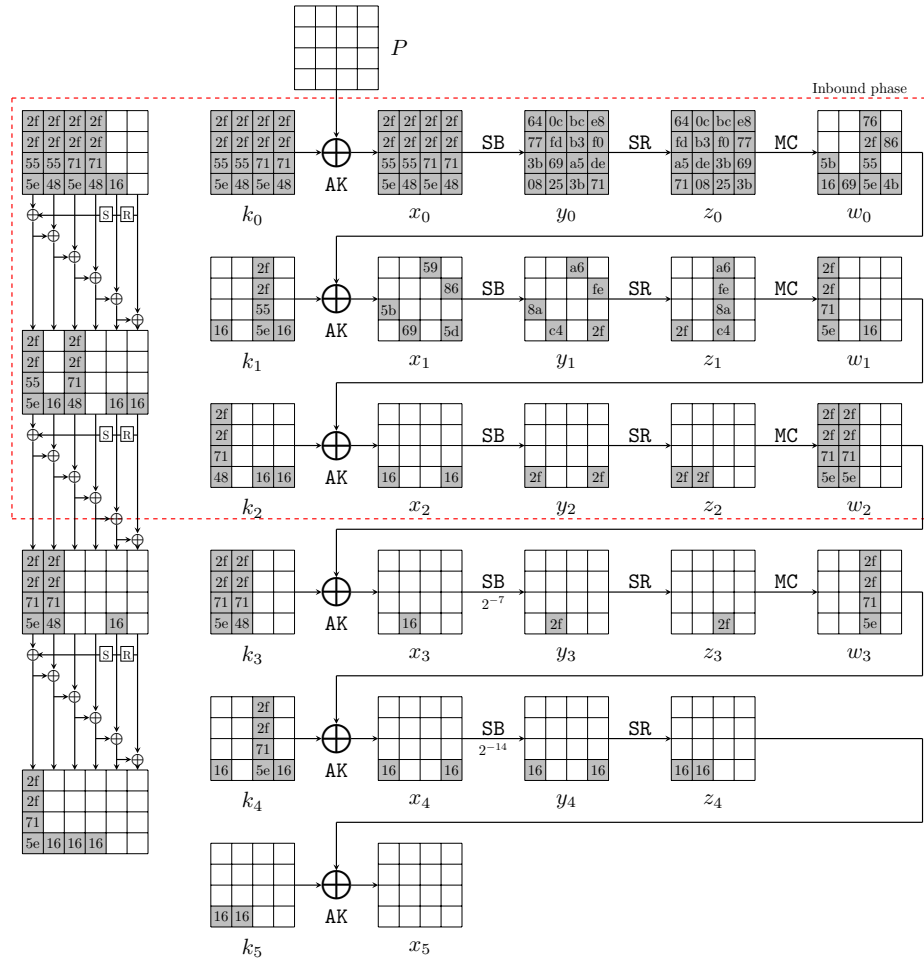


Fig. 15: The related-key differential characteristic on 5-round AES-192 in [53]

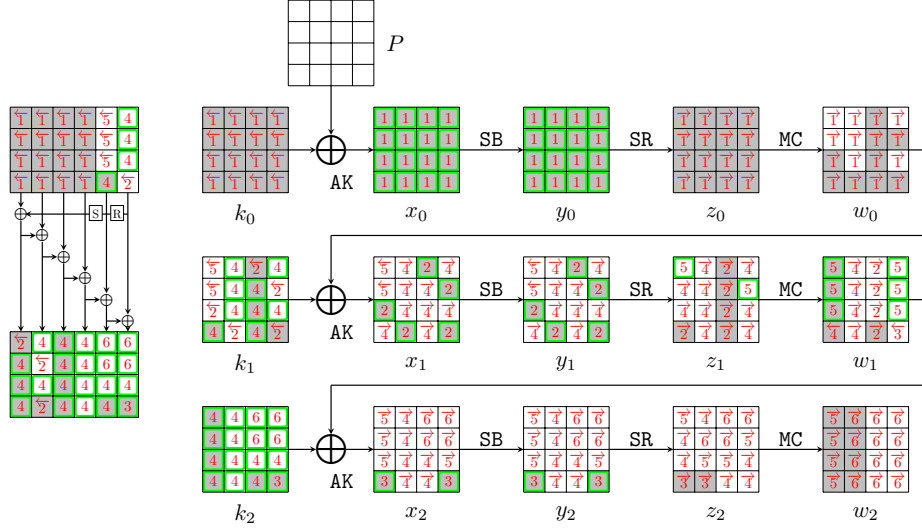


Fig. 16: Steps of the GD in the inbound phase for 5-round AES-192

- 786 (b) Compute backward in round 2 to get $w_1[3] = k_2[3] \oplus x_2[3]$ (marked by $\overrightarrow{4}$).
- 787 $\overrightarrow{4}$). Compute forward to deduce $z_2[1, 2, 4, 11, 14, 15]$ (marked by $\overrightarrow{4}$).
- 788 5. For column 0 and column 3 over the MC operation in round 1, four values
- 789 in the inputs and outputs are known; we can deduce the other four values.
- 790 (a) For column 0, deduce $z_1[0]$ and $w_1[0, 1, 2]$ (marked by $\overrightarrow{5}$) from $z_1[1, 2, 3]$
- 791 and $w_1[3]$.
- 792 (b) For column 3, deduce $z_1[13]$ and $w_1[12, 13, 14]$ (marked by $\overrightarrow{5}$) from
- 793 $z_1[12, 14, 15]$ and $w_1[15]$.
- 794 (c) Compute backward to compute $k_1[0] = w_0[0] \oplus \text{SB}^{-1}(z_1[0])$ and $k_1[1] =$
- 795 $w_0[1] \oplus \text{SB}^{-1}(z_1[13])$ (marked by $\overrightarrow{5}$).
- 796 (d) Compute forward to get $z_2[0, 6, 10, 13]$ and $w_2[0, 1, 2, 3]$ (marked by $\overrightarrow{5}$).
- 797 6. According to the key relations, we can deduce $k_2[8, 9, 12, 13]$ (marked by $\overrightarrow{6}$).
- 798 Compute forward to get columns 1, 2, and 3 of w_2 (marked by $\overrightarrow{6}$). So we
- 799 totally determine the starting point.

800 Degree of freedom and complexity.

- 801 – There are totally 24 active Sboxes in the 3-round inbound phase, including 21
- 802 active Sboxes with probability $s_1 = 2^{-7}$ and 3 active Sboxes with probability
- 803 $s_2 = 2^{-6}$. Therefore, by accessing the DDT, there expect $2^{21+6}/2 = 2^{26}$
- 804 combinations for the 24 active Sboxes, i.e., there are 2^{26} choices for the
- 805 bytes marked by $\overrightarrow{1}$, $\overrightarrow{2}$, and $\overrightarrow{3}$ in Fig. 16.
- 806 – There is no conflict in the GD, i.e., $c_{in} = 0$. The probability of the outbound
- 807 phase is $2^{-p_{out}} = 2^{-21}$. We have enough degrees of freedom to satisfy the
- 808 outbound phase. Therefore, the total complexity of the 5-round key-collision

attack on AES-192 is about $\mathcal{T} = 2^{21}$. We have practically implemented the attack and find some key pairs (K_1, K_2) in Table 3 such that $\text{AES-192}_{K_1}(0) = \text{AES-192}_{K_2}(0)$, where AES-192 is a 5-round one.

1.	$k_0 = x_0 \oplus P$	$w_0 = \text{MC} \circ \text{SR}(y_0)$
2.	$k_1[2, 7, 8, 13, 15] = (x_1 \oplus w_0)[2, 7, 8, 13, 15]$	$w_1[8, 9, 10, 11] = \text{MC}(z_1[8, 9, 10, 11])$
3.	$w_1[15] = k_2[15] \oplus x_2[15]$	
4.	$k_1[5] = \text{SB}^{-1}(k_1[8] \oplus k_0[0] \oplus \text{const})$	$k_1[10] = k_0[2] \oplus \text{SB}(k_1[7])$
	$k_1[14] = k_0[6] \oplus k_1[10]$	$k_2[2] = k_0[10] \oplus k_1[14]$
	$k_2[6] = k_0[14] \oplus k_2[2]$	$k_2[10] = k_1[2] \oplus k_2[6]$
	$k_1[12] = k_0[4] \oplus k_1[8]$	$k_2[0] = k_0[8] \oplus k_1[12]$
	$k_2[4] = k_0[12] \oplus k_2[0]$	$k_1[9] = k_1[13] \oplus k_0[5]$
	$k_1[6] = \text{SB}^{-1}(k_1[9] \oplus k_0[1])$	$k_1[11] = k_1[15] \oplus k_0[7]$
	$k_1[4] = \text{SB}^{-1}(k_1[11] \oplus k_0[3])$	$k_2[1] = k_0[9] \oplus k_1[13]$
	$k_2[5] = k_0[13] \oplus k_2[1]$	$k_2[3] = k_0[11] \oplus k_1[15]$
	$k_2[7] = k_0[15] \oplus k_2[3]$	$k_2[14] = k_1[6] \oplus k_2[10]$
	$k_2[11] = k_1[7] \oplus k_2[15]$	$k_1[3] = k_2[11] \oplus k_2[7]$
	$w_1[4, 5, 6, 7] = \text{MC}(z_1[4, 5, 6, 7])$	$w_1[3] = k_2[3] \oplus x_2[3]$
5.	$z_1[0], w_1[0, 1, 2] = \text{MC}(z_1[1, 2, 3], w_1[3])$	$k_1[0] = w_0[0] \oplus \text{SB}^{-1}(z_1[0])$
	$z_1[13], w_1[12, 13, 14] = \text{MC}(z_1[12, 14, 15], w_1[15])$	$k_1[1] = w_0[1] \oplus \text{SB}^{-1}(z_1[13])$
6.	$k_2[8] = k_1[0] \oplus k_2[4]$	$k_2[9] = k_1[1] \oplus k_2[5]$
	$k_2[12] = k_1[4] \oplus k_2[8]$	$k_2[13] = k_1[5] \oplus k_2[9]$

Table 7: Equations in the guess-and-determine steps for 5-round AES-192.

5.2 The Quantum Key Collision Attack on 6-round AES-192

We find a new quantum key collision attack on 6-round AES-192. The differential characteristic for 6-round AES-192 is shown in Fig. 17, with a probability of 2^{-184} . The inbound phase covers the first three rounds and has 22 active Sboxes, including 1 active Sbox in the key schedule. The probabilities of the inbound phase and outbound phase are 2^{-150} and 2^{-34} , respectively. In the GD of the inbound phase, there are 5 conflicts, which are all of Type III, *i.e.*, $c_{in} = c_3 = 5$ and $c_1 = c_2 = 0$. The guess-and-determine steps of the GD in the inbound phase are given below and in Fig. 18. The detail equations are given in Table 8.

Guess-and-determine procedure of the inbound phase.

- With the fixed differences in $\Delta x_0[2, 7]$ and $\Delta y_0[2, 7]$, we can deduce $x_0[2, 7]$ and $y_0[2, 7]$ (marked by 1) by accessing the DDT. Similarly, deduce $x_1[7, 8, 9, 11, 15]$, $y_1[7, 8, 9, 11, 15]$, $x_2[0-8, 10, 12-15]$, and $y_2[0-8, 10, 12-15]$ (marked by 1). Since the input difference and output difference of $k_1[7]$ are known, deduce $k_1[7]$ (marked by 1) by accessing the DDT.
 - In round 0, compute $k_0[2, 7] = x_0[2, 7] \oplus P[2, 7]$ (marked by 1). Compute forward to get $z_0[10, 11] = y_0[2, 7]$, marked by 1.

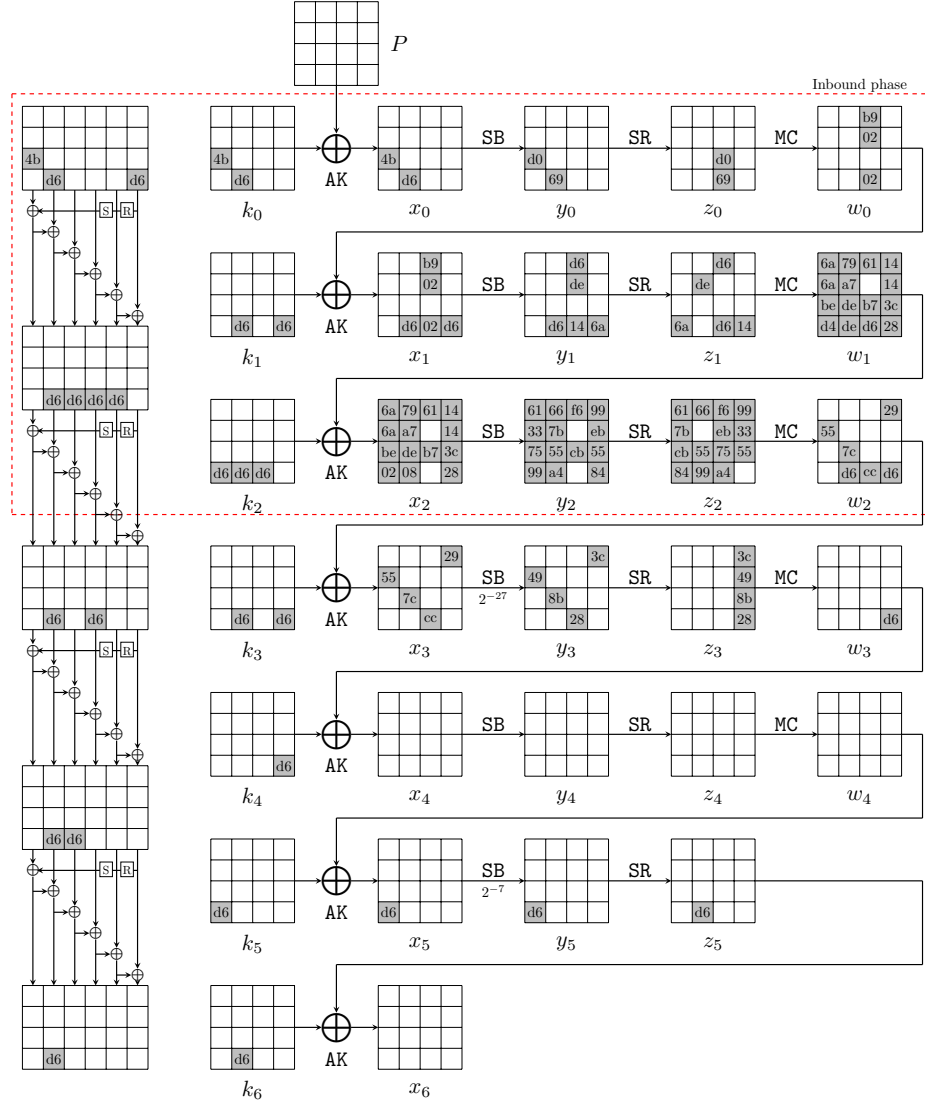


Fig. 17: The related-key differential characteristic on 6-round AES-192

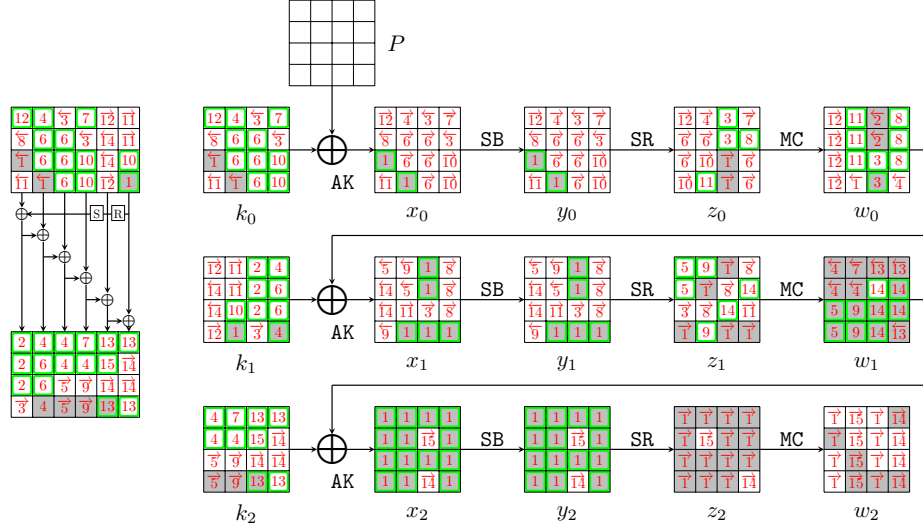


Fig. 18: Steps of the GD in the inbound phase for 6-round AES-192

- 829 (b) Compute backward in round 1 to get $w_0[7] = k_1[7] \oplus x_1[7]$ (marked by $\overleftarrow{1}$). Compute forward to get $z_1[3, 5, 8, 11, 15]$ (marked by $\overrightarrow{1}$).
830
831 (c) Compute forward in round 2 to get $z_2[0-4, 6-14]$, marked by $\overrightarrow{1}$. Com-
832 pute $w_2[0, 1, 2, 3] = \text{MC}(z_2[0, 1, 2, 3])$ and $w_2[8, 9, 10, 11] = \text{MC}(z_2[8, 9, 10, 11])$
833 (marked by $\overrightarrow{1}$).
834 2. According to the key relations, we can deduce $k_1[10]$ (marked by $\overrightarrow{2}$).
835 Guess $k_1[8, 9]$ (marked by $\overrightarrow{2}$). Compute $w_0[8, 9]$ backward (marked by $\overleftarrow{2}$).
836 3. For column 2 over the MC operation in round 0, four values in the inputs
837 and outputs are known, and we can deduce the other four values. That is,
838 deduce $z_0[8, 9]$ and $w_0[10, 11]$ (marked by $\overrightarrow{3}$) from $z_0[10, 11]$ and $w_0[8, 9]$.
839 (a) Compute backward to compute $k_0[8, 13] = P[8, 13] \oplus \text{SB}^{-1}(z_0[8, 9])$ (marked
840 by $\overleftarrow{3}$).
841 (b) Compute forward to get $k_1[11] = w_0[11] \oplus x_1[11]$ and $x_1[10] = w_0[10] \oplus$
842 $k_1[10]$ (marked by $\overrightarrow{3}$). Then deduce $z_1[2]$ (marked by $\overrightarrow{3}$).
843 4. Guess $k_2[0, 1]$ (marked by $\overrightarrow{4}$). According to the key relations, we can deduce
844 $k_0[4]$, $k_1[12, 15]$, and $k_2[5]$ (marked by $\overrightarrow{4}$).
845 (a) Compute $w_0[15]$ and $w_1[0, 1, 5]$ backward (marked by $\overleftarrow{4}$).
846 (b) Compute $z_0[4]$ forward (marked by $\overrightarrow{4}$).
847 5. For column 0 over the MC operation in round 1, deduce $z_1[0, 1]$ and $w_1[2, 3]$
848 (marked by $\overrightarrow{5}$) from $z_1[2, 3]$ and $w_1[0, 1]$.
849 (a) Compute backward to compute $x_1[0, 5] = \text{SB}^{-1}(z_1[0, 1])$ (marked by $\overleftarrow{5}$).
850 (b) Compute forward to get $k_2[2, 3] = w_1[2, 3] \oplus x_2[2, 3]$ (marked by $\overrightarrow{5}$).
851 6. Guess $k_1[13, 14]$ (marked by $\overrightarrow{6}$). According to the key relations, we can de-
852 deduce $k_0[5, 6, 9, 10, 11]$ (marked by $\overrightarrow{6}$). Compute forward to compute $z_0[1, 2, 5, 14, 15]$
853 (marked by $\overrightarrow{6}$).

- 854 7. Guess $k_0[12]$ (marked by $\overrightarrow{7}$). According to the key relations, we can deduce
855 $k_2[4]$ (marked by $\overrightarrow{7}$).
- 856 (a) In round 0, compute forward to compute $z_0[12]$ (marked by $\overrightarrow{7}$).
857 (b) In round 2, compute backward to get $w_1[4]$ (marked by $\overleftarrow{7}$).
- 858 8. For column 3 over the MC operation in round 0, deduce $z_0[13]$ and $w_0[12, 13, 14]$
859 (marked by $\overrightarrow{8}$) from $z_0[12, 14, 15]$ and $w_0[15]$.
- 860 (a) Compute backward to compute $x_0[1]$ and $k_0[1]$ (marked by $\overleftarrow{8}$).
861 (b) Compute forward to get $x_1[12, 13, 14]$ and $z_1[6, 9, 12]$ (marked by $\overrightarrow{8}$).
- 862 9. For column 1 over the MC operation in round 1, deduce $z_1[4, 7]$ and $w_1[6, 7]$
863 (marked by $\overrightarrow{9}$) from $z_1[5, 6]$ and $w_1[4, 5]$.
- 864 (a) Compute backward to compute $x_1[3, 4]$ (marked by $\overleftarrow{9}$).
865 (b) Compute forward to get $k_2[6, 7]$ (marked by $\overrightarrow{9}$).
- 866 10. According to the key relations, we can deduce $k_0[14, 15]$ and $k_1[6]$ (marked
867 by $\overrightarrow{10}$). Compute forward to get $z_0[3, 6]$ (marked by $\overrightarrow{10}$).
- 868 11. For column 1 over the MC operation in round 0, deduce $z_0[7]$ and $w_0[4, 5, 6]$
869 (marked by $\overrightarrow{11}$) from $z_0[4, 5, 6]$ and $w_0[7]$.
- 870 (a) Compute backward to compute $x_0[3]$ and $k_0[3]$ (marked by $\overleftarrow{11}$).
871 (b) Compute forward to get $k_1[4, 5]$ and $z_1[14]$ (marked by $\overrightarrow{11}$).
872 (c) Since $k_0[3] \oplus \text{SB}(k_1[4]) = k_1[11]$ and $k_1[11]$ (marked by $\overrightarrow{3}$) are deduced
873 in Step 3, there is a conflict of Type III with probability of 2^{-8} .
- 874 12. According to the key relations, we can deduce $k_0[0]$ (marked by $\overrightarrow{12}$). Com-
875 pute forward to get $z_0[0]$ (marked by $\overrightarrow{12}$). For column 0 over the MC opera-
876 tion in round 0, deduce $w_0[0, 1, 2, 3]$ (marked by $\overrightarrow{12}$) from $z_0[0, 1, 2, 3]$. Then
877 compute $k_1[0, 3]$ (marked by $\overrightarrow{12}$).
- 878 13. According to the key relations, we can deduce $k_2[8, 11, 12, 15]$ (marked by
879 $\overrightarrow{13}$). Compute backward to $w_1[8, 12, 15]$ (marked by $\overleftarrow{13}$).
- 880 14. For column 2 over the MC operation in round 1, deduce $z_1[10]$ and $w_1[9, 10, 11]$
881 (marked by $\overrightarrow{14}$) from $z_1[8, 9, 11]$ and $w_1[8]$. For column 3 over the MC opera-
882 tion in round 1, since five values are known, there is a conflict of Type III
883 with a probability of 2^{-8} . Then deduce $z_1[13]$ and $w_1[13, 14]$ (marked by $\overrightarrow{14}$)
884 from $z_1[12, 14, 15]$ and $w_1[12, 15]$.
- 885 (a) Compute backward to compute $x_1[1, 2]$ and $k_1[1, 2]$ (marked by $\overleftarrow{14}$).
886 (b) Compute forward to get $k_2[10, 13, 14]$ and $x_2[11]$ (marked by $\overrightarrow{14}$). Then
887 deduce $z_2[15]$ and $w_2[12, 13, 14, 15]$ (marked by $\overrightarrow{14}$).
888 (c) Since $k_1[2] \oplus k_2[10] = k_2[6]$ (marked by $\overrightarrow{9}$) and $k_2[14] \oplus k_2[10] = k_1[6]$
889 (marked by $\overrightarrow{10}$), there are two conflicts of Type III with a probability of
890 2^{-16} .
- 891 15. According to the key relations, we can deduce $k_2[9] = k_1[1] \oplus k_2[5] = k_2[13] \oplus$
892 $k_1[5]$ (marked by $\overrightarrow{15}$), which is a conflict of Type III with a probability of 2^{-8} .
893 Compute forward to $x_2[9]$ and $w_2[4, 5, 6, 7]$ (marked by $\overrightarrow{15}$).

894 Degree of Freedom and Complexity.

- 895 – In step 1, we deduce the values for active bytes from the input/output dif-
896 ferences in the inbound phase. There are 22 active Sboxes, including $s_1 = 18$
897 Sboxes with probability 2^{-7} and $s_2 = 4$ Sboxes with probability 2^{-6} . There-
898 fore, there are $2^{18+8}/2 = 2^{25}$ combinations for the 22 active bytes, *i.e.* there
899 are 2^{25} choices for the bytes marked by 1 in Fig. 18.
- 900 – Given one out of 2^{25} choices marked by 1, seven bytes $k_1[8, 9], k_2[0, 1], k_1[13, 14], k_0[12]$
901 (marked by a wavy line) are guessed in step 2, 4, 6 and 7. In step 11, 14 and
902 15, there are 5 conflicts with a total probability of 2^{-40} marked by under-
903 line. Therefore, there expect $2^{25+56-40} = 2^{41}$ starting points satisfying the
904 inbound differential.
- 905 – The time of the GD to find one starting point is about $\mathcal{T}_{GD} = 2^{40}$. Since the
906 probability of the outbound phase is $2^{-p_{out}} = 2^{-34}$, we have to collect 2^{34}
907 starting points to expect one collision and the degree of freedom is enough.
908 The classical time complexity of the full key collision attack is about $\mathcal{T} =$
909 $2^{40+34} = 2^{74}$ and the time complexity is larger than the birthday bound 2^{64} .

910 **Quantum Attack on 6-round AES-192.** Although a classical attack is invalid,
911 we can give a valid quantum one. We select 2^{18} choices of bytes marked by 1
912 and traverse 2^{56} possible values of $k_0[12], k_1[8, 9, 13, 14], k_2[0, 1]$.

- 913 1. Deduce the pairs (m_i^0, m_i^1) ($i = 0, 1, \dots, 21$) for 22 active Sboxes by accessing
914 the DDT, and store them in a qRAM L , whose size is about 44 bytes.
- 915 2. Given $|l_0, l_1, \dots, l_{17}\rangle$ and $l_i \in \{0, 1\}$, O_L is a quantum oracle that computes

$$O_L(|l_0, l_1, \dots, l_{17}\rangle |0\rangle) = |l_0, l_1, \dots, l_{17}\rangle |m_0^{l_0}, m_1^{l_1}, \dots, m_{17}^{l_{17}}, m_{18}^0, m_{19}^0, m_{20}^0, m_{21}^0\rangle \quad (7)$$

- 916 3. Define $F : \mathbb{F}_2^{18+56} \mapsto \mathbb{F}_2$ and its quantum oracle,

$$U_F : |l_0, \dots, l_{17}, k_0[12], k_1[8, 9, 13, 14], k_2[0, 1]\rangle |y\rangle \mapsto y \oplus F(l_0, \dots, l_{17}, k_0[12], k_1[8, 9, 13, 14], k_2[0, 1]), \quad (8)$$

917 Implementation of U_F :

- 918 (a) Access O_L to get $|m_0^{l_0}, m_1^{l_1}, \dots, m_{17}^{l_{17}}, m_{18}^0, m_{19}^0, m_{20}^0, m_{21}^0\rangle$.
- 919 (b) Fix the 22 bytes marked by 1 as $(m_0^{l_0}, m_1^{l_1}, \dots, m_{17}^{l_{17}}, m_{18}^0, m_{19}^0, m_{20}^0, m_{21}^0)$.
- 920 (c) Run Step 1-15 (or Table 8) with 7-byte $(k_0[12], k_1[8, 9, 13, 14], k_2[0, 1])$.
- 921 (d) Check if the 5 conflicts with a probability of 2^{-40} in Table 8 are satisfied.
922 If so, set a 1-bit flag flag_1 as $\text{flag}_1 := 1$. Else, set $\text{flag}_1 := 0$
- 923 (e) Check if the outbound phase with a probability of 2^{-34} is satisfied. If so,
924 set a 1-bit flag flag_2 as $\text{flag}_2 := 1$. Else, set $\text{flag}_2 := 0$
- 925 (f) Return 1 as the value of F if $\text{flag}_1 = \text{flag}_2 = 1$. Return 0 otherwise.
- 926 (g) Uncompute steps (a)-(e).
- 927 4. Run Grover's algorithm [28] on U_F to find the collision.

1.	$k_0[2, 7] = x_0[2, 7] \oplus P[2, 7]$ $w_2[0, 1, 2, 3] = \text{MC}(z_2[0, 1, 2, 3])$	$w_0[7] = k_1[7] \oplus x_1[7]$ $w_2[8, 9, 10, 11] = \text{MC}(z_2[8, 9, 10, 11])$
2.	$k_1[10] = k_0[2] \oplus \text{SB}(k_1[7])$	$w_0[8, 9] = \widetilde{k_1[8, 9]} \oplus x_1[8, 9]$
3.	$z_0[8, 9], w_0[10, 11] = \text{MC}(z_0[10, 11], w_0[8, 9])$ $k_1[11] = w_0[11] \oplus x_1[11]$	$k_0[8, 13] = P[8, 13] \oplus \text{SB}^{-1}(z_0[8, 9])$ $z_1[2] = \text{SB}(w_0[10] \oplus k_1[10])$
4.	$k_1[15] = k_0[7] \oplus k_1[11]$ $k_0[4] = k_1[12] \oplus k_1[8]$	$k_1[12] = k_0[8] \oplus \widetilde{k_2[0]}$ $k_2[5] = k_0[13] \oplus \widetilde{k_2[1]}$
5.	$z_1[0, 1], w_1[2, 3] = \text{MC}(z_1[2, 3], w_1[0, 1])$ $k_2[2, 3] = w_1[2, 3] \oplus x_2[2, 3]$	$x_1[0, 5] = \text{SB}^{-1}(z_1[0, 1])$
6.	$k_0[11] = k_2[3] \oplus k_1[15]$ $k_0[6] = \widetilde{k_1[14]} \oplus k_1[10]$ $k_0[10] = k_2[2] \oplus k_1[14]$	$k_0[5] = \widetilde{k_1[13]} \oplus k_1[9]$ $k_0[9] = k_2[1] \oplus k_1[13]$
7.	$k_2[4] = \widetilde{k_0[12]} \oplus k_2[0]$	
8.	$z_0[13], w_0[12, 13, 14] = \text{MC}(z_0[12, 14, 15], w_0[15])$	$k_0[1] = P[1] \oplus \text{SB}^{-1}(z_0[12])$
9.	$z_1[4, 7], w_1[6, 7] = \text{MC}(z_1[5, 6], w_1[4, 5])$	$k_2[6, 7] = w_1[6, 7] \oplus x_2[6, 7]$
10.	$k_0[14] = k_2[6] \oplus k_2[2]$ $k_1[6] = \text{SB}^{-1}(k_1[9] \oplus k_0[1])$	$k_0[15] = k_2[7] \oplus k_2[3]$
11.	$z_0[7], w_0[4, 5, 6] = \text{MC}(z_0[4, 5, 6], w_1[7])$ $k_1[4, 5] = w_0[4, 5] \oplus x_1[4, 5]$ $z_1[14] = \text{SB}(k_1[6] \oplus w_0[6])$	$k_0[3] = P[3] \oplus \text{SB}^{-1}(z_0[7])$ $k_0[3] \oplus \text{SB}(k_1[4]) \stackrel{?}{=} k_1[11]$
12.	$k_0[0] = k_1[8] \oplus \text{SB}(k_1[5]) \oplus \text{const}$ $w_0[0, 1, 2, 3] = \text{MC}(z_0[0, 1, 2, 3])$	$z_0[0] = \text{SB}(P[0] \oplus k_0[0])$ $k_1[0, 3] = w_0[0, 3] \oplus x_1[0, 3]$
13.	$k_2[8, 11] = k_1[0, 3] \oplus k_2[4, 7]$ $w_1[8, 12, 15] = k_2[8, 12, 15] \oplus x_2[8, 12, 15]$	$k_2[12, 15] = k_1[4, 7] \oplus k_2[8, 11]$
14.	$z_1[10], w_1[9, 10, 11] = \text{MC}(z_1[8, 9, 11], w_1[8])$ $k_1[1, 2] = w_1[1, 2] \oplus \text{SB}^{-1}(z_1[10, 13])$ $k_1[2] \oplus k_2[10] \stackrel{?}{=} k_2[6]$ $x_2[11] = w_1[11] \oplus k_2[11]$	$z_1[13], w_1[13, 14] = \text{MC}(z_1[12, 14, 15], w_1[12, 15]) ?$ $k_2[10, 13, 14] = w_1[10, 13, 14] \oplus x_2[10, 13, 14]$ $k_2[14] \oplus k_2[10] \stackrel{?}{=} k_1[6]$ $w_2[12, 13, 14, 15] = \text{MC}(z_2[12, 13, 14, 15])$
15.	$k_2[9] = k_1[1] \oplus k_2[5] \stackrel{?}{=} k_2[13] \oplus k_1[5]$ $w_2[4, 5, 6, 7] = \text{MC}(z_2[4, 5, 6, 7])$	$x_2[9] = w_1[9] \oplus k_2[9]$

Table 8: Equations in the guess-and-determine steps for 6-round AES-192. The blue bytes are guessed. The red equations are conflicts.

Quantum Complexity. Given a choice of bytes marked by 1 and a guess for the 7-byte $(k_0[12], k_1[8, 9, 13, 14], k_2[0, 1])$ and taking the uncomputation into account, the cost of U_F is about four 6-round AES-192. The probability of finding the collision is roughly $2^{-40-34} = 2^{-74}$. Therefore, the quantum time complexity is about

$$\frac{\pi}{4} \sqrt{2^{74}} \cdot 4 \approx 2^{38.7} \text{ 6-round AES-192.}$$

6 Key Collision Attacks on Reduced AES-256

In this section, we discuss the fixed-target-plaintext key collision on 6-round AES-256 in [53]. Then we give a practical key collision attack on 6-round AES-256 and quantum attacks on 7/8-round AES-256.

6.1 The Invalid Key Collision on 6-round AES-256 in [53]

In [53], Taiyama *et al.* gave a related-key differential characteristic for key collision attack on 6-round AES-256, which is listed in Fig. 19. For $k_1[12]$, the differences $\Delta k_1[12] = 0x02$ and $\Delta SB(k_1[12]) = 0x48$ are fixed. There is $DDT(0x02, 0x48) = 0$ for the Sbox of AES, but [53] regards that the probability of the active Sbox is 2^{-7} . It is not a valid instantiation of the related-key truncated differential and one can not make a correct attack with this differential.

It seems that a simple way to correct this differential is to modify $\Delta SB(k_1[12])$ to ensure $DDT(0x02, \Delta SB(k_1[12])) > 0$ and $DDT(\Delta SB(k_1[12]), 0x01) > 0$. However, even if $\Delta SB(k_1[12])$ is modified correctly, there is still another problem in this differential that makes the attack fail. We briefly recall the attack in [53], where the 0th and 1st rounds in the EN path is the inbound phase and the remaining parts including the KS are the outbound phase. The attack procedures are as follows.

1. Choose 2^{51} values of $x_0[0-15]$ and $y_0[0-15]$ that satisfy the differences in Δx_0 and Δy_0 . Deduce 2^{51} values of $k_0[0-15]$.
2. Choose 2^{11} values of $x_1[12-15]$ and $y_1[12-15]$ that satisfy the differences in $\Delta x_1[12-15]$ and $\Delta y_1[12-15]$. Deduce 2^{51+11} values of $\{k_1[12-15], k_2[0-15]\}$. Since the differences in $\Delta k_1[12-15]$, $\Delta k_2[13]$, $\Delta SB(k_1[12-15])$ and $\Delta SB(k_2[13])$ are fixed, there is a filter of 2^{-35} . Then $2^{51+11-35} = 2^{27}$ values will remain.
3. Choose 2^{22} values of $x_1[4-11]$ and $y_1[4-11]$ satisfying the differences in $\Delta x_1[4-11]$ and $\Delta y_1[4-11]$. Deduce 2^{27+22} values of $k_1[4-11]$.
4. Choose 2^{12} values of $x_1[0-3]$ and $y_1[0-3]$ satisfying the differences in $\Delta x_1[0-3]$ and $\Delta y_1[0-3]$. Deduce 2^{49+12} starting points. Since the probability of the remaining parts is 2^{-61} , one collision is expected.

The probability of the inbound phase is 2^{-118} . Since the probability of generating k_2 and k_3 in the KS is 2^{-35} , the probability of the outbound phase should be 2^{-96} . So the total probability is $2^{-118-94} = 2^{-214}$, not 2^{-179} in [53]. As above

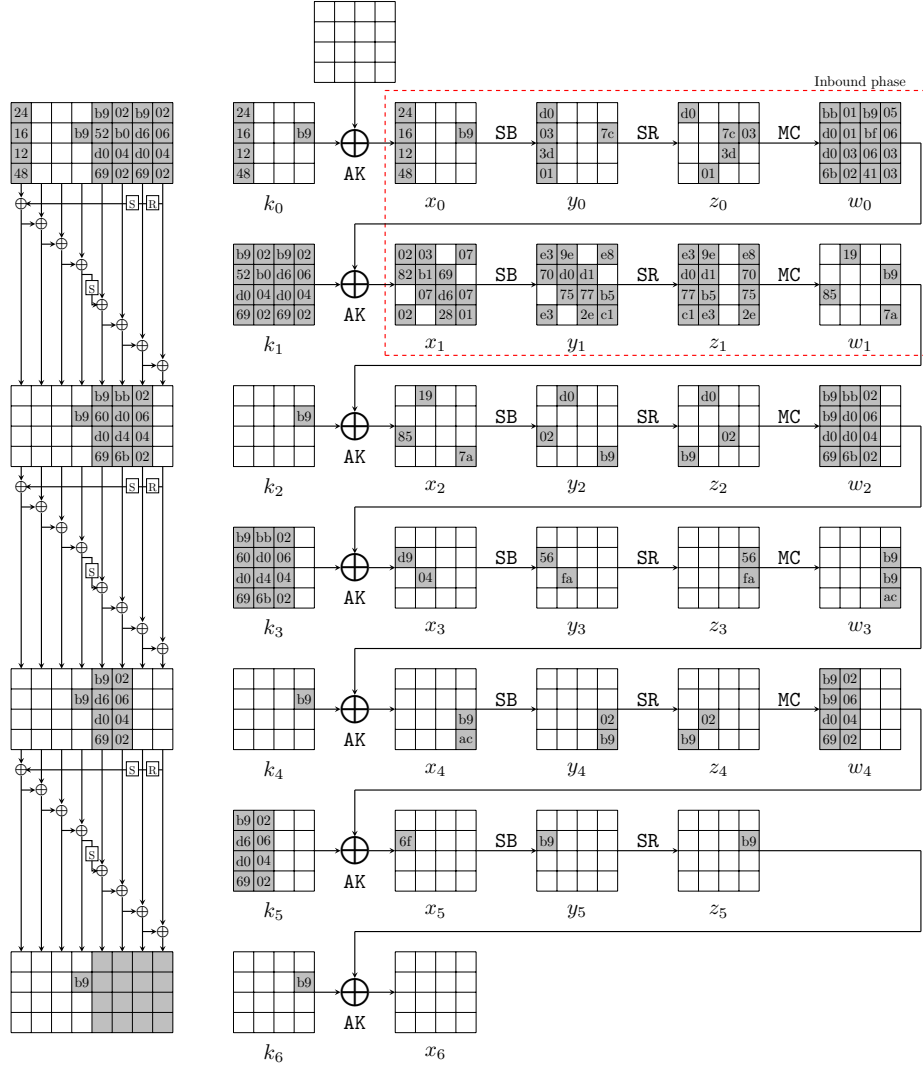


Fig. 19: The related-key differential characteristic on 6-round AES-256 in [53]

steps, the freedom seems enough to find one collision. But in fact, for some specific byte, the freedom is not enough. For $x_2[2]$, there is

$$\begin{aligned} x_2[2] &= w_1[2] \oplus k_2[2] \\ &= y_1[0] \oplus y_1[5] \oplus 02 \cdot y_1[10] \oplus 03 \cdot y_1[15] \oplus x_0[2] \oplus P[2] \oplus \text{SB}(k_1[15]). \end{aligned} \quad (9)$$

The values of $x_0[2]$ and $y_1[0, 5, 10, 15]$ are directly chosen in step 1 to 4, and the value of $k_1[15]$ is filtered in step 2 to satisfy the differential. We list the values of $x_0[2]$, $y_1[0, 5, 10, 15]$, $k_1[15]$ in Table 9, where there are 2^6 combinations in total. In fact, the value of $x_0[2]$ is fixed to one value in step 1. With 2^5 combinations of $x_0[2]$, $y_1[0, 5, 10, 15]$, $k_1[15]$, there are 2^5 possible values of $x_2[2]$ with fixed $P[2]$. The probability of the active Sbox for $x_2[2]$ is 2^{-7} . When $P = 0$ and $x_0[2]$ is fixed to 0x87 or 0x95, all the 2^5 values of $x_2[2]$ don't match the differences unfortunately. So in step 4, after the filter there is no collision found.

State	$x_0[2]$	$y_1[0]$	$y_1[5]$	$y_1[10]$	$y_1[15]$	$k_1[15]$
Values	{0x87, 0x95}	{0x10, 0xf3}	{0xc3, 0x13}	{0x59, 0x2e}	{0xcd, 0x0c}	{0x5c, 0x5e}

Table 9: The possible values of states in Equation 9

6.2 Practical Key Collision Attack on 6-round AES-256

We find a new related-key differential characteristic on 6-round AES-256 with a probability of 2^{-214} , which is shown in Fig. 20. Compared to the differential in Fig. 19 in [53], the two differentials follow the same related-key truncated differential, but are different instantiations. The inbound phase covers the first four rounds and has 28 active Sboxes with a probability of 2^{-193} , including 6 active Sboxes in the key schedule. The probability of the outbound phase is $2^{-p_{out}} = 2^{-21}$. The steps of the GD are listed below and in Fig. 21. The detailed equations are listed in Table 10.

Guess-and-determine procedures of the inbound phase.

1. Deduce the values of $x_0[0, 1, 2, 3, 13]$, $y_0[0, 1, 2, 3, 13]$, $x_1[0, 1, 3-6, 9-12, 14, 15]$, $y_1[0, 1, 3-6, 9-12, 14, 15]$, $x_2[2, 4, 15]$, $y_2[2, 4, 15]$, $x_3[1, 6]$ and $y_3[1, 6]$ with the fixed differences by accessing the DDT, which are all marked by 1. Similarly, deduce the values of $k_1[12, 13, 14, 15]$ and $k_2[13]$ (marked by 1) by accessing the DDT, according to the fixed $\Delta k_1[12, 13, 14, 15]$, $\Delta k_2[13]$, $\Delta \text{SB}(k_1[12, 13, 14, 15])$ and $\Delta \text{SB}(k_2[13])$.
 (a) According to the known values, we have

$$y_1[0] \oplus y_1[5] \oplus 02 \cdot y_1[10] \oplus 03 \cdot y_1[15] \oplus x_2[2] \oplus x_0[2] \oplus P[2] \oplus \text{SB}(k_1[15]) = 0, \quad (10)$$

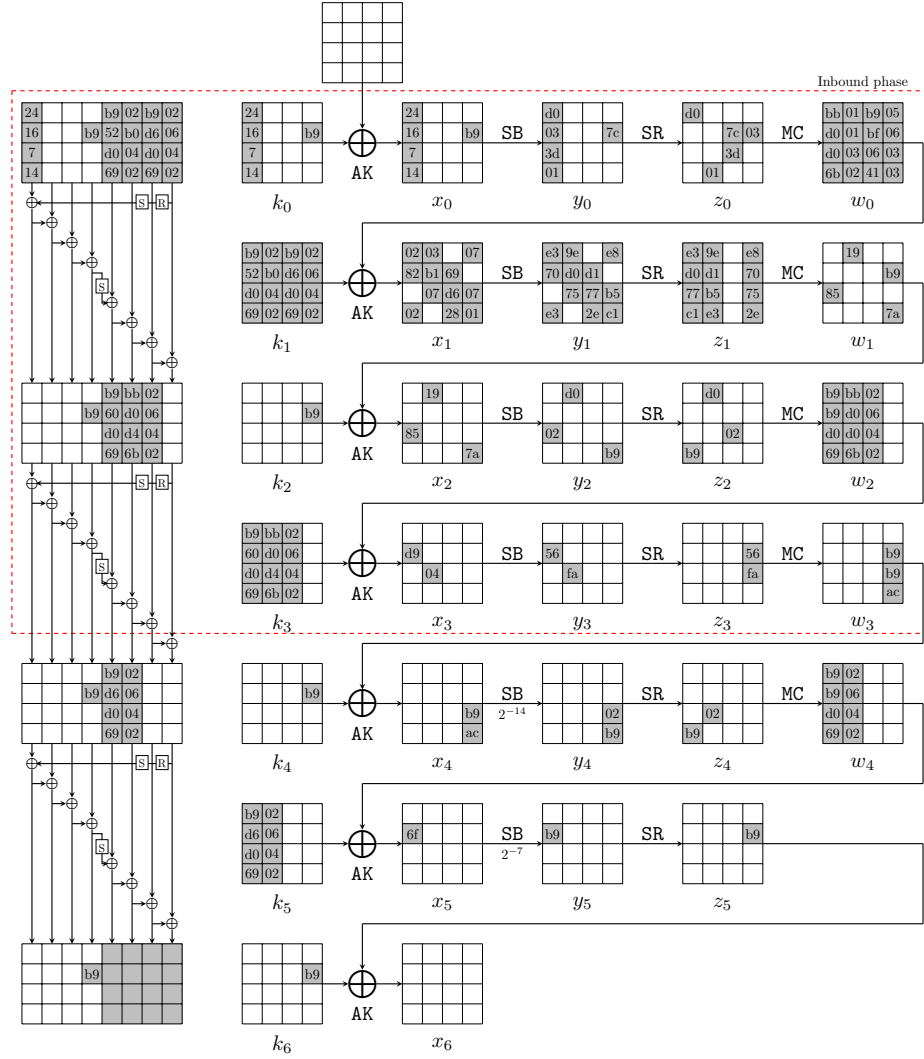


Fig. 20: The new related-key differential characteristic on 6-round AES-256

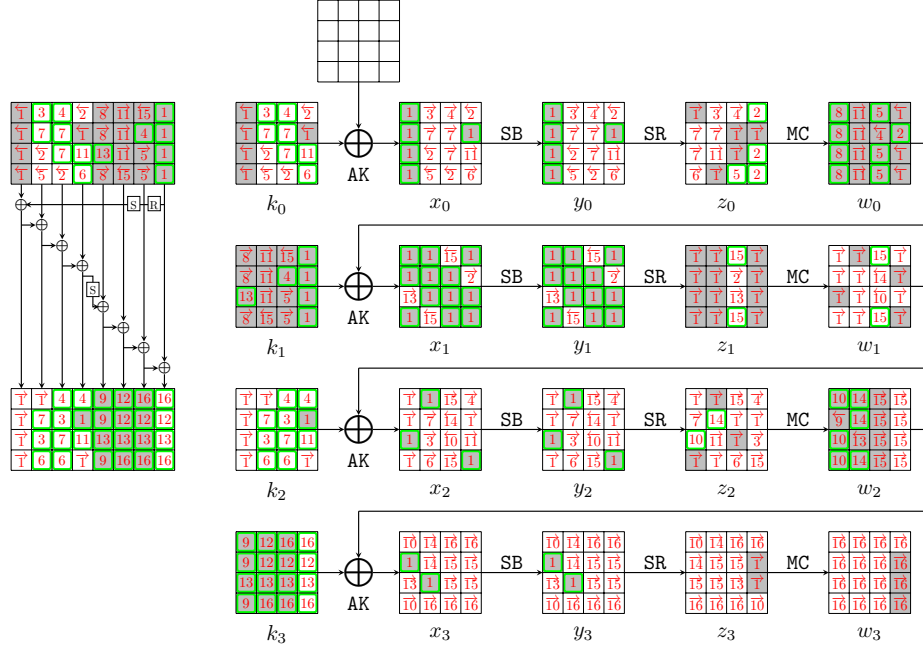


Fig. 21: Steps of the GD in the inbound phase for 6-round AES-256

which is a conflict of Type II. The bytes marked by red are known by accessing the DDT. We precompute the values of $y_1[0, 5, 10, 15]$, $x_2[2]$, $x_0[2]$ and $k_1[15]$ to satisfy Equation 10 and solve the conflict. Note that the same conflict also exists in the differential in [53], and they can not fulfill Equation 10 for $P = 0$ (see details in Supplementary Material 6.1).

- (b) In round 0, compute backward to get $k_0[0, 1, 2, 3, 13]$ (marked by $\overleftarrow{1}$). Compute forward to $z_0[0, 7, 9, 10, 13]$ (marked by $\overrightarrow{1}$).

- (c) In round 1, compute backward to $w_0[12, 14, 15]$ (marked by $\overleftarrow{1}$). Compute $\text{MC} \circ \text{SR}(y_1)$ and get columns 0, 1, 3 of z_1 and w_1 (marked by $\overrightarrow{1}$).

- (d) In round 2, compute $k_2[2, 4, 15]$ (marked by $\overleftarrow{1}$) from $w_1[2, 4, 15]$ and $x_2[2, 4, 15]$. According to the key relations, compute $k_2[0, 1, 2, 3]$ (marked by $\overrightarrow{1}$) from $k_0[0, 1, 2, 3]$ and $k_1[12, 13, 14, 15]$. As step 1(a), the two values of $k_2[2]$ computed are equal of probability 1 after solving the conflict. Then deduce $x_2[0, 1, 3, 13]$ and $z_2[0, 3, 4, 7, 9, 10, 13]$ (marked by $\overrightarrow{1}$).

- (e) In round 3, compute forward to $z_3[13, 14]$ (marked by $\overrightarrow{1}$).

2. For column 3 over the MC operation in round 0, compute $z_0[12, 14, 15]$ and $w_0[13]$ (marked by $\overrightarrow{2}$) from $z_0[13]$ and $w_0[12, 14, 15]$.

- (a) Compute backward to get $k_0[6, 11, 12]$ (marked by $\overleftarrow{2}$).

- (b) Compute forward to $x_1[13]$ as well as $z_1[9]$ (marked by $\overrightarrow{2}$).

3. According to the key relations, deduce the key values $k_0[4]$, $k_2[6, 9]$ (marked by $\overrightarrow{3}$). Compute forward to $z_0[4]$ and $z_2[14]$ (marked by $\overrightarrow{3}$).

- 1009 4. Guess $k_0[8]$ and $k_1[9]$ (marked by 4), and deduce $k_2[8, 12]$ (marked by 4)
 1010 according to the key relations.
 1011 (a) Compute forward to $z_0[8]$ (marked by 4) in round 0, and to $z_2[12]$
 1012 (marked by 4) in round 2.
 1013 (b) Compute backward to $w_0[9]$ (marked by 4) in round 1.
 1014 5. For column 2 over the MC operation in round 0, compute $w_0[8, 10, 11]$ and
 1015 $z_0[11]$ (marked by 5) from $z_1[8, 9, 10]$ and $w_1[9]$.
 1016 (a) Compute forward to $k_1[10, 11]$ (marked by 5).
 1017 (b) Compute backward to $k_0[7]$ (marked by 5) in round 0.
 1018 6. According to the key relations, compute $k_2[7, 11]$ and $k_0[15]$ (marked by 6),
 1019 and compute forward to get $z_0[3]$ and $z_2[11]$ (marked by 6).
 1020 7. Guess $k_0[5]$ and $k_0[10]$ (marked by 7), and deduce $k_2[5, 10]$ and $k_0[9]$ (marked
 1021 by 7) according to the key relations. Then compute forward to $z_0[1, 2, 5]$ and
 1022 $z_2[1]$ (marked by 7).
 1023 8. For column 0 over the MC operation in round 0, compute $w_0[0, 1, 2, 3]$ (marked
 1024 by 8) from $z_0[0, 1, 2, 3]$. Then deduce $k_1[0, 1, 3] = x_1[0, 1, 3] \oplus w_0[0, 1, 3]$
 1025 (marked by 8).
 1026 9. According to the key relations, we can deduce $k_3[0, 1, 3]$ (marked by 9).
 1027 Then compute backward to $w_2[1]$ (marked by 9).
 1028 10. For column 0 over the MC operation in round 2, compute $w_2[0, 2, 3]$ and $z_2[2]$
 1029 (marked by 10) from $z_2[0, 1, 3]$ and $w_2[1]$.
 1030 (a) Compute backward to $x_2[10]$ and $w_1[10]$ (marked by 10) in round 2.
 1031 (b) Compute forward to $x_3[0, 3]$ and $z_3[0, 15]$ (marked by 10) in round 3.
 1032 11. Guess $k_0[14]$ (marked by 11) and deduce $k_2[14]$ (marked by 11). Com-
 1033 pute forward to $z_0[6]$ and $z_2[6]$ (marked by 11), and deduce $w_0[4, 5, 6, 7] =$
 1034 $\text{MC}(z_0[4, 5, 6, 7])$ (marked by 11). Deduce $k_1[4, 5, 6] = x_1[4, 5, 6] \oplus w_0[4, 5, 6]$
 1035 (marked by 11).
 1036 12. According to the key relations, we deduce $k_3[4, 5, 9, 13]$ (marked by 12).
 1037 13. Guess $k_1[2]$ and deduce $k_3[2, 6, 10, 14]$ according to the key relations (marked
 1038 by 13).
 1039 (a) Compute forward to get $z_1[10]$ and $z_3[10]$ (marked by 13).
 1040 (b) Compute backward to get $w_2[6]$ (marked by 13).
 1041 14. For column 1 over the MC operation in round 2, compute $w_2[4, 5, 7]$ and $z_2[5]$
 1042 (marked by 14) from $z_2[4, 6, 7]$ and $w_2[6]$.
 1043 (a) Compute backward in round 2 to $w_1[9]$ (marked by 14).
 1044 (b) Compute forward in round 3 to $x_3[4, 5]$ and $z_3[4, 1]$ (marked by 14).
 1045 15. For column 2 over the MC operation in round 1, compute $z_1[8, 11]$ and
 1046 $w_1[8, 11]$ (marked by 15) from $z_1[9, 10]$ and $w_1[9, 10]$.
 1047 (a) Compute backward in round 1 to $x_1[7, 8]$ and deduce $k_1[7, 8]$ (marked by
 1048 15).
 1049 (b) Compute forward in round 2 to $x_2[8, 11]$ and $z_2[8, 15]$ (marked by 15).
 1050 Deduce columns 2 and 3 of w_2 and $z_3[2, 5, 6, 9]$ (marked by 15).
 1051 16. According to the key relations, compute $k_3[7, 8, 11, 12, 15]$ (marked by 16).
 1052 Compute $w_3 = \text{MC} \circ \text{SR} \circ \text{SB}(k_3 \oplus w_2)$. So we deduce all states of the starting
 1053 point.

1.	$k_0[0, 1, 2, 3, 13] = (x_0 \oplus P)[0, 1, 2, 3, 13]$	$w_1[0, 1, 2, 3] = \text{MC}(z_1[0, 1, 2, 3])$
	$w_1[4, 5, 6, 7] = \text{MC}(z_1[4, 5, 6, 7])$	$w_1[12, 13, 14, 15] = \text{MC}(z_1[12, 13, 14, 15])$
	$k_2[2, 4, 15] = x_2[2, 4, 15] \oplus w_1[2, 4, 15]$	$k_2[0] = k_0[0] \oplus \text{SB}(k_1[13]) \oplus \text{const}$
	$k_2[1, 2, 3] = k_0[1, 2, 3] \oplus \text{SB}(k_1[14, 15, 12])$	$k_2[2] = w_1[2] \oplus x_2[2] \stackrel{?}{=} k_0[2] \oplus \text{SB}(k_1[15])$
2.	$z_0[12, 14, 15], w_0[13] = \text{MC}^{-1}(z_0[13], w_0[12, 14, 15])$	$k_0[6] = P[6] \oplus \text{SB}^{-1}(z_0[14])$
	$k_0[11] = P[11] \oplus \text{SB}^{-1}(z_0[15])$	$k_0[12] = P[12] \oplus \text{SB}^{-1}(z_0[12])$
3.	$k_0[4] = k_2[4] \oplus k_2[0]$	$k_2[6] = k_0[6] \oplus k_2[2]$
	$k_2[9] = k_0[13] \oplus k_2[13]$	
4.	$k_2[8] = \underbrace{k_0[8]} \oplus k_2[4]$	$k_2[12] = k_0[12] \oplus k_2[8]$
	$w_0[9] = \underbrace{k_1[9]} \oplus x_1[9]$	
5.	$w_0[8, 10, 11], z_0[11] = \text{MC}(z_0[8, 9, 10], w_0[9])$	$k_1[10, 11] = w_0[10, 11] \oplus x_1[10, 11]$
	$k_0[7] = \text{SB}^{-1}(z_0[11]) \oplus P[7]$	
6.	$k_2[7] = k_0[7] \oplus k_2[3]$	$k_2[11] = k_0[11] \oplus k_2[7]$
	$k_0[15] = k_2[15] \oplus k_2[11]$	
7.	$k_2[5] = \underbrace{k_0[5]} \oplus k_2[1]$	$k_0[9] = k_2[5] \oplus k_2[9]$
	$k_2[10] = \underbrace{k_0[10]} \oplus k_2[6]$	
8.	$w_0[0, 1, 2, 3] = \text{MC}(z_0[0, 1, 2, 3])$	$k_1[0, 1, 3] = x_1[0, 1, 3] \oplus w_0[0, 1, 3]$
9.	$k_3[0, 1, 3] = k_1[0, 1, 3] \oplus \text{SB}(k_2[12, 13, 15])$	
10.	$w_2[0, 2, 3], z_2[2] = \text{MC}(z_2[0, 1, 3], w_2[1])$	
11.	$z_0[6] = \text{SB}(\underbrace{k_0[14]}) \oplus x_0[14]$	$k_2[14] = \underbrace{k_0[14]} \oplus k_2[10]$
	$w_0[4, 5, 6, 7] = \text{MC}(z_0[4, 5, 6, 7])$	$k_1[4, 5, 6] = x_1[4, 5, 6] \oplus w_0[4, 5, 6]$
12.	$k_3[4] = k_1[4] \oplus k_3[0]$	$k_3[5] = k_1[5] \oplus k_3[1]$
	$k_3[9] = k_1[9] \oplus k_3[5]$	$k_3[13] = k_1[13] \oplus k_3[9]$
13.	$k_3[2] = \underbrace{k_1[2]} \oplus \text{SB}(k_2[14])$	$k_3[6] = k_1[6] \oplus k_3[2]$
	$k_3[10] = k_1[10] \oplus k_3[6]$	$k_3[14] = k_1[14] \oplus k_3[10]$
14.	$w_2[4, 5, 7], z_2[5] = \text{MC}(z_2[4, 6, 7], w_2[6])$	
15.	$z_1[8, 11], w_1[8, 11] = \text{MC}(z_1[9, 10], w_1[9, 10])$	$k_1[7, 8] = \text{SB}^{-1}(z_1[11, 8]) \oplus w_0[7, 8]$
	$z_2[8, 15] = \text{SB}(w_1[8, 11] \oplus k_2[8, 11])$	$w_2[8, 9, 10, 11] = \text{MC}(z_2[8, 9, 10, 11])$
	$w_2[12, 13, 14, 15] = \text{MC}(z_2[12, 13, 14, 15])$	
16.	$k_3[7] = k_1[7] \oplus k_3[3]$	$k_3[11] = k_1[11] \oplus k_3[7]$
	$k_3[15] = k_1[15] \oplus k_3[11]$	$k_3[8] = k_1[8] \oplus k_3[4]$
	$k_3[12] = k_1[12] \oplus k_3[8]$	$w_3 = \text{MC} \circ \text{SR} \circ \text{SB}(k_3 \oplus w_2)$

Table 10: Equations in the guess-and-determine steps for 6-round AES-256. The blue bytes are guessed. The red equation is the conflict.

1054 Degree of freedom and complexity.

- 1055 – There are total 28 active Sboxes in the 4-round inbound phase, including
1056 $s_1 = 25$ active Sboxes with probability 2^{-7} and $s_2 = 3$ active Sboxes with
1057 probability 2^{-6} . There is $c_{in} = c_2 = 1$ conflict as Equation 10, and we fix the
1058 7-byte values of $y_1[0, 5, 10, 15]$, $x_2[2]$, $x_0[2]$ and $k_1[15]$ to satisfy Equation 10.
1059 Then, by accessing the DDT for the other 21 active Sboxes, we expect at least
1060 $2^{21}/2 = 2^{20}$ combinations for the 21 active Sboxes, *i.e.*, there are at least
1061 2^{20} choices for the bytes marked by [1] in Fig. 21.
1062 – Given one out of 2^{20} choices marked by [1], six bytes $k_0[5, 8, 10, 14]$ and
1063 $k_1[2, 9]$ (marked by a wavy line) are guessed in step 4,7,11,13. Therefore,

1064 there expect $2^{20+48} = 2^{68}$ states satisfying the inbound differential in total,
 1065 which can act as the starting points for the outbound phase.
 1066 – Since the probability of the outbound phase is $2^{-p_{out}} = 2^{-21}$, we have enough
 1067 degrees of freedom to satisfy the outbound phase. The overall time complex-
 1068 ity is $\mathcal{T} = 2^{21}$ and the memory complexity is negligible. We have practically
 1069 implemented the attack and could find one key collision in several minutes.
 1070 Some key pairs (K_1, K_2) are listed in Table 3 such that $\text{AES-256}_{K_1}(0) =$
 1071 $\text{AES-256}_{K_2}(0)$, where AES-256 is a 6-round one.

1072 6.3 Quantum Key Collision Attack on 7-round AES-256

1073 We give a new quantum key collision attack on 7-round AES-256. The differential
 1074 characteristic with a probability of 2^{-228} is shown in Fig. 22. The inbound phase
 1075 covers the first four rounds of the EN and KS path, which has 30 active Sboxes
 1076 with a probability of 2^{-198} . The outbound phase has 5 active Sboxes, including
 1077 1 active Sboxes in the key schedule, with a probability of $2^{-p_{out}} = 2^{-30}$. In the
 1078 GD procedure of inbound phase, there are $c_{in} = 5$ conflicts, where $c_1 = c_2 = 0$
 1079 and $c_3 = 5$. The guess-and-determine steps of the GD are listed as follows, as in
 1080 Fig. 23. The detailed equations are listed in Table 11.

1081 Guess-and-determine procedures of the inbound phase.

- 1082 1. Deduce the values of $x_0[3, 11]$, $y_0[3, 11]$, $x_1[4 - 7, 12 - 15]$, $y_1[4 - 7, 12 -$
 1083 $15]$, $x_2[0 - 15]$, $y_2[0 - 15]$, $x_3[0, 5, 10, 15]$ and $y_3[0, 5, 10, 15]$ with the fixed
 1084 differences by accessing the DDT, which are all marked by 1 in Fig. 23.
 1085 (a) In round 0, compute backward to get $k_0[3, 11]$ (marked by 1), and com-
 1086 pute forward to get $z_0[7, 15]$ (marked by 1).
 1087 (b) In round 1, compute forward to get $z_1[1, 3, 4, 6, 9, 11, 12, 14]$ (marked by
 1088 1).
 1089 (c) In round 2, compute forward to get the whole state $w_2 = \text{MC} \circ \text{SR}(y_2)$
 1090 (marked by 1).
 1091 (d) In round 3, compute backward to deduce $k_3[0, 5, 10, 15] = x_3[0, 5, 10, 15] \oplus$
 1092 $w_2[0, 5, 10, 15]$ (marked by 1). Compute forward to get the $w_3[0, 1, 2, 3]$
 1093 (marked by 1).
 1094 2. Guess $k_0[7]$, $k_1[12]$ and $k_2[0, 4, 8]$ (marked by 2), then deduce the $k_0[4, 8]$
 1095 and $k_2[3, 7, 11]$ (marked by 2) according to the key relations.
 1096 (a) In round 0, compute forward to get $z_0[4, 8, 11]$ (marked by 2).
 1097 (b) In round 1, compute backward to get $w_0[12]$ (marked by 2).
 1098 (c) In round 2, compute backward to get $w_1[0, 3, 4, 7, 8, 11]$ (marked by 2).
 1099 3. For columns 0, 1, 2 over the MC operation in round 1, compute $w_1[1, 2, 5, 6, 9, 10]$
 1100 and $z_1[0, 2, 5, 7, 8, 10]$ (marked by 3) from $z_1[1, 3, 4, 6, 9, 11]$ and $w_1[0, 3, 4, 7, 8, 11]$.
 1101 (a) Compute backward to get $x_1[0, 2, 3, 8, 9, 10]$ (marked by 3).
 1102 (b) Compute forward to get $k_2[1, 2, 5, 6, 9, 10]$ (marked by 3).

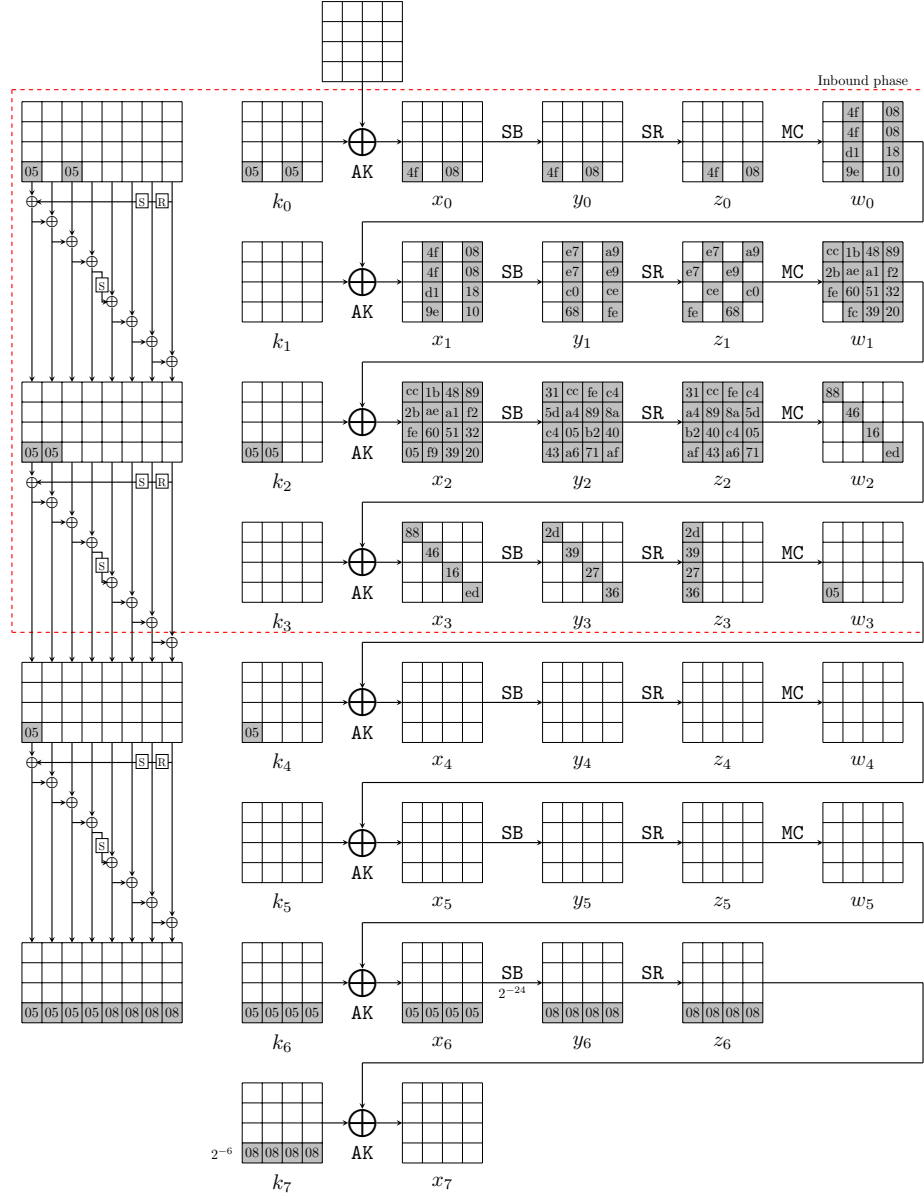


Fig. 22: The related-key differential characteristic on 7-round AES-256

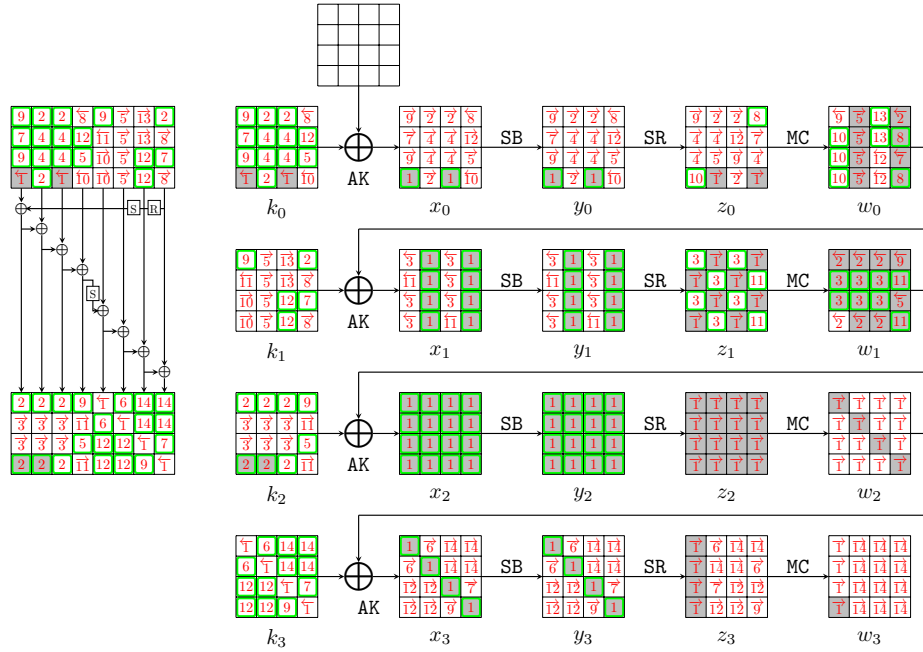


Fig. 23: Steps of the GD in the inbound phase for 7-round AES-256

4. According to the key relations, deduce $k_0[5, 6, 9, 10]$ (marked by 4). Compute forward then get $z_0[1, 2, 5, 14]$ (marked by 4).
5. Guess $k_0[14]$ (marked by 5) and deduce $k_2[14]$ (marked by 5).
 - (a) Compute forward to get $z_0[6]$ (marked by 5). Then compute $w_0[4, 5, 6, 7]$ (marked by 5) from $z_0[4, 5, 6, 7]$, and deduce $k_1[4, 5, 6, 7]$ (marked by 5).
 - (b) Compute backward to get $w_1[14]$ (marked by 5).
6. According to the key relations, deduce $k_3[1, 4]$ (marked by 6). Compute forward to get $x_3[1, 4]$ and $z_3[4, 13]$ (marked by 6).
7. Guess $k_0[1]$ (marked by 7) and deduce $k_1[14]$ and $k_3[14]$ with the key relations (marked by 7).
 - (a) In round 0, compute forward get $x_0[1]$ and $z_0[13]$ (marked by 7).
 - (b) In round 1, compute backward get $w_0[14]$ (marked by 7).
 - (c) In round 3, compute forward get $x_3[14]$ and $z_3[6]$ (marked by 7).
8. For column 3 over the MC operation in round 0, compute $w_0[13, 15]$ and $z_0[12]$ (marked by 8) from $z_0[13, 14, 15]$ and $w_0[12, 14]$. Since five values are known in the inputs/outputs over the MC operation, there is a conflict of Type III of 2^{-8} probability.
 - (a) Compute forward to $k_1[13, 15]$ (marked by 8).
 - (b) Compute backward to $k_0[12]$ (marked by 8).

- 1122 9. According to the key relations, deduce $k_0[0, 2]$, $k_1[0]$, $k_2[12]$ and $k_3[11]$ (marked
1123 by 9).
- 1124 (a) In round 0, compute forward to $x_0[0, 2]$ and $z_0[0, 10]$ (marked by $\overrightarrow{9}$).
1125 (b) In round 1, compute backward to $w_0[0]$ (marked by $\overleftarrow{9}$).
1126 (c) In round 2, compute backward to $w_1[12]$ (marked by $\overleftarrow{9}$).
1127 (d) In round 3, compute forward to $x_3[11]$ and $z_3[15]$ (marked by $\overrightarrow{9}$).
- 1128 10. For column 0 over the MC operation in round 0, compute $w_0[1, 2, 3]$ and $z_0[3]$
1129 (marked by 10) from $z_0[0, 1, 2]$ and $w_0[0]$.
1130 (a) Compute forward to $k_1[2, 3]$ (marked by $\overrightarrow{10}$).
1131 (b) Compute backward to $k_0[15]$ (marked by $\overleftarrow{10}$).
- 1132 11. For column 3 over the MC operation in round 1, compute $w_1[13, 15]$ and
1133 $z_1[13, 15]$ (marked by 11) from $z_1[12, 14]$ and $w_1[12, 14]$.
1134 (a) Compute backward to $x_1[1, 11]$ and $k_1[1]$ (marked by $\overleftarrow{11}$).
1135 (b) Compute forward to $k_2[13, 15]$ (marked by $\overrightarrow{11}$).
1136 (c) According to the key relations, we have $k_2[15] = k_0[15](\overleftarrow{10}) \oplus k_2[11](2)$
1137 and $\text{SB}(k_2[13]) \oplus k_1[1] = k_3[1](6)$, which are two conflicts of Type III
1138 with a total probability of 2^{-16} .
- 1139 12. According to the key relations, deduce $k_0[13]$, $k_1[10, 11]$, $k_3[2, 3, 6, 7]$ (marked
1140 by 12).
- 1141 (a) In round 0, compute forward to $z_0[9]$ (marked by $\overrightarrow{12}$).
1142 (b) In round 1, compute backward to $w_0[10, 11]$ (marked by $\overleftarrow{12}$).
1143 (c) In round 3, compute forward to $z_3[7, 10, 11, 14]$ (marked by $\overrightarrow{12}$).
- 1144 13. For column 2 over the MC operation in round 0, compute $w_0[8, 9]$ (marked
1145 by 13) from $z_0[8, 9, 10, 11]$ and $w_0[10, 11]$. Since six values are known in the
1146 inputs/outputs over the MC operation, there are two conflicts of Type III
1147 with a total probability of 2^{-16} . Compute forward to $k_1[8, 9]$ (marked by
1148 $\overrightarrow{13}$).
- 1149 14. According to the key relations, deduce $k_3[8, 9, 12, 13]$ (marked by 14). Com-
1150 pute forward to $z_3[5, 8, 9, 12]$ (marked by $\overrightarrow{14}$) and deduce columns 1,2,3 of
1151 $w_3 = \text{MC}(z_3)$ (marked by $\overrightarrow{14}$). So we deduce all states of the starting point.

1152 Degree of freedom and complexity.

- 1153 – In step 1, we deduce the values for active bytes from the input/output dif-
1154 ferences in the inbound phase. There are 30 active Sboxes, including $s_1 = 18$
1155 Sboxes with probability 2^{-7} and $s_2 = 12$ Sboxes with probability 2^{-6} . There-
1156 fore, there are $2^{18+24}/2 = 2^{41}$ combinations for the 30 active bytes, *i.e.*, there
1157 are 2^{41} choices for the bytes marked by 1 in Fig. 23.
- 1158 – Given one out of 2^{41} choices marked by 1, seven bytes $k_0[1, 7, 14]$, $k_1[12]$, $k_2[0, 4, 8]$
1159 (marked by a wavy line) are guessed in step 2, 5, 7. In step 8, 11, 13, there are
1160 $c_3 = 5$ conflicts with a total probability of 2^{-40} marked by underline. There-
1161 fore, there expect $2^{41+56-40} = 2^{57}$ starting points satisfying the inbound
1162 differential.

1.	$k_0[3, 11] = (x_0 \oplus P)[3, 11]$ $k_3[0, 5, 10, 15] = (x_3 \oplus w_2)[0, 5, 10, 15]$	$w_2 = \text{MC} \circ \text{SR}(y_2)$ $w_3[0, 1, 2, 3] = \text{MC}(y_3[0, 5, 10, 15])$
2.	$k_2[3] = k_0[3] \oplus \text{SB}(\textcolor{blue}{k_1[12]})$ $k_2[11] = k_0[11] \oplus k_2[7]$ $k_0[8] = \textcolor{blue}{k_2[8]} \oplus \textcolor{blue}{k_2[4]}$ $w_1[3, 7, 11] = x_2[3, 7, 11] \oplus k_2[3, 7, 11]$	$k_2[7] = \textcolor{blue}{k_0[7]} \oplus k_2[3]$ $k_0[4] = \textcolor{blue}{k_2[4]} \oplus \textcolor{blue}{k_2[0]}$ $w_1[0, 4, 8] = x_2[0, 4, 8] \oplus \textcolor{blue}{k_2[0, 4, 8]}$
3.	$w_1[1, 2], z_1[0, 2] = \text{MC}(z_1[1, 3], w_1[0, 3])$ $w_1[5, 6], z_1[5, 7] = \text{MC}(z_1[4, 6], w_1[4, 7])$ $w_1[9, 10], z_1[8, 10] = \text{MC}(z_1[9, 11], w_1[8, 11])$	$k_2[1, 2] = x_2[1, 2] \oplus w_1[1, 2]$ $k_2[5, 6] = x_2[5, 6] \oplus w_1[5, 6]$ $k_2[9, 10] = x_2[9, 10] \oplus w_1[9, 10]$
4.	$k_0[5] = k_2[5] \oplus k_2[1]$ $k_0[9] = k_2[9] \oplus k_2[5]$	$k_0[6] = k_2[6] \oplus k_2[2]$ $k_0[10] = k_2[10] \oplus k_2[6]$
5.	$k_2[14] = \textcolor{blue}{k_0[14]} \oplus k_2[10]$ $w_0[4, 5, 6, 7] = \text{MC}(z_0[4, 5, 6, 7])$	$z_0[6] = \text{SB}(\textcolor{blue}{k_0[14]} \oplus P[14])$ $k_1[4, 5, 6, 7] = x_1[4, 5, 6, 7] \oplus w_0[4, 5, 6, 7]$
6.	$k_3[1] = k_3[5] \oplus k_1[5]$	$k_3[4] = k_1[4] \oplus k_3[0]$
7.	$k_1[14] = \text{SB}^{-1}(k_2[1] \oplus \textcolor{blue}{k_0[1]})$ $z_0[13] = \text{SB}(\textcolor{blue}{k_0[1]} \oplus P[1])$	$k_3[14] = k_1[14] \oplus k_3[10]$
8.	$w_0[13, 15], z_0[12] = \textcolor{red}{\text{MC}(z_0[13, 14, 15], w_0[12, 14]) ?}$ $k_0[12] = P[12] \oplus \text{SB}^{-1}(z_0[12])$	$k_1[13, 15] = w_0[13, 15] \oplus x_1[13, 15]$
9.	$k_0[0] = k_2[0] \oplus \text{SB}(k_1[13]) \oplus \text{const}$ $k_2[12] = k_0[12] \oplus k_2[8]$ $k_3[11] = k_3[15] \oplus k_1[15]$	$k_0[2] = k_2[2] \oplus \text{SB}(k_1[15])$ $k_1[0] = k_3[0] \oplus \text{SB}(k_2[12])$
10.	$w_0[1, 2, 3], z_0[3] = \text{MC}(z_0[0, 1, 2], w_0[0])$ $k_0[15] = P[15] \oplus \text{SB}^{-1}(z_0[3])$	$k_1[2, 3] = w_0[2, 3] \oplus x_1[2, 3]$
11.	$w_1[13, 15], z_1[13, 15] = \text{MC}(z_1[12, 14], w_1[12, 14])$ $k_2[13, 15] = w_1[13, 15] \oplus x_2[13, 15]$ $\textcolor{red}{\text{SB}(k_2[13]) \oplus k_1[1] \stackrel{?}{=} k_3[1]}$	$k_1[1] = w_0[1] \oplus \text{SB}^{-1}(z_1[13])$ $\textcolor{red}{k_2[15] \stackrel{?}{=} k_0[15] \oplus k_2[11]}$
12.	$k_0[13] = k_2[13] \oplus k_2[9]$ $k_3[6, 7] = k_1[6, 7] \oplus k_3[2, 3]$	$k_3[2, 3] = k_1[2, 3] \oplus \text{SB}(k_2[14, 15])$ $k_1[10, 11] = k_3[6, 7] \oplus k_3[10, 11]$
13.	$w_0[8, 9] = \textcolor{red}{\text{MC}(z_0[8, 9, 10, 11], w_0[10, 11]) ?}$	$k_1[8, 9] = w_0[8, 9] \oplus x_1[8, 9]$
14.	$k_3[8, 9] = k_3[4, 5] \oplus k_1[8, 9]$	$k_3[12, 13] = k_3[8, 9] \oplus k_1[12, 13]$

Table 11: Equations in the guess-and-determine steps for 7-round AES-256. The blue bytes are guessed. The red equations are conflicts.

1163 – The time of the GD to find one starting point is about $\mathcal{T}_{\text{GD}} = 2^{40}$. Since the
 1164 probability of the outbound phase is $2^{-p_{\text{out}}} = 2^{-30}$, we have to collect 2^{30}
 1165 starting points to expect one collision and the degree of freedom is enough.
 1166 The classical time complexity of the full key collision attack is about $\mathcal{T} =$
 1167 $2^{40+30} = 2^{70}$ and the time complexity is larger than the birthday bound 2^{64} .

1168 **Quantum attack on 7-round AES-256.** Although a classical attack is invalid,
 1169 we can give a valid quantum one. We select 2^{14} choices of bytes marked by 1
 1170 and traverse 2^{56} possible values of $k_0[1, 7, 14], k_1[12], k_2[0, 4, 8]$.

1171 1. Deduce the pairs (m_i^0, m_i^1) ($i = 0, 1, \dots, 29$) for 30 active Sboxes by accessing
 1172 the DDT, and store them in a qRAM L , whose size is about 60 bytes.

1173 2. Given $|l_0, l_1, \dots, l_{13}\rangle$ and $l_i \in \{0, 1\}$, O_L is a quantum oracle that computes

$$O_L(|l_0, l_1, \dots, l_{13}\rangle |0\rangle) = |l_0, l_1, \dots, l_{13}\rangle |m_0^{l_0}, m_1^{l_1}, \dots, m_{13}^{l_{13}}, m_{14}^0, \dots, m_{29}^0\rangle \quad (11)$$

1174 3. Define $F : \mathbb{F}_2^{14+56} \mapsto \mathbb{F}_2$ and its quantum oracle,

$$U_F : |l_0, \dots, l_{13}, k_0[1, 7, 14], k_1[12], k_2[0, 4, 8]\rangle |y\rangle \mapsto y \oplus F(l_0, \dots, l_{13}, k_0[1, 7, 14], k_1[12], k_2[0, 4, 8]), \quad (12)$$

1175 Implementation of U_F :

- 1176 (a) Access O_L to get $|m_0^{l_0}, m_1^{l_1}, \dots, m_{13}^{l_{13}}, m_{14}^0, \dots, m_{29}^0\rangle$.
- 1177 (b) Fix the 30 bytes marked by 1 as $(m_0^{l_0}, m_1^{l_1}, \dots, m_{13}^{l_{13}}, m_{14}^0, \dots, m_{29}^0)$.
- 1178 (c) Run Step 1-14 (or Table 11) with 7-byte $(k_0[1, 7, 14], k_1[12], k_2[0, 4, 8])$.
- 1179 (d) Check if the 5 conflicts in Table 11 are satisfied with a probability of
- 1180 2^{-40} . If so, set a 1-bit flag \mathbf{flag}_1 as $\mathbf{flag}_1 := 1$. Else, set $\mathbf{flag}_1 := 0$.
- 1181 (e) Check if the outbound phase is satisfied with a probability of 2^{-30} . If so,
- 1182 set a 1-bit flag \mathbf{flag}_2 as $\mathbf{flag}_2 := 1$. Else, set $\mathbf{flag}_2 := 0$.
- 1183 (f) Return 1 as the value of F if $\mathbf{flag}_1 = \mathbf{flag}_2 = 1$. Return 0 otherwise.
- 1184 (g) Uncompute steps (a)-(e).
- 1185 4. Run Grover's algorithm [28] on U_F to find the collision.

Quantum Complexity. Given a choice of bytes marked by 1 and a guess for the 7-byte $(k_0[1, 7, 14], k_1[12], k_2[0, 4, 8])$ and taking the uncomputation into account, the cost of U_F is about four 7-round AES-256. The probability of finding the collision is roughly $2^{-40-30} = 2^{-70}$. Therefore, the quantum time complexity is about

$$\frac{\pi}{4} \sqrt{2^{70}} \cdot 4 \approx 2^{36.7} \text{ 7-round AES-256.}$$

1186 6.4 Quantum Key Collision Attack on 8-round AES-256

1187 We give a new quantum key collision attack on 8-round AES-256. The differential
 1188 characteristic with a probability of 2^{-249} is shown in Fig. 24. The inbound phase
 1189 covers the first four rounds of the EN and KS path, which has 22 active Sboxes
 1190 with a probability of 2^{-152} . The outbound phase has 14 active Sboxes, including
 1191 4 active Sboxes in the key schedule, with a probability of $2^{-p_{out}} = 2^{-97}$. In the
 1192 GD procedure of inbound phase, there is no conflict, where $c_{in} = 0$. The guess-
 1193 and-determine steps of the GD are listed as follows, as in Fig. 25. The detailed
 1194 equations are listed in Table 12.

1195 Guess-and-determine procedures of the inbound phase.

- 1196 1. Deduce the values of $x_0[1-7, 9-15]$, $y_0[1-7, 9-15]$, $x_1[5, 8, 10, 15]$,
 1197 $y_1[5, 8, 10, 15]$, $x_2[0, 4]$, $y_2[0, 4]$, $x_3[0, 4]$ and $y_3[0, 4]$ with the fixed differences
 1198 by accessing the DDT, which are all marked by 1 in Fig. 25.
- 1199 (a) In round 0, compute backward to get $k_0[1-7, 9-15]$ (marked by ←1),
 1200 and compute forward to get $z_0[1-7, 9-15]$ and $w_0[4-7, 12-15]$ (marked
 1201 by →1)

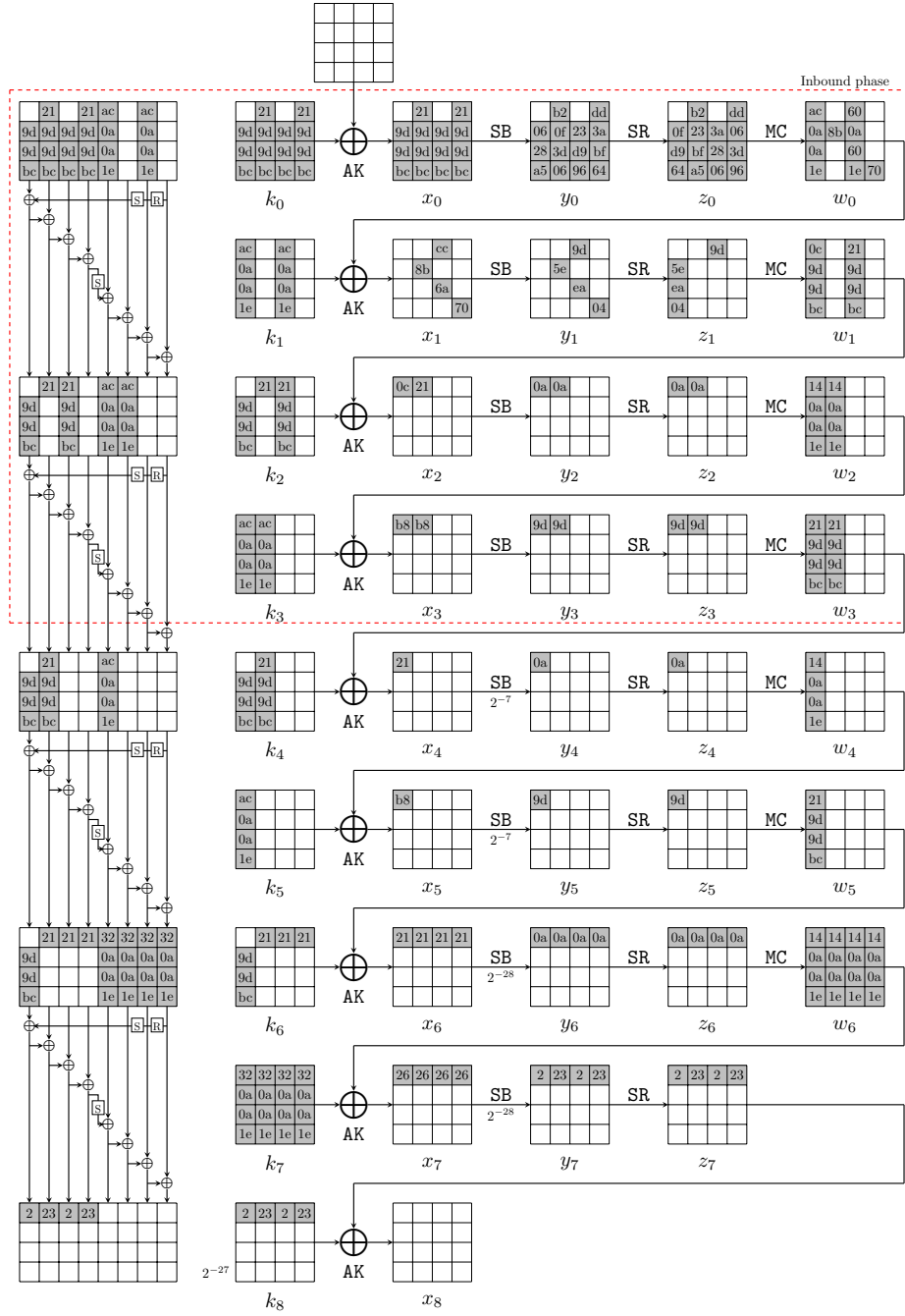


Fig. 24: The related-key differential characteristic on 8-round AES-256

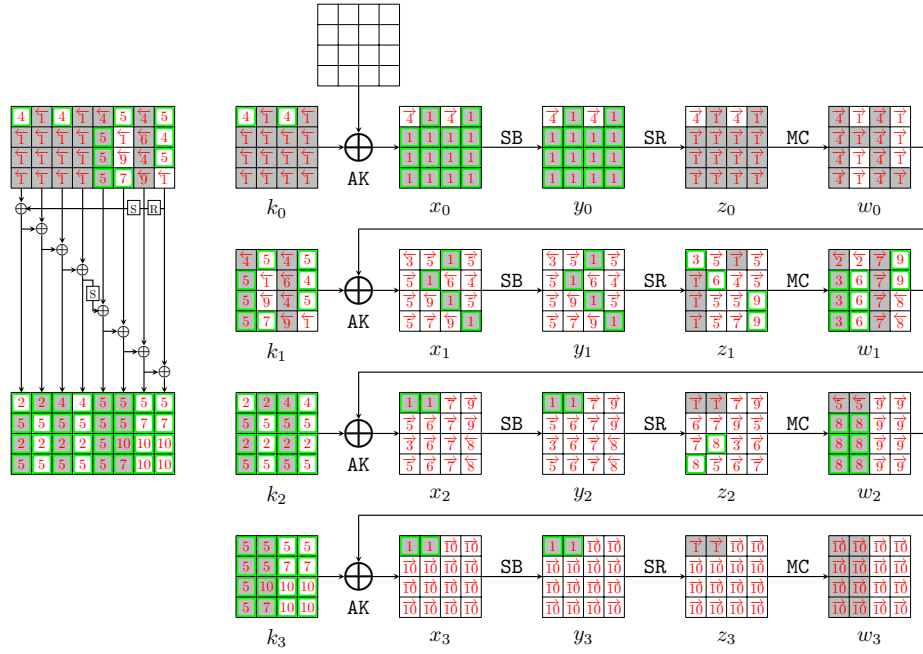


Fig. 25: Steps of the GD in the inbound phase for 8-round AES-256

- 1202 (b) In round 1, compute backward to get $k_1[5, 15]$ (marked by $\overleftarrow{1}$), and com-
 1203 pute forward to get $z_1[1 - 3, 8]$ (marked by $\overrightarrow{1}$).
- 1204 (c) In round 2, compute forward to get $z_2[0, 4]$ (marked by $\overrightarrow{1}$).
- 1205 (d) In round 3, compute forward to get $z_3[0, 4]$ (marked by $\overrightarrow{1}$).
- 1206 2. Guess $k_2[0]$ (marked by $\overrightarrow{2}$), then deduce the $k_2[2, 4, 6, 10, 14]$ (marked by $\overrightarrow{2}$)
 1207 according to the key relations. Compute backward to get $w_1[0, 4]$ (marked
 1208 by $\overleftarrow{2}$).
- 1209 3. For column 0 over the MC operation in round 1, compute $w_1[1, 2, 3]$ and $z_1[0]$
 1210 (marked by $\overrightarrow{3}$) from $z_1[1, 2, 3]$ and $w_1[0]$. Compute backward to get $x_1[0]$
 1211 (marked by $\overleftarrow{3}$) and compute forward to get $x_2[2]$ and $z_2[10]$ (marked by $\overrightarrow{3}$).
- 1212 4. Guess $k_0[0, 8]$ (marked by $\overrightarrow{4}$) and deduce $k_1[13]$ and $k_2[8, 12]$ (marked by
 1213 $\overrightarrow{4}$).
- 1214 (a) In round 0, compute forward to $z_0[0, 8]$ and get $w_0[0 - 3, 8 - 11]$ (marked
 1215 by $\overrightarrow{4}$).
- 1216 (b) In round 1, compute backward to $k_1[0, 8, 10]$ (marked by $\overleftarrow{4}$) and compute
 1217 forward to $z_1[9]$ (marked by $\overrightarrow{4}$).
- 1218 5. Guess $k_1[1, 2, 3, 4, 12, 14]$ (marked by $\overrightarrow{5}$) and deduce $k_2[1, 3, 5, 7, 9, 11, 13, 15]$
 1219 and $k_3[0, 1, 2, 3, 4, 5, 8, 12]$ (marked by $\overrightarrow{5}$). In round 1 and round 2, compute
 1220 forward to get $z_1[4, 6, 7, 10, 12, 13]$, $z_2[7, 13]$ (marked by $\overrightarrow{5}$). Compute back-
 1221 ward to get $w_2[0, 4]$ (marked by $\overleftarrow{5}$).

- 1222 6. For column 1 over the MC operation in round 1, compute $w_1[5, 6, 7]$ and
 1223 $z_1[5]$ (marked by 6) from $z_1[4, 6, 7]$ and $w_1[4]$. Compute backward to get
 1224 $k_1[9]$ (marked by ←6) and compute forward to get $z_2[1, 14, 11]$ (marked by
 1225 →6).
- 1226 7. Guess $k_1[7]$ (marked by 7) and deduce $k_3[7, 9, 13]$ (marked by 7). In round
 1227 1, compute forward to get $z_1[11]$ and $w_1[8, 9, 10, 11]$ (marked by →7). Then
 1228 Compute forward to get $x_2[8, 9, 10, 11]$ and $z_2[8, 5, 2, 15]$ (marked by →7).
- 1229 8. For columns 0 and 1 over the MC operation in round 2, compute $w_2[1, 2, 3, 5, 6, 7]$
 1230 and $z_2[3, 6]$ (marked by 8) from $z_2[0, 1, 2, 4, 5, 7]$ and $w_2[0, 4]$. Compute back-
 1231 ward to get $x_2[14, 15]$ and $w_1[14, 15]$ (marked by ←8).
- 1232 9. For column 3 over the MC operation in round 1, compute $w_1[12, 13]$ and
 1233 $z_1[14, 15]$ (marked by 9) from $z_1[12, 13]$ and $w_1[14, 15]$. Compute backward
 1234 to get $k_1[6, 11]$ (marked by ←9) and compute forward to $z_2[9, 12]$ and columns
 1235 2,3 of w_2 (marked by →9).
- 1236 10. According to the key relations, deduce $k_3[6, 10, 11, 14, 15]$ (marked by 10).
 1237 Compute forward to w_3 (marked by →10). So we deduce all states of the
 1238 starting point.

1239 Degree of freedom and complexity.

- 1240 – In step 1, we deduce the values for active bytes from the input/output dif-
 1241 ferences in the inbound phase. There are 22 active Sboxes, including $s_1 = 20$
 1242 Sboxes with probability 2^{-7} and $s_2 = 2$ Sboxes with probability 2^{-6} . There-
 1243 fore, there are $2^{20+4}/2 = 2^{23}$ combinations for the 22 active bytes, *i.e.*, there
 1244 are 2^{23} choices for the bytes marked by 1 in Fig. 25.
- 1245 – Given one out of 2^{23} choices marked by 1, ten bytes $k_0[0, 8], k_1[1, 2, 3, 4, 7, 12, 14], k_2[0]$
 1246 (marked by a wavy line) are guessed in step 2, 4, 5, 7. There is no conflict
 1247 and expect $2^{23+80} = 2^{123}$ starting points satisfying the inbound differential.
- 1248 – The time of the GD to find one starting point is about $\mathcal{T}_{GD} = 1$. Since the
 1249 probability of the outbound phase is $2^{-p_{out}} = 2^{-97}$, we have to collect 2^{97}
 1250 starting points to expect one collision and the degree of freedom is enough.
 1251 The classical time complexity of the full key collision attack is about $\mathcal{T} = 2^{97}$
 1252 and the time complexity is larger than the birthday bound 2^{64} .

1253 **Quantum attack on 8-round AES-256.** Although a classical attack is invalid,
 1254 we can give a valid quantum one. We select 2^{17} choices of bytes marked by 1
 1255 and traverse 2^{80} possible values of $k_0[0, 8], k_1[1, 2, 3, 4, 7, 12, 14], k_2[0]$.

- 1256 1. Deduce the pairs (m_i^0, m_i^1) ($i = 0, 1, \dots, 21$) for 22 active Sboxes by accessing
 1257 the DDT, and store them in a qRAM L , whose size is about 44 bytes.
- 1258 2. Given $|l_0, l_1, \dots, l_{16}\rangle$ and $l_i \in \{0, 1\}$, O_L is a quantum oracle that computes

$$O_L(|l_0, l_1, \dots, l_{16}\rangle |0\rangle) = |l_0, l_1, \dots, l_{16}\rangle |m_0^{l_0}, m_1^{l_1}, \dots, m_{16}^{l_{16}}, m_{17}^0, \dots, m_{21}^0\rangle \quad (13)$$

1.	$k_0[1-7, 9-15] = (x_0 \oplus P)[1-7, 9-15]$	$w_0[4, 5, 6, 7] = \text{MC}(y_0[4, 9, 14, 3])$
	$w_0[12, 13, 14, 15] = \text{MC}(y_0[12, 1, 6, 11])$	$k_1[5, 15] = (x_1 \oplus w_0)[5, 15]$
2.	$k_2[4] = k_0[4] \oplus \textcolor{blue}{k_2[0]}$	$k_2[2] = k_0[2] \oplus \text{SB}(k_1[15])$
	$k_2[6] = k_0[6] \oplus k_2[2]$	$k_2[10] = k_0[10] \oplus k_2[6]$
	$k_2[14] = k_0[14] \oplus k_2[10]$	
3.	$w_1[1, 2, 3], z_1[0] = \text{MC}(z_1[1, 2, 3], w_1[0])$	
4.	$k_1[13] = \text{SB}^{-1}(k_2[0] \oplus \textcolor{blue}{k_0[0]} \oplus \text{const})$	$k_2[8] = \textcolor{blue}{k_0[8]} \oplus k_2[4]$
	$k_2[12] = k_0[12] \oplus k_2[8]$	$z_0[0, 8] = \text{SB}(\textcolor{blue}{k_0[0, 8]} \oplus P[0, 8])$
	$w_0[0, 1, 2, 3] = \text{MC}(z_0[0, 1, 2, 3])$	$w_0[8, 9, 10, 11] = \text{MC}(z_0[8, 9, 10, 11])$
	$k_1[0, 8, 10] = x_1[0, 8, 10] \oplus w_0[0, 8, 10]$	
5.	$k_2[1] = k_0[1] \oplus \text{SB}(\textcolor{blue}{k_1[14]})$	$k_2[3] = k_0[3] \oplus \text{SB}(\textcolor{blue}{k_1[12]})$
	$k_2[5] = k_0[5] \oplus k_2[1]$	$k_2[7] = k_0[7] \oplus k_2[3]$
	$k_2[9] = k_0[9] \oplus k_2[5]$	$k_2[11] = k_0[11] \oplus k_2[7]$
	$k_2[13] = k_0[13] \oplus k_2[9]$	$k_2[15] = k_0[15] \oplus k_2[11]$
	$k_3[0] = k_1[0] \oplus \text{SB}(k_2[12])$	$k_3[1] = \textcolor{blue}{k_1[1]} \oplus \text{SB}(k_2[13])$
	$k_3[2] = \textcolor{blue}{k_1[2]} \oplus \text{SB}(k_2[14])$	$k_3[3] = \textcolor{blue}{k_1[3]} \oplus \text{SB}(k_2[15])$
	$k_3[4] = \textcolor{blue}{k_1[4]} \oplus k_3[0]$	$k_3[5] = k_1[5] \oplus k_3[1]$
	$k_3[8] = k_1[8] \oplus k_3[4]$	$k_3[12] = k_1[12] \oplus k_3[8]$
6.	$w_1[5, 6, 7], z_1[5] = \text{MC}(z_1[4, 6, 7], w_1[4])$	$k_1[9] = w_0[9] \oplus \text{SB}^{-1}(z_1[5])$
7.	$k_3[7] = \textcolor{blue}{k_1[7]} \oplus k_3[3]$	$k_3[9] = k_1[9] \oplus k_3[5]$
	$k_3[13] = k_1[13] \oplus k_3[9]$	$w_1[8, 9, 10, 11] = \text{MC}(z_1[8, 9, 10, 11])$
8.	$w_2[1, 2, 3], z_2[3] = \text{MC}(z_2[0, 1, 2], w_2[0])$	$w_2[5, 6, 7], z_2[6] = \text{MC}(z_2[4, 5, 7], w_2[4])$
9.	$w_1[12, 13], z_1[14, 15] = \text{MC}(z_1[12, 13], w_1[14, 15])$	$k_1[6, 11] = w_0[6, 11] \oplus \text{SB}^{-1}(z_1[14, 15])$
10.	$k_3[6] = k_1[6] \oplus k_3[2]$	$k_3[10] = k_1[10] \oplus k_3[6]$
	$k_3[11] = k_1[11] \oplus k_3[7]$	$k_3[14] = k_1[14] \oplus k_3[10]$
	$k_3[15] = k_1[15] \oplus k_3[1]$	

Table 12: Equations in the guess-and-determine steps for 8-round AES-256. The blue bytes are guessed.

1259 3. Define $F : \mathbb{F}_2^{17+80} \mapsto \mathbb{F}_2$ and its quantum oracle,

$$\begin{aligned}
 U_F : |l_0, \dots, l_{16}, k_0[0, 8], k_1[1, 2, 3, 4, 7, 12, 14], k_2[0]\rangle |y\rangle \\
 \mapsto y \oplus F(l_0, \dots, l_{16}, k_0[0, 8], k_1[1, 2, 3, 4, 7, 12, 14], k_2[0]),
 \end{aligned} \tag{14}$$

1260 Implementation of U_F :

- 1261 (a) Access O_L to get $|m_0^{l_0}, m_1^{l_1}, \dots, m_{16}^{l_{16}}, m_{17}^0, \dots, m_{21}^0\rangle$.
- 1262 (b) Fix the 22 bytes marked by 1 as $(m_0^{l_0}, m_1^{l_1}, \dots, m_{16}^{l_{16}}, m_{17}^0, \dots, m_{21}^0)$.
- 1263 (c) Run Step 1-10 (or Table 12) with 10-byte $(k_0[0, 8], k_1[1, 2, 3, 4, 7, 12, 14], k_2[0])$.
- 1264 (d) Check if the outbound phase is satisfied with a probability of 2^{-97} . If so,
- 1265 set a 1-bit flag flag as $\text{flag} := 1$. Else, set $\text{flag} := 0$.
- 1266 (e) Return 1 as the value of F if $\text{flag} = 1$. Return 0 otherwise.
- 1267 (f) Uncompute steps (a)-(d).

1268 4. Run Grover's algorithm 28 on U_F to find the collision.

Quantum Complexity. Given a choice of bytes marked by 1 and a guess for the 10-byte $(k_0[0, 8], k_1[1, 2, 3, 4, 7, 12, 14], k_2[0])$ and taking the uncomputation

into account, the cost of U_F is about four 8-round AES-256. The probability of finding the collision is roughly 2^{-97} . Therefore, the quantum time complexity is about

$$\frac{\pi}{4} \sqrt{2^{97}} \cdot 4 \approx 2^{50.2} \text{ 8-round AES-256.}$$

1269 7 Key Collision Attack on 3-round Rijndael-256

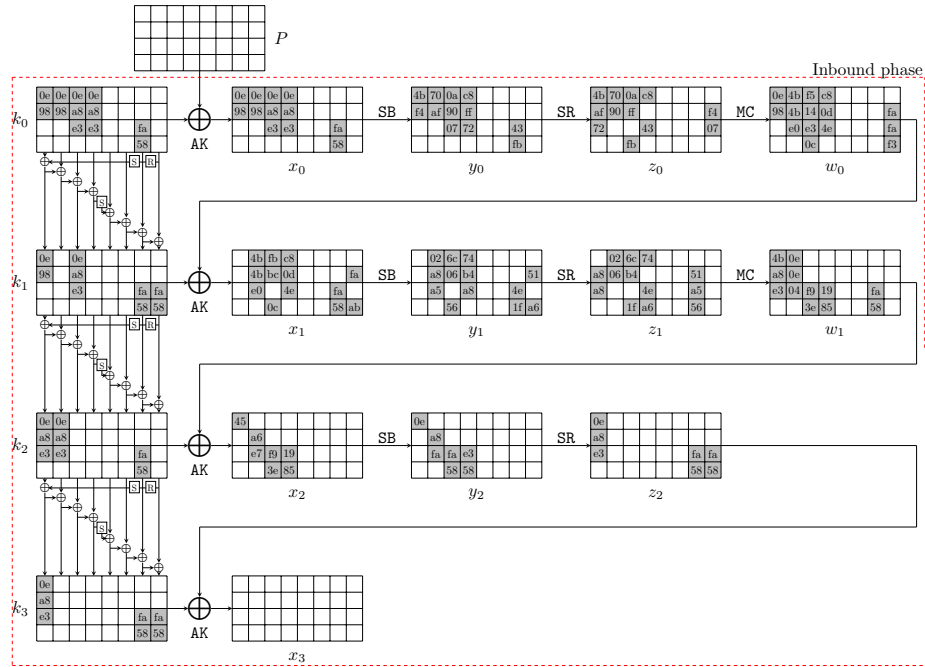


Fig. 26: The related-key differential characteristic on 3-round Rijndael-256

1270 We give a new key collision attack on 3-round Rijndael-256 based on a related-
 1271 key differential characteristic as shown in Fig. 26, which has a probability of
 1272 2^{-231} . We choose the all states of the EN and KS as the inbound phase, with
 1273 a probability of 2^{-231} . The outbound phase has a probability of 1. The steps
 1274 of the GD for the inbound phase are marked in Fig. 27 with equations listed in
 1275 Table 13.

1276 Guess-and-determine procedures of the inbound phase.

- 1277 1. With the fixed differences in the differential, deduce $x_0[0, 1, 4, 5, 8 - 10, 12 -$
 1278 $14, 26, 27]$, $y_0[0, 1, 4, 5, 8 - 10, 12 - 14, 26, 27]$, $x_1[4 - 6, 8, 9, 11 - 14, 26, 27, 29, 31]$,

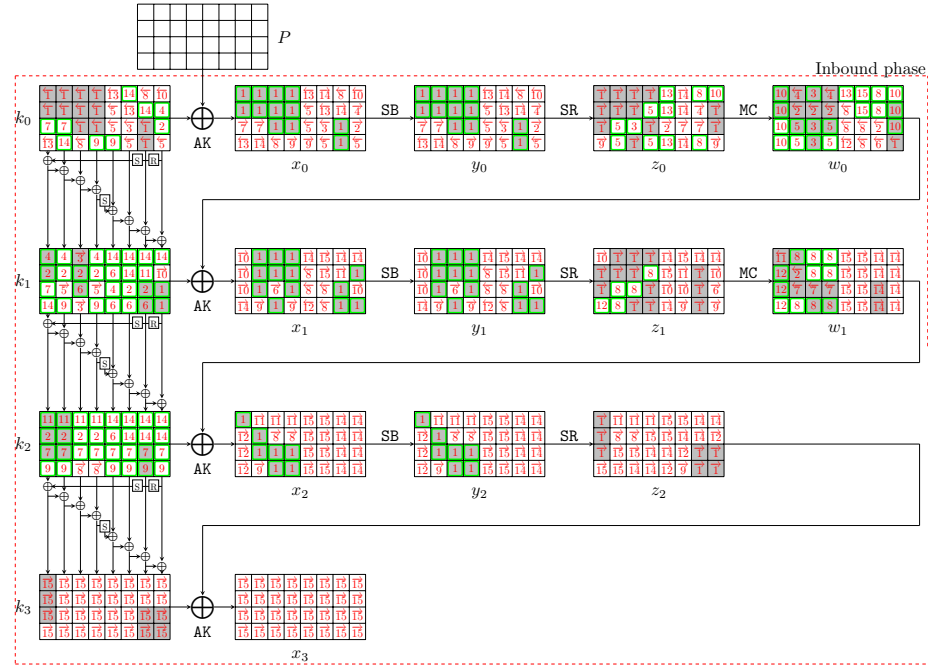


Fig. 27: Steps of the GD in the inbound phase for 3-round Rijndael-256

- 1279 $y_1[4-6, 8, 9, 11-14, 26, 27, 29, 31]$, $x_2[0, 5, 6, 10, 11, 14, 15]$, $y_2[0, 5, 6, 10, 11, 14, 15]$
 1280 (marked by 1 in Fig. 27) by accessing the DDT. Since the differences $\Delta k_1[30, 31]$
 1281 and $\Delta SB(k_1[30, 31])$ are known, deduce $k_1[30, 31]$ (marked by 1) by access-
 1282 ing the DDT.
- 1283 (a) In round 0, deduce $k_0[0, 1, 4, 5, 8-10, 12-14, 26, 27]$ (marked by 1).
 1284 Compute forward to $z_0[0-2, 4, 5, 8, 9, 11, 12, 14, 29, 30]$ (marked by 1).
 1285 (b) In round 1, compute backward to get $w_0[31]$ (marked by 1) and compute
 1286 forward to get $z_1[1, 2, 4, 5, 8, 9, 11, 12, 14, 15, 25-27]$ (marked by 1).
- 1287 2. Guess $k_1[1]$ (marked by 2), and deduce $k_0[30]$, $k_1[5, 9, 13, 22, 26]$ and $k_2[1, 5, 9, 13]$
 1288 (marked by 2) as Table 13. Then deduce $z_0[18]$ (marked by 2), and $w_0[5, 9, 13, 26]$
 1289 and $w_1[5]$ (marked by 2).
- 1290 3. For column 2 over the MC operation of round 0, deduce $w_0[8, 10, 11]$ and
 1291 $z_0[10]$ (marked by 3) from $z_0[8, 9, 11]$ and $w_0[9]$.
 1292 (a) Compute backward to get $k_0[22]$ (marked by 3).
 1293 (b) Compute forward to get $k_1[8, 11]$ (marked by 3).
- 1294 4. According to the key relations, deduce $k_0[29]$ and $k_1[0, 4, 12, 18]$ (marked by
 1295 4). Deduce $z_0[25]$ (marked by 4) and $w_0[4, 12]$ (marked by 4).
- 1296 5. For columns 1 and 3 over the MC operation of round 0, deduce $w_0[6, 7, 14, 15]$
 1297 and $z_0[6, 7, 13, 15]$ (marked by 5) from $z_0[4, 5, 12, 14]$ and $w_0[4, 5, 12, 13]$.
 1298 (a) Compute backward to get $k_0[17, 18, 23, 31]$ (marked by 5).

- 1299 (b) Compute forward to get $k_1[6, 14]$ (marked by $\overrightarrow{5}$).
- 1300 (c) Since $k_0[18] \oplus \text{SB}(k_1[14]) = k_1[18]$ and $k_1[18]$ is deduced in step 4,
- 1301 there is a conflict of Type III with a probability of 2^{-8} .
- 1302 6. According to the key relations, deduce $k_1[10]$ (marked by $\overrightarrow{6}$), where has a conflict
- 1303 of Type III with a probability of 2^{-8} since $k_1[10]$ is deduced twice as Table 13.
- 1304 Then deduce $k_1[17, 19, 23, 27]$ and $k_2[17]$ (marked by $\overrightarrow{6}$). Compute $z_1[30]$
- 1305 (marked by $\overrightarrow{6}$) and $w_0[27]$ (marked by $\overleftarrow{6}$).
- 1306 7. Guess $k_0[2]$ (marked by $\overrightarrow{7}$) and deduce $k_0[6]$, $k_1[2]$ and $k_2[2, 6, 10, 14, 18, 22, 26, 30]$
- 1307 (marked by $\overrightarrow{7}$). Compute $z_0[22, 26]$ (marked by $\overrightarrow{7}$) and $w_1[6, 10, 14]$ (marked
- 1308 by $\overleftarrow{7}$).
- 1309 8. For column 6 over the MC operation of round 0, deduce $w_0[24, 25]$ and
- 1310 $z_0[24, 27]$ (marked by $\overrightarrow{8}$) from $z_0[25, 26]$ and $w_0[26, 27]$. For columns 1,2,3
- 1311 over the MC operation of round 1, deduce $w_1[4, 7, 8, 9, 11, 12, 13, 15]$ and
- 1312 $z_1[6, 7, 10, 13]$ (marked by $\overrightarrow{8}$) from $z_1[4, 5, 8, 9, 11, 12, 14, 15]$ and $w_1[5, 6, 10, 14]$.
- 1313 (a) In round 0, compute backward to get $k_0[11, 24]$ (marked by $\overleftarrow{8}$).
- 1314 (b) In round 1, compute forward to get $k_2[11, 15]$ and $x_2[9, 13]$ (marked
- 1315 by $\overrightarrow{8}$). Compute backward to get $x_1[17, 18, 22, 23]$ and $w_0[17, 18, 22, 23]$
- 1316 (marked by $\overleftarrow{8}$).
- 1317 9. According to the key relations, deduce $k_0[15, 19]$, $k_1[7, 15]$ and $k_2[3, 7, 19, 23, 27, 31]$
- 1318 (marked by $\overrightarrow{9}$). Compute forward to get $z_0[3, 31]$, $z_1[23, 31]$ and $x_2[7]$ (marked
- 1319 by $\overrightarrow{9}$).
- 1320 10. For columns 0 and 7 over the MC operation of round 0, deduce $w_0[0, 1, 2, 3, 28, 29, 30]$
- 1321 and $z_0[28]$ (marked by $\overrightarrow{10}$) from $z_0[0, 1, 2, 3, 29, 30, 31]$ and $w_0[31]$.
- 1322 (a) Compute backward to get $k_0[28]$ (marked by $\overleftarrow{10}$).
- 1323 (b) Compute forward to get $k_1[29]$ and $z_1[0, 18, 22, 29]$ (marked by $\overrightarrow{10}$).
- 1324 11. According to the key relations, deduce $k_1[25]$ and $k_2[0, 4, 8, 12]$ (marked by
- 1325 $\overrightarrow{11}$). Compute forward to get $z_1[21]$ and $x_2[4, 8, 12]$ (marked by $\overrightarrow{11}$). Compute
- 1326 backward to get $w_1[0]$ (marked by $\overleftarrow{11}$).
- 1327 12. For column 0 over the MC operation of round 1, deduce $w_1[1, 2, 3]$ and $z_1[3]$
- 1328 (marked by $\overrightarrow{12}$) from $z_1[0, 1, 2]$ and $w_1[0]$.
- 1329 (a) Compute backward to get $x_1[19]$ and $w_0[19]$ (marked by $\overleftarrow{12}$).
- 1330 (b) Compute forward to get $x_2[1, 2, 3]$ (marked by $\overrightarrow{12}$).
- 1331 13. For column 4 over the MC operation of round 0, deduce $w_0[16]$ and $z_0[16, 17, 19]$
- 1332 (marked by $\overrightarrow{13}$) from $z_0[18]$ and $w_0[17, 18, 19]$. Compute backward to get
- 1333 $k_0[3, 16, 21]$ (marked by $\overleftarrow{13}$).
- 1334 14. According to the key relations, deduce $k_0[7, 20, 25]$, $k_1[3, 16, 20, 21, 24, 28]$
- 1335 and $k_2[16, 20, 21, 24, 25, 28, 29]$ (marked by $\overrightarrow{14}$).
- 1336 (a) In round 0, compute forward to get $z_0[20, 21, 23]$ (marked by $\overrightarrow{14}$).
- 1337 (b) In round 1, compute forward to get $z_1[16, 19, 24, 28]$ and $w_1[24 - 31]$
- 1338 (marked by $\overrightarrow{14}$).
- 1339 (c) In round 2, compute forward to get $x_2[24 - 31]$ (marked by $\overrightarrow{14}$).

- 1340 15. For column 5 over the MC operation of round 0, deduce $w_0[20, 21]$ (marked by
 1341 15) from $z_0[20, 21, 22, 23]$ and $w_0[22, 23]$. Since six values are known in the
 1342 inputs/outputs over the MC operation, there are two conflicts of Type III
 1343 with a total probability 2^{-16} . Then we get all the states of the starting point.

1344 Degree of freedom and complexity.

- 1345 – In step 1, we deduce the values for active bytes from the input/output differ-
 1346 ences in the inbound phase. There are 34 active Sboxes with a total proba-
 1347 bility 2^{-231} , including $s_1 = 27$ active Sboxes with probability 2^{-7} and $s_2 = 7$
 1348 active Sboxes with probability 2^{-6} . Therefore, there are $2^{27+14-1}/2 = 2^{40}$
 1349 combinations for the 34 active bytes, *i.e.*, there are 2^{40} choices for the bytes
 1350 marked by 1 in Fig. 27.
- 1351 – Given one out of 2^{40} choices marked by 1, two bytes $k_1[1]$ and $k_0[2]$ (marked
 1352 by a wavy line) are guessed in step 2 and 7. In step 5, 6 and 15, there are four
 1353 filters of 2^{-8} marked by underline. Therefore, there expect $2^{40+16-32} = 2^{24}$
 1354 states satisfying the inbound trial in total, which act as the starting points
 1355 for the outbound phase.
- 1356 – Since there are four conflict of Type III in the inbound phase, *i.e.*, $c_{in} = 4$, the
 1357 time of the GD to find one starting point is $\mathcal{T}_{GD} = 2^{32}$. Since the probability
 1358 of the outbound phase is 1, each starting point is corresponding to one
 1359 collision. The overall time complexity is $\mathcal{T} = 2^{32}$ and the memory complexity
 1360 is negligible, which is practical. We find key collisions in several hours on a
 1361 desktop equipped with Intel Core i7-13700F @2.1 GHz and 16G RAM using
 1362 one CPU core, and some examples are listed in Table 3.

1363 8 Semi-Free-Start Collisions on Reduced AES-DM and 1364 Rijndael-DM

1365 The DM mode is $h_i = \text{AES}_{m_i}(h_{i-1}) \oplus h_{i-1}$ shown in Fig. 28, where the message
 1366 block m_i acts as the key of the block cipher. The semi-free-start (SFS) collision
 1367 is to find two message blocks (m_i, m'_i) , such that $h_i = \text{AES}_{m_i}(h_{i-1}) \oplus h_{i-1} =$
 1368 $h'_i = \text{AES}_{m'_i}(h_{i-1}) \oplus h_{i-1}$. This is equivalent to $\text{AES}_{m_i}(h_{i-1}) = \text{AES}_{m'_i}(h_{i-1})$,
 1369 *i.e.*, the free-target-plaintext key collision in Fig. 5.

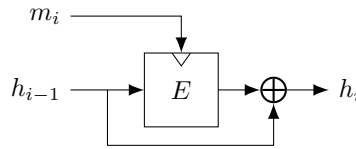


Fig. 28: Davies-Meyer (DM) mode

1.	$k_0[0, 1, 4, 5, 8 - 10, 12 - 14, 26, 27] = (x_0 \oplus P)[0, 1, 4, 5, 8 - 10, 12 - 14, 26, 27]$	
2.	$k_0[30] = \text{SB}^{-1}(\widetilde{k_1[1]} \oplus k_0[1])$	$k_1[5] = \widetilde{k_1[1]} \oplus k_0[5]$
	$k_1[9] = k_0[9] \oplus k_1[5]$	$k_1[13] = k_0[13] \oplus k_1[9]$
	$k_1[26] = k_0[30] \oplus k_1[30]$	$k_1[22] = k_0[26] \oplus k_1[26]$
	$k_2[1] = \widetilde{k_1[1]} \oplus \text{SB}(k_1[30])$	$k_2[5] = k_1[5] \oplus k_2[1]$
	$k_2[9] = k_1[9] \oplus k_2[5]$	$k_2[13] = k_1[13] \oplus k_2[9]$
3.	$w_0[8, 10, 11], z_0[10] = \text{MC}(z_0[8, 9, 11], w_0[9])$	$k_0[22] = P[22] \oplus \text{SB}^{-1}(z_0[10])$
	$k_1[8, 11] = (w_0 \oplus x_1)[8, 11]$	
4.	$k_1[4] = k_1[8] \oplus k_0[8]$	$k_1[0] = k_1[4] \oplus k_0[4]$
	$k_0[29] = \text{SB}^{-1}(k_1[0] \oplus k_0[0] \oplus \text{const})$	$k_1[12] = k_0[12] \oplus k_1[8]$
	$k_1[18] = k_0[22] \oplus k_1[22]$	
5.	$w_0[6, 7], z_0[6, 7] = \text{MC}(z_0[4, 5], w_0[4, 5])$	$w_0[14, 15], z_0[13, 15] = \text{MC}(z_0[12, 14], w_0[12, 13])$
	$k_0[17, 18, 23, 31] = P[17, 18, 23, 31] \oplus \text{SB}^{-1}(z_0[13, 6, 7, 15])$	
	$k_1[6, 14] = (w_0 \oplus x_1)[6, 14]$	$\text{SB}(k_1[14]) \oplus k_0[18] \stackrel{?}{=} k_1[18]$
6.	$k_1[10] = k_0[10] \oplus k_1[6] \stackrel{?}{=} k_1[14] \oplus k_0[14]$	$k_1[17] = k_0[17] \oplus \text{SB}(k_1[13])$
	$k_1[27] = k_1[31] \oplus k_0[31]$	$k_1[23] = k_1[27] \oplus k_0[27]$
	$k_1[19] = k_1[23] \oplus k_0[23]$	$k_2[17] = k_1[17] \oplus \text{SB}(k_2[13])$
7.	$k_1[2] = \widetilde{k_0[2]} \oplus \text{SB}(k_0[31])$	$k_0[6] = k_1[6] \oplus k_1[2]$
	$k_2[2] = k_1[2] \oplus \text{SB}(k_1[31])$	$k_2[6, 10, 14] = k_1[6, 10, 14] \oplus k_2[2, 6, 10]$
	$k_2[18] = k_1[18] \oplus \text{SB}(k_2[14])$	$k_2[22, 26, 30] = k_1[22, 26, 30] \oplus k_2[18, 22, 26]$
8.	$w_0[24, 25], z_0[24, 27] = \text{MC}(z_0[25, 26], w_0[26, 27])$	$w_1[4, 7], z_1[6, 7] = \text{MC}(z_1[4, 5], w_1[5, 6])$
	$w_1[8, 9, 11], z_1[10] = \text{MC}(z_1[8, 9, 11], w_1[10])$	$w_1[12, 13, 15], z_1[13] = \text{MC}(z_1[12, 14, 15], w_1[14])$
	$k_0[11, 24] = P[11, 24] \oplus \text{SB}^{-1}(z_0[27, 24])$	$k_2[11, 15] = (w_1 \oplus x_2)[11, 15]$
9.	$k_1[7] = k_1[11] \oplus k_0[11]$	$k_2[7] = k_1[11] \oplus k_2[11]$
	$k_2[3] = k_1[7] \oplus k_2[7]$	$k_1[15] = k_2[15] \oplus k_2[11]$
	$k_2[19] = k_1[19] \oplus \text{SB}(k_2[15])$	$k_2[23, 27, 31] = k_1[23, 27, 31] \oplus k_2[19, 23, 27]$
	$k_0[15] = k_1[15] \oplus k_1[11]$	$k_0[19] = k_1[19] \oplus \text{SB}(k_1[15])$
10.	$w_0[0, 1, 2, 3] = \text{MC}(z_0[0, 1, 2, 3])$	$w_0[28, 29, 30], z_0[28] = \text{MC}(z_0[29, 30, 31], w_0[31])$
	$k_0[28] = P[28] \oplus \text{SB}^{-1}(z_0[28])$	$k_1[29] = (w_0 \oplus x_1)[29]$
11.	$k_1[25] = k_1[29] \oplus k_0[29]$	$k_2[0] = k_1[0] \oplus \text{SB}(k_1[29]) \oplus \text{const}$
	$k_2[4, 8, 12] = k_1[4, 8, 12] \oplus k_2[0, 4, 8]$	
12.	$w_1[1, 2, 3], z_1[3] = \text{MC}(z_1[0, 1, 2], w_1[0])$	
13.	$w_0[16], z_0[16, 17, 19] = \text{MC}(z_0[18], w_0[17, 18, 19])$	$k_0[3, 16, 21] = P[3, 16, 21] \oplus \text{SB}^{-1}(z_0[19, 16, 17])$
14.	$k_1[3] = k_0[3] \oplus \text{SB}(k_0[28])$	$k_0[7] = k_1[7] \oplus k_1[3]$
	$k_1[16] = k_0[16] \oplus \text{SB}(k_1[12])$	$k_1[21] = k_0[21] \oplus k_1[17]$
	$k_0[25] = k_1[25] \oplus k_1[21]$	$k_1[28] = \text{SB}^{-1}(k_2[3] \oplus k_1[3])$
	$k_2[16] = k_1[16] \oplus \text{SB}(k_2[12])$	$k_2[21, 25, 29] = k_1[21, 25, 29] \oplus k_2[17, 21, 25]$
	$k_1[24] = k_0[28] \oplus k_1[28]$	$k_1[20] = k_0[24] \oplus k_1[24]$
	$k_0[20] = k_1[16] \oplus k_1[20]$	$k_2[20, 24, 28] = k_1[20, 24, 28] \oplus k_2[16, 20, 24]$
15.	$w_0[20, 21] = \text{MC}(z_0[20, 21, 22, 23], w_0[22, 23])$?	

Table 13: Equations in the GD steps for 3-round Rijndael-256. The blue bytes are guessed. The red equations are conflicts.

8.1 The Practical SFS Collision Attack on 5-round AES-128-DM

We give a semi-free-start collision attack on 5-round AES-128-DM with the differential characteristic in [53]. The differential has a probability of 2^{-251} , which is shown in Fig. 29. The inbound phase covers the whole KS and 3 rounds of the

EN path, *i.e.*, round 1 to round 3. The inbound phase has 32 active Sboxes, including 1 active Sbox in the key schedule. The probabilities of the inbound phase and the outbound phase are 2^{-220} and 2^{-31} , respectively. In the GD of the inbound phase, there is 1 conflict of Type III, *i.e.*, $c_{in} = c_3 = 1$ and $c_1 = c_2 = 0$. The guess and determination steps of the GD in the inbound phase are listed below, also in Fig. 30. The detailed equations are listed in Table 14.

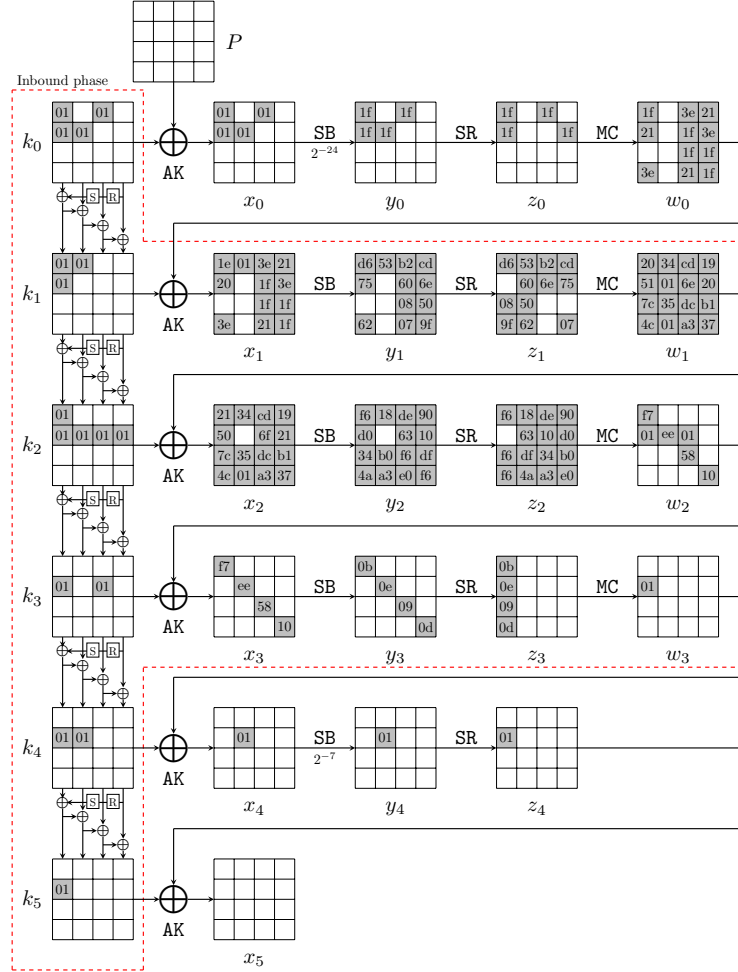


Fig. 29: The related-key differential characteristic on 5-round AES-128 in [53]

Guess-and-determine procedure of the inbound phase.

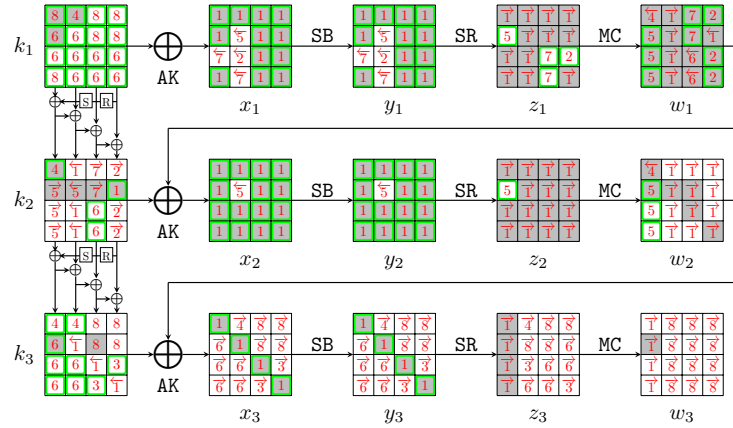


Fig. 30: Steps of the GD in the inbound phase for 5-round AES-128-DM

- 1381 1. Deduce the values of $x_1[0, 1, 3, 4, 8-15]$, $y_1[0, 1, 3, 4, 8-15]$, $x_2[0-4, 6-15]$,
 1382 $y_2[0-4, 6-15]$, $x_3[0, 5, 10, 15]$ and $y_3[0, 5, 10, 15]$ with the fixed differences
 1383 by accessing the DDT, which are all marked by 1. Since $\Delta k_2[13]$ and
 1384 $\Delta SB(k_2[13])$ are known (see Fig. 29), deduce $k_2[13]$ (marked by 1) by ac-
 1385 cessing the DDT.
 1386 (a) In round 1, compute forward to get $z_1[0, 2-9, 12, 13, 15]$ and $w_1[4, 5, 6, 7]$
 1387 (marked by → 1).
 1388 (b) In round 2, compute backward to $w_1[13]$ and deduce $k_2[4, 6, 7] = x_2[4, 6, 7] \oplus$
 1389 $w_1[4, 6, 7]$ (marked by ← 1). Compute forward to get $z_2[0, 2-15]$ and
 1390 $w_2[4-15]$ (marked by → 1).
 1391 (c) In round 3, compute backward to deduce $k_3[5, 10, 15] = x_3[5, 10, 15] \oplus$
 1392 $w_2[5, 10, 15]$ (marked by ← 1). Compute forward to get $w_3[0, 1, 2, 3]$ (marked
 1393 by → 1).
 1394 2. For column 3 over the MC operation in round 1, compute $w_1[12, 14, 15]$ and
 1395 $z_1[14]$ (marked by 2) from $z_1[12, 13, 15]$ and $w_1[13]$.
 1396 (a) Compute backward to get $x_1[6]$ (marked by ← 2).
 1397 (b) Compute forward to get $k_2[12, 14, 15]$ (marked by → 2).
 1398 3. According to the key relations, deduce $k_3[11, 14]$ (marked by 3). Compute
 1399 forward to get $z_3[6, 15]$ (marked by → 3).
 1400 4. Guess $k_2[0]$ (marked by 4) and deduce $k_1[4]$ and $k_3[0, 4]$ (marked by 4)
 1401 according to the key relations. Then compute backward to $w_1[0]$ and $w_2[0]$
 1402 (marked by ← 4). Compute backward to $z_3[4]$ (marked by ← 4).
 1403 5. For column 0 over the MC operation in round 1, compute $w_1[1, 2, 3]$ and
 1404 $z_1[1]$ (marked by 5) from $z_1[0, 2, 3]$ and $w_1[0]$. For column 0 over the MC
 1405 operation in round 2, compute $w_2[1, 2, 3]$ and $z_2[1]$ (marked by 5) from
 1406 $z_2[0, 2, 3]$ and $w_2[0]$.
 1407 (a) In round 1, compute backward to get $x_1[5]$ (marked by ← 5). Compute
 1408 forward to deduce $k_2[1, 2, 3]$ (marked by → 5).

- 1409 (b) In round 2, compute forward to deduce $k_2[5]$ (marked by $\overleftarrow{5}$).
- 1410 6. According to the key relations, deduce $k_1[1, 2, 5, 6, 7, 10, 11, 14, 15]$, $k_2[10, 11]$
- 1411 and $k_3[1, 2, 3, 6, 7]$ following the order in Table 14 (marked by $\overrightarrow{6}$). Since the
- 1412 $k_3[1]$ can be computed twice from different key relations, there is a conflict of
- 1413 Type III with a probability of 2^{-8} . Compute backward to get $w_1[10, 11]$ (marked
- 1414 by $\overleftarrow{6}$). Compute forward to get $z_3[7, 10, 11, 13, 14]$ (marked by $\overrightarrow{6}$).
- 1415 7. For column 2 over the MC operation in round 1, compute $z_1[10, 11]$ and
- 1416 $w_1[8, 9]$ (marked by $\overrightarrow{7}$) from $z_1[8, 9]$ and $w_1[10, 11]$.
- 1417 (a) Compute backward to get $x_1[2, 7]$ (marked by $\overleftarrow{7}$).
- 1418 (b) Compute forward to get $k_2[8, 9]$ (marked by $\overrightarrow{7}$).
- 1419 8. According to the key relations, deduce $k_1[0, 3, 8, 9, 12, 13]$ and $k_3[8, 9, 12, 13]$
- 1420 (marked by $\overrightarrow{8}$) following the order in Table 15. Compute forward to deduce
- 1421 the columns 1,2,3 of $w_3 = \text{MC}(z_3)$ (marked by $\overrightarrow{8}$).

1.	$k_2[4, 6, 7] = (x_2 \oplus w_1)[4, 6, 7]$	$k_3[5, 10, 15] = (x_3 \oplus w_2)[5, 10, 15]$
2.	$w_1[12, 14, 15], z_1[14] = \text{MC}(z_1[12, 13, 15], w_1[13])$	$k_2[12, 14, 15] = (w_1 \oplus x_2)[12, 14, 15]$
3.	$k_3[14] = k_2[14] \oplus k_3[10]$	$k_3[11] = k_2[15] \oplus k_3[15]$
4.	$k_1[4] = k_2[4] \oplus \underline{k_2[0]}$	$k_3[0] = \underline{k_2[0]} \oplus \text{SB}(k_2[13]) \oplus \text{const}$
	$k_3[4] = k_3[0] \oplus k_2[4]$	
5.	$w_1[1, 2, 3], z_1[1] = \text{MC}(z_1[0, 2, 3], w_1[0])$	$k_2[1, 2, 3] = (w_1 \oplus x_2)[1, 2, 3]$
	$w_2[1, 2, 3], z_2[1] = \text{MC}(z_2[0, 2, 3], w_2[0])$	$k_2[5] = w_1[5] \oplus \text{SB}^{-1}(z_2[1])$
6.	$k_1[5] = k_2[5] \oplus k_2[1]$	$k_1[6] = k_2[6] \oplus k_2[2]$
	$k_1[7] = k_2[7] \oplus k_2[3]$	$k_3[1] = k_2[1] \oplus \text{SB}(k_2[14]) \stackrel{?}{=} k_3[5] \oplus k_2[5]$
	$k_3[2] = k_2[2] \oplus \text{SB}(k_2[15])$	$k_3[3] = k_2[3] \oplus \text{SB}(k_2[12])$
	$k_3[6] = k_2[6] \oplus k_3[2]$	$k_3[7] = k_2[7] \oplus k_3[3]$
	$k_2[10] = k_3[6] \oplus k_3[10]$	$k_2[11] = k_3[7] \oplus k_3[11]$
	$k_1[14] = k_2[10] \oplus k_2[14]$	$k_1[15] = k_2[11] \oplus k_2[15]$
	$k_1[10] = k_2[10] \oplus k_2[6]$	$k_1[11] = k_2[11] \oplus k_2[7]$
	$k_1[1] = k_2[1] \oplus \text{SB}(k_1[14])$	$k_1[2] = k_2[2] \oplus \text{SB}(k_1[15])$
7.	$w_1[8, 9], z_1[10, 11] = \text{MC}(z_1[8, 9], w_1[10, 11])$	$k_2[8, 9] = (w_1 \oplus x_2)[8, 9]$
8.	$k_1[8] = k_2[8] \oplus k_2[4]$	$k_1[9] = k_2[9] \oplus k_2[5]$
	$k_1[12] = k_2[8] \oplus k_2[12]$	$k_1[13] = k_2[9] \oplus k_2[13]$
	$k_1[0] = k_2[0] \oplus \text{SB}(k_1[13]) \oplus \text{const}$	$k_1[3] = k_2[3] \oplus \text{SB}(k_1[12])$
	$k_3[8] = k_2[8] \oplus k_3[4]$	$k_3[9] = k_2[9] \oplus k_3[5]$
	$k_3[12] = k_3[8] \oplus k_2[12]$	$k_3[13] = k_3[9] \oplus k_2[13]$

Table 14: Equations in the guess-and-determine steps for 5-round AES-128-DM. The blue bytes are guessed. The red equation is conflict.

1422 Degree of freedom and complexity.

- 1423 – There are totally 32 active Sboxes in the inbound phase, including $s_1 = 28$
- 1424 active Sboxes with probability 2^{-7} and $s_2 = 4$ active Sboxes with probability

1425 2^{-6} . Therefore, by accessing the DDT, there expect $2^{28+8}/2 = 2^{35}$ combina-
 1426 tions for the 32 active Sboxes, *i.e.*, there are 2^{35} choices for the bytes marked
 1427 by 1.
 1428 – Given one out of 2^{35} choices marked by 1, 1 byte $k_2[0]$ (marked by a wavy
 1429 line) is guessed in step 4. And in step 6, there is a conflict with a probability
 1430 of 2^{-8} . Therefore, there expect $2^{35+8-8} = 2^{35}$ starting points satisfying the
 1431 inbound differential.
 1432 – The time of the GD to find one starting point is about $\mathcal{T}_{\text{GD}} = 2^8$. Since the
 1433 probability of the outbound phase is $2^{-p_{\text{out}}} = 2^{-31}$, we have to collect 2^{31}
 1434 starting points to expect one collision and the degree of freedom is enough.
 1435 The total complexity of the 5-round key-collision attack on AES-128-DM is
 1436 about $\mathcal{T} = 2^{39}$. We have practically implemented the attack and found some
 1437 key pairs (K_1, K_2) and free plaintexts P in Table 3.

1438 8.2 The Practical SFS Collision Attack on 7-round AES-192-DM

1439 We give a practical semi-free-start collision attack on 7-round AES-192-DM. We
 1440 reuse the differential characteristic for AES-192 with a probability of 2^{-248} in
 1441 [53], which is shown in Fig. 31. The inbound phase covers the whole KS and
 1442 4 rounds of the EN path, *i.e.*, round 1 to round 4. The inbound phase has 33
 1443 active Sboxes, including 1 active Sbox in the key schedule. The probabilities of
 1444 the inbound phase and outbound phase are 2^{-228} and 2^{-20} , respectively. There
 1445 is no conflict in the GD of the inbound phase, *i.e.*, $c_{\text{in}} = 0$. The guess-and-
 1446 determine steps of the GD of the inbound phase are listed below, also in Fig. 32.
 1447 The detailed equations are listed in Table 15.

1448 Guess-and-determine procedure of the inbound phase.

- 1449 1. Deduce the values of $x_1[6, 12, 13]$, $y_1[6, 12, 13]$, $x_2[2, 6, 8-11, 13-15]$, $y_2[2, 6, 8-$
 1450 $11, 13-15]$, $x_3[0-15]$, $y_3[0-15]$, $x_4[0, 5, 10, 15]$ and $y_4[0, 5, 10, 15]$ with the
 1451 fixed differences by accessing the DDT, which are all marked by 1. Since
 1452 $\Delta k_1[6]$ and $\Delta \text{SB}(k_1[6])$ are known (see Fig. 31), deduce $k_1[6]$ (marked by 1)
 1453 by accessing the DDT.
 1454 (a) In round 1, compute forward to get $z_1[9, 12, 14]$ (marked by →1).
 1455 (b) In round 2, compute forward to get $z_2[2, 3, 5, 6, 8-10, 14, 15]$ (marked
 1456 by →1).
 1457 (c) In round 3, compute forward to get the whole state $w_3 = \text{MC} \circ \text{SR}(y_3)$
 1458 (marked by →1).
 1459 (d) In round 4, compute backward to deduce $k_4[0, 5, 10, 15] = x_4[0, 5, 10, 15] \oplus$
 1460 $w_3[0, 5, 10, 15]$ (marked by ←1). Compute forward to get the $w_4[0, 1, 2, 3]$
 1461 (marked by →1).
 1462 2. Guess $k_3[8, 12, 13]$ (marked by 2) and deduce $k_1[0]$ and $k_2[4, 8]$ according to
 1463 the key relations. Then compute backward to $w_2[8, 12, 13]$ and $w_1[8]$ (marked
 1464 by ←2).

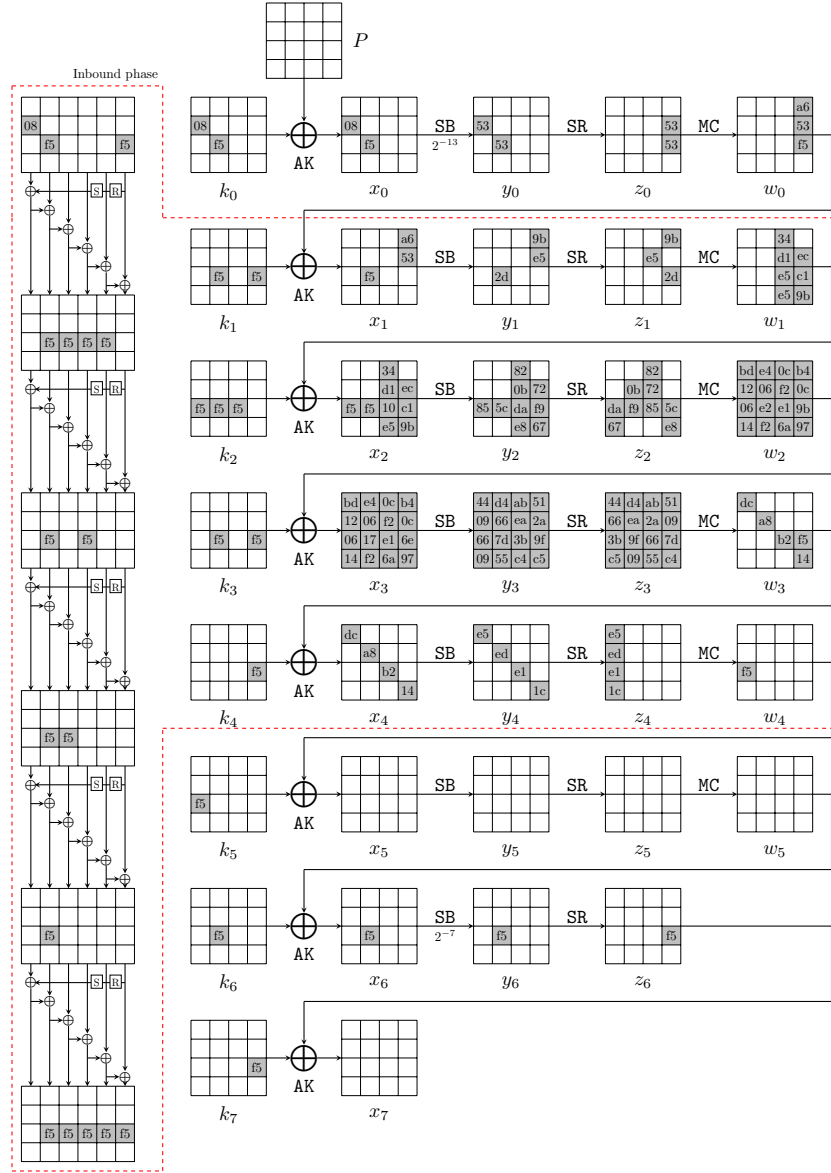


Fig. 31: The related-key differential characteristic on 7-round AES-192 in [53]

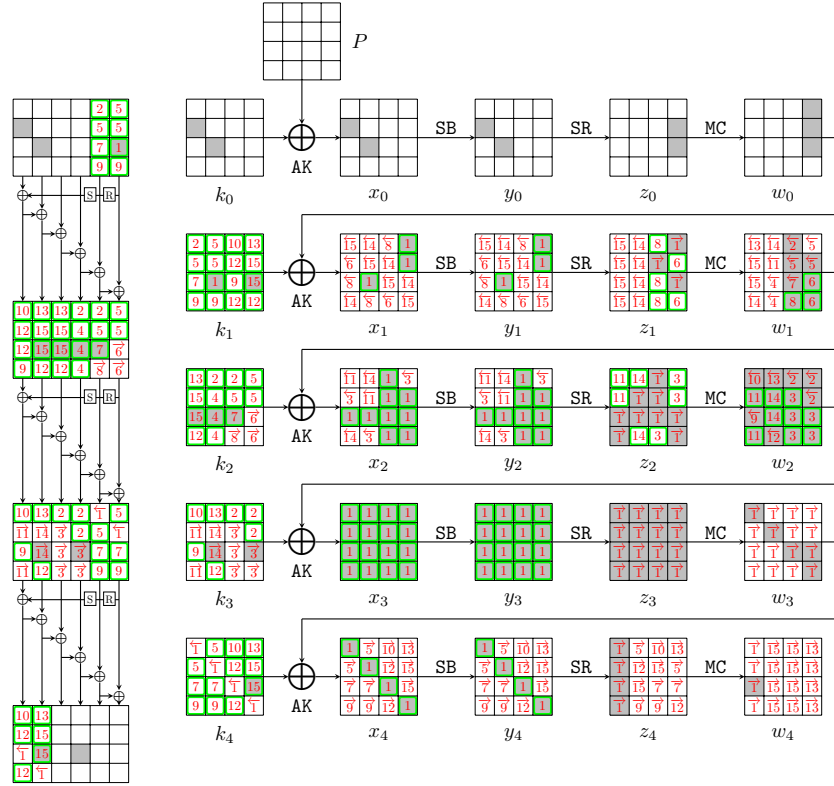


Fig. 32: Steps of the GD in the inbound phase for 7-round AES-192-DM

- 1465 3. For columns 2,3 over the MC operation in round 2, compute $w_2[9, 10, 11, 14, 15]$
 1466 and $z_2[11, 12, 13]$ (marked by $\boxed{3}$) from $z_2[8, 9, 10, 14, 15]$ and $w_2[8, 12, 13]$.
 1467 (a) Compute backward to get $x_2[1, 7, 12]$ (marked by $\overleftarrow{3}$).
 1468 (b) Compute forward to get $k_3[9, 10, 11, 14, 15]$ (marked by $\overrightarrow{3}$).
 1469 4. According to the key relations, deduce $k_2[5, 6, 7]$ (marked by $\boxed{4}$). Compute
 1470 backward and get $w_1[6, 7]$ (marked by $\overleftarrow{4}$).
 1471 5. Guess $k_2[12, 13]$ (marked by $\boxed{5}$) and deduce $k_1[1, 4, 5]$, $k_2[9]$ and $k_4[1, 4]$
 1472 (marked by $\boxed{5}$) following the order in Table 15. Compute backward to
 1473 $w_1[9, 12, 13]$ (marked by $\overleftarrow{5}$) and compute forward to $z_4[4, 13]$ (marked by
 1474 $\overrightarrow{5}$).
 1475 6. For column 3 over the MC operation in round 1, compute $w_1[14, 15]$ and
 1476 $z_1[13, 15]$ (marked by $\boxed{6}$) from $z_1[12, 14]$ and $w_1[12, 13]$.
 1477 (a) Compute backward to get $x_1[1, 11]$ (marked by $\overleftarrow{6}$).
 1478 (b) Compute forward to get $k_2[14, 15]$ (marked by $\overrightarrow{6}$).
 1479 7. According to the key relations, deduce $k_1[2]$, $k_2[10]$ and $k_4[2, 6]$ (marked by
 1480 $\boxed{7}$). Compute backward to get $w_1[10]$ (marked by $\overleftarrow{7}$). Compute forward to
 1481 get $z_4[10, 14]$ (marked by $\overrightarrow{7}$).
 1482 8. For column 2 of the MC operation in round 1, compute $z_1[8, 10, 11]$ and
 1483 $w_1[11]$ (marked by $\boxed{8}$) from $z_1[9]$ and $w_1[8, 9, 10]$.
 1484 (a) Compute backward to get $x_1[2, 7, 8]$ (marked by $\overleftarrow{8}$).
 1485 (b) Compute forward to get $k_2[11]$ (marked by $\overrightarrow{8}$).
 1486 9. According to the key relations, deduce $k_1[3, 7, 10]$, $k_3[2]$ and $k_4[3, 7]$ (marked
 1487 by $\boxed{9}$) following the order in Table 15.
 1488 (a) Compute backward to get $w_2[2]$ (marked by $\overleftarrow{9}$).
 1489 (b) Compute forward to get $x_4[3, 7]$ and $z_4[7, 11]$ (marked by $\overrightarrow{9}$).
 1490 10. Guess $k_3[0]$ (marked by $\boxed{10}$) and deduce $k_1[8]$ and $k_4[8]$ (marked by $\boxed{10}$).
 1491 Compute backward to $w_2[0]$ (marked by $\overleftarrow{10}$) and compute forward to $z_4[8]$
 1492 (marked by $\overrightarrow{10}$).
 1493 11. For column 1 over the MC operation in round 2, compute $z_2[0, 1]$ and $w_2[1, 3]$
 1494 (marked by $\boxed{11}$) from $z_2[2, 3]$ and $w_2[0, 2]$.
 1495 (a) Compute backward to get $x_2[0, 5]$ and $w_1[5]$ (marked by $\overleftarrow{11}$).
 1496 (b) Compute forward to get $k_3[1, 3]$ (marked by $\overrightarrow{11}$).
 1497 12. According to the key relations, deduce $k_1[9, 11, 15]$, $k_2[3]$, $k_3[7]$ and $k_4[9, 11]$
 1498 (marked by $\boxed{12}$) following the order in Table 15.
 1499 (a) Compute backward to get $w_2[7]$ (marked by $\overleftarrow{12}$).
 1500 (b) Compute forward to get $x_4[9, 11]$ and $z_4[5, 15]$ (marked by $\overrightarrow{12}$).
 1501 13. Guess $k_3[4]$ (marked by $\boxed{13}$) and deduce $k_1[12]$, $k_2[0]$ and $k_4[12]$ (marked
 1502 by $\boxed{13}$). Compute backward to $w_1[0]$ and $w_2[4]$ (marked by $\overleftarrow{13}$) and compute
 1503 forward to $z_4[12]$ and $w_4[12, 13, 14, 15]$ (marked by $\overrightarrow{13}$).
 1504 14. For column 1 over the MC operation in round 2, compute $z_2[4, 7]$ and $w_2[5, 6]$
 1505 (marked by $\boxed{14}$) from $z_2[5, 6]$ and $w_2[4, 7]$.
 1506 (a) Compute backward to get $x_2[3, 4]$ and $w_1[3, 4]$ (marked by $\overleftarrow{14}$). Then
 1507 compute $x_1[4, 9, 14, 3] = \text{SB}^{-1} \circ \text{MC}^{-1}(w_1[4, 5, 6, 7])$ (marked by $\overleftarrow{14}$).

- 1508 (b) Compute forward to get $k_3[5, 6]$ (marked by $\overrightarrow{14}$).
 1509 15. According to the key relations, deduce $k_1[13, 14]$, $k_2[0, 1]$ and $k_4[13, 14]$ (marked
 1510 by $\overrightarrow{15}$).
 1511 (a) Compute backward to $w_1[1, 2]$ (marked by $\overrightarrow{15}$) and deduce $x_1[0, 5, 10, 15] =$
 1512 $\text{SB}^{-1} \circ \text{MC}^{-1}(w_1[0, 1, 2, 3])$ (marked by $\overrightarrow{15}$).
 1513 (b) Compute forward to $z_4[6, 9]$ (marked by $\overrightarrow{15}$). Deduce columns 1,2 of
 1514 $w_4 = \text{MC}(z_4)$ (marked by $\overrightarrow{15}$).

1.	$w_3 = \text{MC} \circ \text{SR}(y_3)$	$k_4[0, 5, 10, 15] = (x_4 \oplus w_3)[0, 5, 10, 15]$
2.	$k_2[4] = k_3[12] \oplus \underline{k_3[8]}$	$k_2[8] = k_4[0] \oplus \underline{k_3[12]}$
	$k_1[0] = k_2[8] \oplus k_2[4]$	$w_2[8, 12, 13] = x_3[8, 12, 13] \oplus \underline{k_3[8, 12, 13]}$
3.	$w_2[9, 10, 11], z_2[11] = \text{MC}(z_2[8, 9, 10], w_2[8])$	$w_2[14, 15], z_2[12, 13] = \text{MC}(z_2[14, 15], w_2[12, 13])$
	$k_3[9, 10, 11, 14, 15] = (w_2 \oplus x_3)[9, 10, 11, 14, 15]$	
4.	$k_2[5] = k_3[13] \oplus k_3[9]$	$k_2[6] = k_3[14] \oplus k_3[10]$
	$k_2[7] = k_3[15] \oplus k_3[11]$	
5.	$k_1[4] = \underline{k_2[12]} \oplus k_2[8]$	$k_4[4] = \underline{k_2[12]} \oplus k_4[0]$
	$k_4[1] = \underline{k_2[13]} \oplus k_4[5]$	$k_2[9] = k_4[1] \oplus k_3[13]$
	$k_1[5] = \underline{k_2[13]} \oplus k_2[9]$	$k_1[1] = k_2[9] \oplus k_2[5]$
6.	$w_1[14, 15], z_1[13, 15] = \text{MC}(z_1[12, 14], w_1[12, 13])$	$k_2[14, 15] = (w_1 \oplus x_2)[14, 15]$
7.	$k_2[10] = k_2[14] \oplus k_1[6]$	$k_1[2] = k_2[10] \oplus k_2[6]$
	$k_4[2] = k_2[10] \oplus k_3[14]$	$k_4[6] = k_2[14] \oplus k_4[2]$
8.	$z_1[8, 10, 11], w_1[11] = \text{MC}^{-1}(z_1[9], w_1[8, 9, 10])$	$k_2[11] = w_1[11] \oplus x_2[11]$
9.	$k_1[3] = k_2[11] \oplus k_2[7]$	$k_1[7] = k_2[15] \oplus k_2[11]$
	$k_4[3] = k_2[11] \oplus k_3[15]$	$k_4[7] = k_2[15] \oplus k_4[3]$
	$k_3[2] = k_4[10] \oplus \text{SB}(k_4[7])$	$k_1[10] = k_3[2] \oplus \text{SB}(k_2[15])$
10.	$k_1[8] = \underline{k_3[0]} \oplus \text{SB}(k_2[13]) \oplus \text{const}$	$k_4[8] = \underline{k_3[0]} \oplus \text{SB}(k_4[5]) \oplus \text{const}$
11.	$z_2[0, 1], w_2[1, 3] = \text{MC}^{-1}(z_2[2, 3], w_2[0, 2])$	$k_3[1, 3] = w_2[1, 3] \oplus x_3[1, 3]$
12.	$k_1[9] = k_3[1] \oplus \text{SB}(k_2[14])$	$k_1[11] = k_3[3] \oplus \text{SB}(k_2[12])$
	$k_4[9] = k_3[1] \oplus \text{SB}(k_4[6])$	$k_4[11] = k_3[3] \oplus \text{SB}(k_4[4])$
	$k_3[7] = k_4[11] \oplus k_4[15]$	$k_2[3] = k_3[7] \oplus k_3[11]$
	$k_1[15] = k_3[7] \oplus k_3[3]$	
13.	$k_1[12] = \underline{k_3[4]} \oplus k_3[0]$	$k_2[0] = \underline{k_3[4]} \oplus k_3[8]$
	$k_4[12] = \underline{k_3[4]} \oplus k_4[8]$	
14.	$z_2[4, 7], w_2[5, 6] = \text{MC}^{-1}(z_2[5, 6], w_2[4, 7])$	$k_3[5, 6] = w_2[5, 6] \oplus x_3[5, 6]$
15.	$k_1[13] = k_3[5] \oplus k_3[1]$	$k_1[14] = k_3[6] \oplus k_3[2]$
	$k_2[1] = k_3[9] \oplus k_3[5]$	$k_2[2] = k_3[10] \oplus k_3[6]$
	$k_4[13] = k_3[5] \oplus k_4[9]$	$k_4[14] = k_3[6] \oplus k_4[10]$

Table 15: Equations in the guess-and-determine steps for 7-round AES-192-DM. The blue bytes are guessed.

- 1516 – There are totally 33 active Sboxes in the inbound phase, including $s_1 = 30$
 1517 active Sboxes with probability 2^{-7} and $s_2 = 3$ active Sboxes with probability
 1518 2^{-6} . Therefore, by accessing the DDT, there expect $2^{30+6}/2 = 2^{35}$ combina-
 1519 tions for the 33 active Sboxes, *i.e.*, there are 2^{35} choices for the bytes marked
 1520 by 1.
- 1521 – Given one out of 2^{35} choices marked by 1, seven bytes $k_2[12, 13], k_3[0, 4, 8, 12, 13]$
 1522 (marked by a wavy line) are guessed in steps 2, 5, 10 and 13. Since there is
 1523 no conflict, there expect $2^{35+56} = 2^{81}$ starting points satisfying the inbound
 1524 differential.
- 1525 – The probability of the outbound phase is $2^{-p_{out}} = 2^{-20}$. We have enough de-
 1526 grees of freedom to satisfy the outbound phase. Therefore, the total complex-
 1527 ity of the 7-round key-collision attack on AES-192-DM is about $\mathcal{T} = 2^{20}$. We
 1528 have practically implemented the attack and found some key pairs (K_1, K_2)
 1529 and free plaintexts P in Table 3.

1530 8.3 The Practical SFS Collision Attack on 5-round Rijndael-256-DM

1531 We give a practical semi-free-start collision attack on 5-round Rijndael-256-DM
 1532 with a differential in Fig. 33. The differential has a probability of 2^{-420} . The
 1533 inbound phase covers the whole KS and 3 rounds of the EN path, *i.e.*, round 1
 1534 to round 3. The inbound phase has 57 active Sboxes, including 1 active Sbox
 1535 in the key schedule. The probabilities of the inbound phase and the outbound
 1536 phase are 2^{-387} and 2^{-33} , respectively. In the GD of the inbound phase, there
 1537 is no conflict, *i.e.*, $c_{in} = 0$. The guess and determination steps of the GD in the
 1538 inbound phase are listed below, also in Fig. 34. The detailed equations are listed
 1539 in Table 16.

1540 Guess-and-determine procedure of the inbound phase.

- 1541 1. Deduce the values of $x_1[1, 4 - 11, 18, 28 - 31], y_1[1, 4 - 11, 18, 28 - 31], x_2[0 -$
 1542 $5, 8 - 31], y_2[0 - 5, 8 - 31], x_3[1 - 3, 7, 10, 15, 16, 20, 21, 25, 28, 30]$ and $y_3[1 -$
 1543 $3, 7, 10, 15, 16, 20, 21, 25, 28, 30]$ with the fixed differences by accessing the
 1544 DDT, which are all marked by 1. Since $\Delta k_2[30]$ and $\Delta SB(k_2[30])$ are known
 1545 (see Fig. 33), deduce $k_2[30]$ (marked by 1) by accessing the DDT.
 1546 (a) In round 1, compute forward to get $z_1[1, 4 - 6, 8, 15, 18, 23, 25 - 30]$
 1547 (marked by →1).
- 1548 (b) In round 2, compute backward to $w_1[30]$ (marked by ←1) and compute
 1549 forward to get $z_2[0 - 22, 24, 25, 27 - 31]$ and $w_2[0 - 19, 28 - 31]$ (marked
 1550 by →1).
- 1551 (c) In round 3, compute backward to deduce $k_3[1 - 3, 7, 10, 15, 16, 28, 30]$
 1552 (marked by ←1). Compute forward to get $w_3[16 - 23, 28 - 31]$ (marked
 1553 by →1).
- 1554 2. For column 7 over the MC operation in round 1, compute $w_1[28, 29, 31]$ and
 1555 $z_1[31]$ (marked by 2) from $z_1[28, 29, 30]$ and $w_1[30]$. Compute backward to
 1556 get $x_1[15]$ (marked by ←2) and compute forward to get $k_2[28, 29, 31]$ (marked
 1557 by →2).

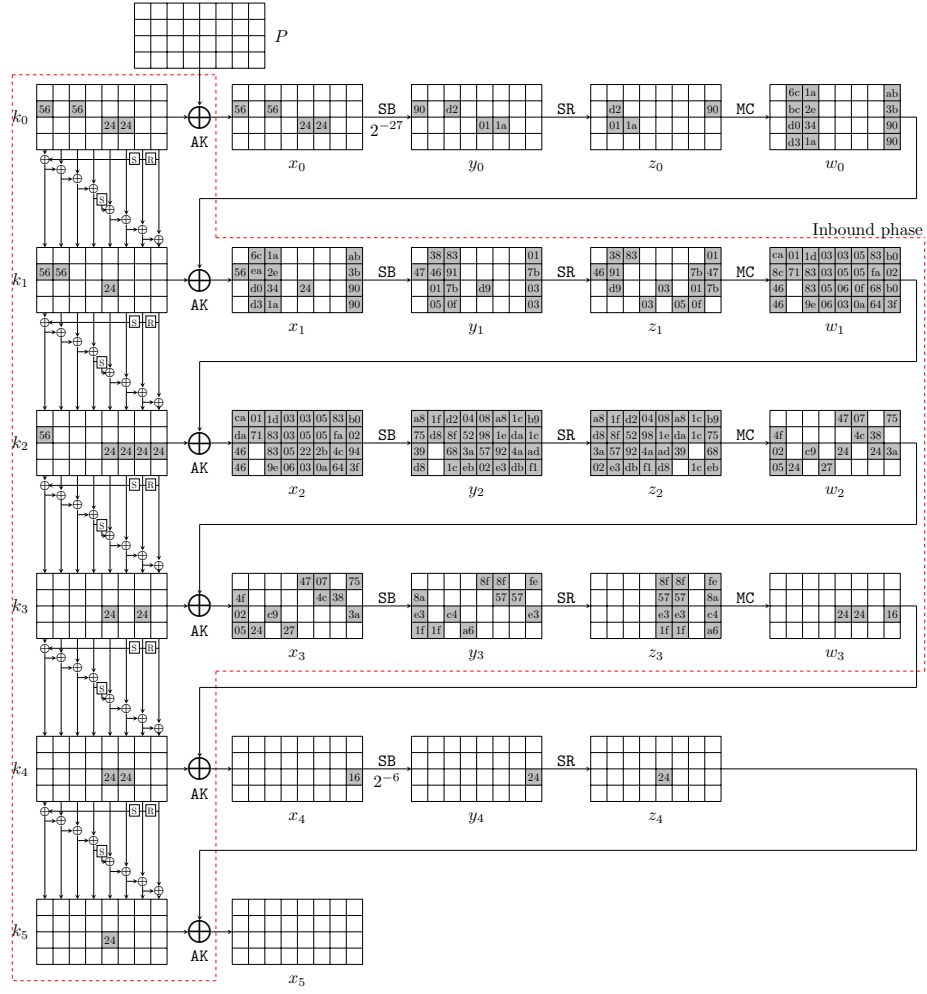


Fig. 33: The related-key differential characteristic on 5-round Rijndael-256

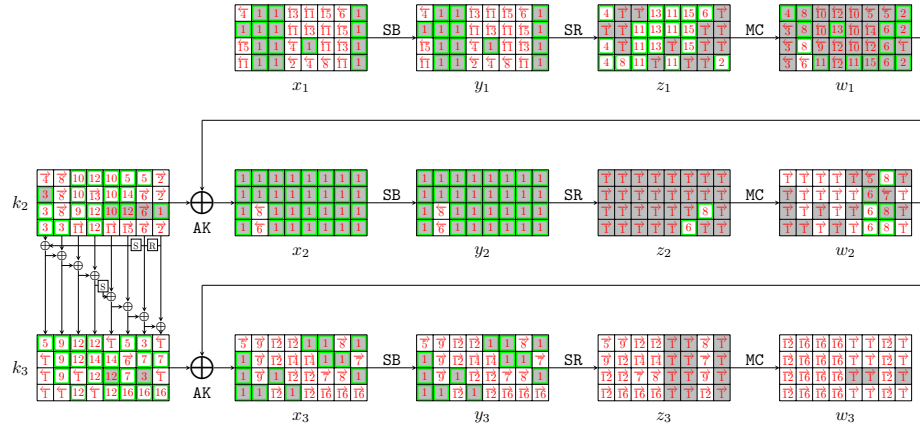


Fig. 34: Steps of the GD in the inbound phase for 5-round Rijndael-256-DM

- 1558 3. According to the key relations, deduce $k_2[1, 2, 3, 7]$ and $k_3[24, 26]$ (marked
1559 by 3). Compute backward to get $w_1[1, 2, 3]$ (marked by ←3).
- 1560 4. For column 0 over the MC operation in round 1, compute $z_1[0, 2, 3]$ and
1561 $w_1[0]$ (marked by 4) from $z_1[1]$ and $w_1[1, 2, 3]$. Compute backward to get
1562 $x_1[0, 14, 19]$ (marked by ←4) and compute forward to get $k_2[0]$ (marked by
1563 →4).
- 1564 5. Guess $k_2[24]$ (marked by 5) and deduce $k_2[20]$ and $k_3[0, 20]$ (marked by 4)
1565 according to the key relations. Then compute backward to $w_1[20, 24]$ and
1566 $w_2[20]$ (marked by ←4). Compute forward to $z_3[0]$ (marked by →5).
- 1567 6. For column 6 over the MC operation in round 1, compute $w_1[25, 26, 27]$ and
1568 $z_1[24]$ (marked by 6) from $z_1[25, 26, 27]$ and $w_1[24]$. For column 5 over the
1569 MC operation in round 2, compute $w_2[21, 22, 23]$ and $z_2[23]$ (marked by 6)
1570 from $z_2[20, 21, 22]$ and $w_2[20]$.
1571 (a) In round 1, compute backward to get $x_1[24]$ (marked by ←6). Compute
1572 forward to deduce $k_2[25, 26, 27]$ (marked by →6).
1573 (b) In round 2, compute backward to deduce $x_2[7]$ and $w_1[7]$ (marked by
1574 ←6). Compute forward to deduce $k_3[21]$ (marked by →6).
- 1575 7. According to the key relations, deduce $k_3[22, 25, 29]$ as Table 14 (marked by
1576 7). Compute backward to get $w_2[25]$ (marked by ←7) and compute forward
1577 to get $z_3[10, 25]$ (marked by →7).
- 1578 8. For column 1 over the MC operation in round 1, compute $w_1[4, 5, 6]$ and
1579 $z_1[7]$ (marked by 8) from $z_1[4, 5, 6]$ and $w_1[7]$. For column 6 over the MC
1580 operation in round 2, compute $w_2[24, 26, 27]$ and $z_2[26]$ (marked by 8) from
1581 $z_2[24, 25, 27]$ and $w_2[25]$.
1582 (a) In round 2, compute backward to deduce $x_2[6]$ (marked by ←8). Compute
1583 forward to $z_3[14, 24]$ (marked by →8).
1584 (b) In round 1, compute backward to get $x_1[23]$ (marked by ←8). Compute
1585 forward to deduce $k_2[4, 5, 6]$ (marked by →8).

- 1586 9. According to the key relations, deduce $k_2[10]$ and $k_3[4, 5, 6]$ (marked by 9).
- 1587 Compute backward to get $w_1[10]$ (marked by 9) and compute forward to
- 1588 get $z_3[1, 4, 26]$ (marked by 9).
- 1589 10. Guess $k_2[8, 9, 16, 17, 18]$ (marked by 10). Compute backward to get $w_1[8, 9, 16, 17, 18]$
- 1590 (marked by 10).
- 1591 11. For columns 2 and 4 over the MC operation in round 1, compute $z_1[9, 10, 11, 16, 17, 19]$
- 1592 and $w_1[11, 19]$ (marked by 11) from $z_1[8, 18]$ and $w_1[8, 9, 10, 16, 17, 18]$. De-
- 1593 duce $k_2[11, 19]$ (marked by 11).
- 1594 12. Guess $k_2[14]$ (marked by 12). According to the key relations, deduce $k_2[12, 15, 22]$
- 1595 and $k_3[8, 9, 11, 12, 14, 18, 19]$ (marked by 12) following the order in Table 16.
- 1596 Compute backward to get $w_1[12, 14, 15, 22]$ (marked by 12).
- 1597 13. For column 3 over the MC operation in round 1, compute $z_1[12, 13, 14]$ and
- 1598 $w_1[13]$ (marked by 13) from $z_1[15]$ and $w_1[12, 14, 15]$. Deduce $k_2[13]$ (marked
- 1599 by 13).
- 1600 14. According to the key relations, deduce $k_2[21]$ and $k_3[13, 17]$ (marked by 14).
- 1601 Compute backward to get $w_1[21]$ (marked by 14).
- 1602 15. For column 5 over the MC operation in round 1, compute $z_1[20, 21, 22]$ and
- 1603 $w_1[23]$ (marked by 15) from $z_1[23]$ and $w_1[20, 21, 22]$. Deduce $k_2[23]$ (marked
- 1604 by 15).
- 1605 16. According to the key relations, deduce $k_3[23, 27, 31]$ (marked by 16). Then
- 1606 we can get all states of the starting point.

1607 Degree of freedom and complexity.

- 1608 – There are totally 57 active Sboxes in the inbound phase, including $s_1 = 45$
- 1609 active Sboxes with probability 2^{-7} and $s_2 = 12$ active Sboxes with prob-
- 1610 ability 2^{-6} . Therefore, by accessing the DDT, there expect $2^{45+24}/2 = 2^{68}$
- 1611 combinations for the 57 active Sboxes, *i.e.*, there are 2^{68} choices for the
- 1612 bytes marked by 1.
- 1613 – Given one out of 2^{68} choices marked by 1, 7 bytes $k_2[8, 9, 14, 16, 17, 18, 24]$
- 1614 (marked by a wavy line) are guessed in steps 5, 10, 12. Therefore, there
- 1615 expect $2^{68+56} = 2^{124}$ starting points satisfying the inbound differential.
- 1616 – The time of the GD to find one starting point is about $\mathcal{T}_{GD} = 1$. Since the
- 1617 probability of the outbound phase is $2^{-p_{out}} = 2^{-33}$, we have to collect 2^{33}
- 1618 starting points to expect one collision and the degree of freedom is enough.
- 1619 The total complexity of the 5-round key-collision attack on Rijndael-256-DM
- 1620 is about $\mathcal{T} = 2^{33}$. We have practically implemented the attack and found
- 1621 some key pairs (K_1, K_2) and free plaintexts P in Table 3.

1622 8.4 The SFS Collision Attack on 6-round Rijndael-256-DM

1623 We give a semi-free-start collision attack on 6-round Rijndael-256-DM. The dif-
 1624 ferential characteristic for Rijndael-256 with a probability of 2^{-465} is shown in

1.	$k_3[1-3, 7, 10, 15, 16, 28, 30] = (x_3 \oplus w_2)[1-3, 7, 10, 15, 16, 28, 30]$	
2.	$w_1[28, 29, 31], z_1[31] = MC(z_1[28, 29, 30], w_1[30])$	$k_2[28, 29, 31] = (w_1 \oplus x_2)[28, 29, 31]$
3.	$k_2[1, 2, 3] = k_3[1, 2, 3] \oplus SB(k_2[30, 31, 28])$ $k_3[24, 26] = k_3[28, 30] \oplus k_2[28, 30]$	$k_2[7] = k_3[7] \oplus k_3[3]$
4.	$z_1[0, 2, 3], w_1[0] = MC^{-1}(z_1[1], w_1[1, 2, 3])$	$k_2[0] = (w_1 \oplus x_2)[0]$
5.	$k_3[20] = k_3[24] \oplus \textcolor{blue}{k_2[24]}$ $k_2[20] = k_3[20] \oplus k_3[16]$	$k_3[0] = k_2[0] \oplus SB(k_2[29]) \oplus const$
6.	$w_1[25, 26, 27], z_1[24] = MC(z_1[25, 26, 27], w_1[24])$ $w_2[21, 22, 23], z_2[23] = MC(z_2[20, 21, 22], w_2[20])$	$k_2[25, 26, 27] = (w_1 \oplus x_2)[25, 26, 27]$ $k_3[21] = (w_2 \oplus x_3)[21]$
7.	$k_3[25] = k_2[25] \oplus k_3[21]$ $k_3[22] = k_3[26] \oplus k_2[26]$	$k_3[29] = k_2[29] \oplus k_3[25]$
8.	$w_1[4, 5, 6], z_1[7] = MC(z_1[4, 5, 6], w_1[7])$ $x_2[6] = SB^{-1}(z_2[26])$	$w_2[24, 26, 27], z_2[26] = MC(z_2[24, 25, 27], w_2[25])$ $k_2[4, 5, 6] = (w_1 \oplus x_2)[4, 5, 6]$
9.	$k_3[4, 5, 6] = k_2[4, 5, 6] \oplus k_3[0, 1, 2]$	$k_2[10] = k_3[10] \oplus k_3[6]$
10.	$w_1[8, 9, 16, 17, 18] = x_2[8, 9, 16, 17, 18] \oplus \textcolor{blue}{k_2[8, 9, 16, 17, 18]}$	
11.	$z_1[9, 10, 11], w_1[11] = MC^{-1}(z_1[8], w_1[8, 9, 10])$ $k_2[11, 19] = (w_1 \oplus x_2)[11, 19]$	$z_1[16, 17, 19], w_1[19] = MC^{-1}(z_1[18], w_1[16, 17, 18])$
12.	$k_3[8, 9, 11] = k_2[8, 9, 11] \oplus k_3[4, 5, 7]$ $k_2[12, 15] = k_3[12, 15] \oplus k_3[8, 11]$ $k_3[18, 19] = k_2[18, 19] \oplus SB(k_3[14, 15])$	$k_3[12] = SB^{-1}(k_3[16] \oplus k_2[16])$ $k_3[14] = \textcolor{blue}{k_2[14]} \oplus k_3[10]$ $k_2[22] = k_3[22] \oplus k_3[18]$
13.	$z_1[12, 13, 14], w_1[13] = MC^{-1}(z_1[15], w_1[12, 14, 15])$	$k_2[13] = (w_1 \oplus x_2)[13]$
14.	$k_3[13] = k_2[13] \oplus k_3[9]$ $k_2[21] = k_3[21] \oplus k_3[17]$	$k_3[17] = k_2[17] \oplus SB(k_3[13])$
15.	$z_1[20, 21, 22], w_1[23] = MC^{-1}(z_1[23], w_1[20, 21, 22])$	$k_2[23] = (w_1 \oplus x_2)[23]$
16.	$k_3[23] = k_2[23] \oplus k_3[19]$ $k_3[31] = k_2[31] \oplus k_3[27]$	$k_3[27] = k_2[27] \oplus k_3[23]$

Table 16: Equations in the guess-and-determine steps for 5-round Rijndael-256-DM. The blue bytes are guessed.

Fig. 35. The inbound phase covers the whole KS, 3 full rounds of the EN path (round 1 to round 3), and the first two columns of the states over the SB operation in round 4. The inbound phase has 60 active Sboxes, including 1 active Sbox in the key schedule. The probabilities of the inbound phase and outbound phase are 2^{-402} and 2^{-63} , respectively. There is 2 conflicts of Type III in the GD of the inbound phase, *i.e.*, $c_{in} = c_3 = 2$. The guess-and-determine steps of the GD of the inbound phase are listed below, also in Fig. 36. The detailed equations are listed in Table 17.

Guess-and-determine procedure of the inbound phase.

1. Deduce the values of $x_1[3, 11, 17, 19, 20-24, 26-31]$, $y_1[3, 11, 17, 19, 20-24, 26-31]$, $x_2[0-2, 4-6, 8, 9, 11-13, 17, 20-24, 26-31]$, $y_2[0-2, 4-6, 8, 9, 11-13, 17, 20-24, 26-31]$, $x_3[0, 2-7, 9, 14, 16, 18-21, 23-25, 29, 30]$, $y_3[0, 2-7, 9, 14, 16, 18-21, 23-25, 29, 30]$, $x_4[2, 7]$ and $y_4[2, 7]$ with the fixed differences by accessing the DDT, which are all marked by 1. Since $\Delta k_3[28]$

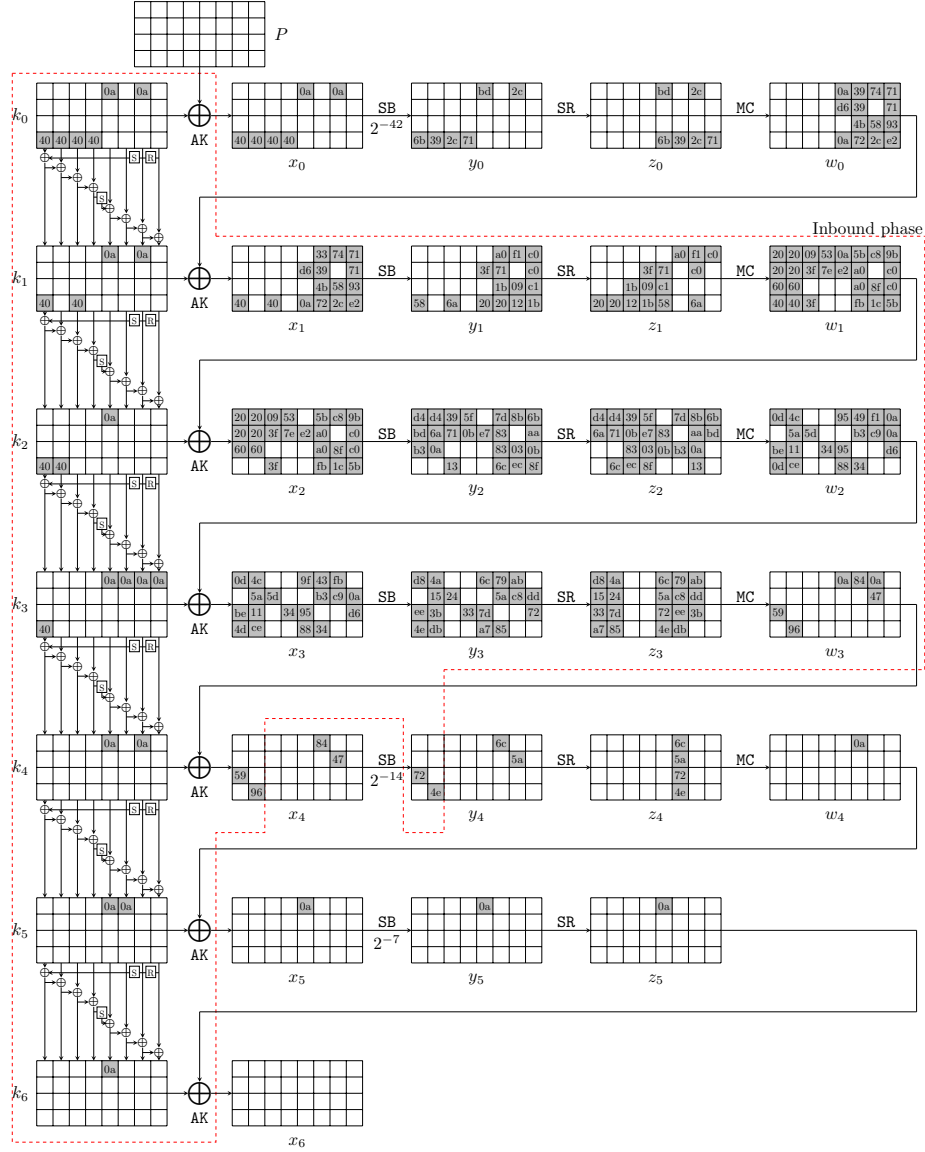


Fig. 35: The related-key differential characteristic on 6-round Rijndael-256

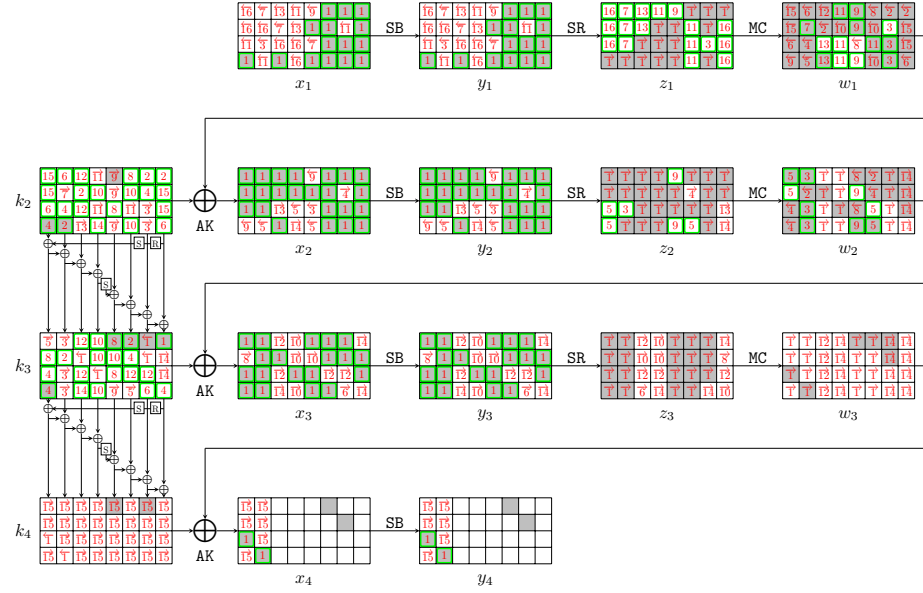


Fig. 36: Steps of the GD in the inbound phase for 6-round Rijndael-256-DM

- 1639 and $\Delta SB(k_3[28])$ are known (see Fig. 35), deduce $k_3[28]$ (marked by 1) by
 1640 accessing the DDT.
 1641 (a) In round 1, compute forward to get $z_1[3, 7, 10, 11, 13-15, 17-20, 24, 25, 27, 28]$
 1642 (marked by →1).
 1643 (b) In round 2, compute forward to get $z_2[0, 1, 4, 5, 7-15, 17, 18, 20, 22, 24-29]$ and $w_2[8-15, 24-27]$ (marked by →1).
 1644 (c) In round 3, compute forward to get $z_3[0-7, 16-26]$ and $w_3[0-7, 16-23]$
 1645 (marked by →1). Compute backward to deduce $k_3[9, 14, 24, 25]$ (marked
 1646 by ←1).
 1647 (d) In round 4, compute backward to deduce $k_4[2, 7]$ (marked by ←1).
 1648 2. Guess $k_2[9, 24]$ (marked by 2) and deduce $k_2[7, 28]$ and $k_3[5, 20]$ according
 1649 to the key relations. Then compute backward to $w_1[9, 24, 25]$ and $w_2[5, 20]$
 1650 (marked by ←2).
 1651 3. For column 6 over the MC operation in round 1, compute $w_1[25, 26, 27]$ and
 1652 $z_1[26]$ (marked by 3) from $z_1[24, 25, 27]$ and $w_1[24]$. For column 1 over the
 1653 MC operation in round 2, compute $w_2[4, 6, 7]$ and $z_2[6]$ (marked by 3) from
 1654 $z_2[4, 5, 7]$ and $w_2[5]$.
 1655 (a) In round 1, compute forward to deduce $k_2[26, 27]$ (marked by →3).
 1656 (b) In round 2, compute backward to get $x_2[18]$ (marked by ←3). Compute
 1657 forward to deduce $k_3[4, 6, 7]$ (marked by →3).
 1658 4. Guess $k_2[25]$ and $k_3[2]$ (marked by 4) and deduce $k_2[3, 6]$ and $k_3[3, 21, 31]$
 1659 (marked by 4). Compute backward and get $w_1[6]$ and $w_2[2, 3, 21]$ (marked
 1660 by ←4). Compute forward and get $z_2[21]$ (marked by →4).
 1661

- 1662 5. For column 0 over the MC operation in round 2, compute $w_2[0, 1]$ and $z_2[2, 3]$
 1663 (marked by 5) from $z_2[0, 1]$ and $w_2[2, 3]$. For column 5 over the MC operation
 1664 in round 2, compute $w_2[22, 23]$ and $z_2[23]$ (marked by 3) from $z_2[20, 21, 22]$
 1665 and $w_2[20, 21]$. Since there are five values known over the MC operation,
 1666 there is a conflict of Type III of 2^{-8} probability.
- 1667 (a) Compute forward to deduce $k_3[0, 23]$ (marked by →5).
- 1668 (b) Compute backward to get $x_2[7, 14, 19]$ and $w_1[7]$ (marked by ←5).
- 1669 6. According to the key relations, deduce $k_2[2, 4, 31]$ and $k_3[27]$ (marked by 6).
- 1670 Compute backward to get $w_1[2, 4, 31]$ (marked by ←6).
- 1671 7. For column 1 over the MC operation in round 1, compute $w_1[5]$ and $z_1[4, 5, 6]$
 1672 (marked by 7) from $z_1[7]$ and $w_1[4, 6, 7]$. Compute forward to deduce $k_2[5]$
 1673 (marked by →7).
- 1674 8. Guess $k_2[18]$ and $k_3[16]$ (marked by 8). Deduce $k_2[20]$ and $k_3[1, 18]$ (marked
 1675 by 8). Compute backward and get $w_1[18, 20]$ and $w_2[16, 18]$ (marked by ←8).
- 1676 9. For column 4 over the MC operation in round 1, compute $w_1[16, 17, 19]$ and
 1677 $z_1[16]$ (marked by 9) from $z_1[17, 18, 19]$ and $w_1[18]$. For column 4 over the
 1678 MC operation in round 2, compute $w_2[17, 19]$ and $z_2[16, 19]$ (marked by 9)
 1679 from $z_2[17, 18]$ and $w_2[16, 18]$.
- 1680 (a) In round 2, compute forward to deduce $k_3[19]$ (marked by →9). And
 1681 compute backward to get $x_2[3, 16]$ (marked by ←9).
- 1682 (b) In round 1, compute forward to get $k_2[16, 17, 19]$ (marked by →9). Com-
 1683 pute backward to deduce $w_1[3]$ (marked by ←9).
- 1684 10. Guess $k_2[13]$ (marked by 10) and deduce $k_2[21, 23]$ and $k_3[12, 13, 15, 17]$
 1685 (marked by 10). Compute backward and get $w_1[13, 21, 23]$ (marked by ←10).
- 1686 11. For columns 3 and 5 over the MC operation in round 1, compute $w_1[12, 14, 15, 22]$
 1687 and $z_1[12, 21, 22, 23]$ (marked by 11) from $z_1[13, 14, 15, 20]$ and $w_1[13, 20, 21, 23]$.
 1688 Compute forward to get $k_2[12, 14, 22]$ (marked by →11).
- 1689 12. According to the key relations, deduce $k_2[8, 10]$ and $k_3[8, 10, 22, 26]$ (marked
 1690 by 12). Compute backward and get $w_1[8]$ (marked by ←12).
- 1691 13. For column 2 over the MC operation in round 1, compute $w_1[10, 11]$ and
 1692 $z_1[8, 9]$ (marked by 13) from $z_1[10, 11]$ and $w_1[8, 9]$. Compute forward to get
 1693 $k_2[11]$ and $z_2[30]$ (marked by →13).
- 1694 14. According to the key relations, deduce $k_3[11]$ and $k_2[15]$ (marked by 14).
- 1695 Compute forward to $z_2[31]$ and $w_2[28, 29, 30, 31]$ (marked by →14). Then de-
 1696 duce $k_3[29, 30]$ (marked by ←14).
- 1697 15. According to the key relations, deduce $k_2[0, 1, 29, 30]$ (marked by 15). Com-
 1698 pute backward to $w_1[0, 1, 29, 30]$ (marked by ←15).
- 1699 16. For columns 0 and 7 over the MC operation in round 1, compute $z_1[0, 1, 2, 29, 30, 31]$
 1700 (marked by 16) from $z_1[3, 28]$ and $w_1[0, 1, 2, 3, 28, 29, 30, 31]$. There are two conflicts of
 1701 Type III with a total 2^{-16} probability. Then we can get all states of the
 1702 starting point.

1.	$k_3[9, 14, 24, 25] = (x_3 \oplus w_2)[9, 14, 24, 25]$	$k_4[2, 7] = (x_4 \oplus w_3)[2, 7]$
2.	$k_3[5] = k_3[9] \oplus \widetilde{k_2[9]}$	$k_3[20] = k_3[24] \oplus \widetilde{k_2[24]}$
	$k_2[28] = k_3[28] \oplus k_3[24]$	$k_2[7] = k_4[7] \oplus \text{SB}(k_3[28])$
3.	$w_1[25, 26, 27], z_1[26] = \text{MC}(z_1[24, 25, 27], w_1[24])$	$w_2[4, 6, 7], z_2[6] = \text{MC}(z_2[4, 5, 7], w_2[5])$
	$k_2[26, 27] = (w_1 \oplus x_2)[26, 27]$	$k_3[4, 6, 7] = (w_2 \oplus x_3)[4, 6, 7]$
4.	$k_3[21] = k_3[25] \oplus \widetilde{k_2[25]}$	$k_3[31] = \text{SB}^{-1}(k_4[2] \oplus \widetilde{k_3[2]})$
	$k_2[6] = k_3[6] \oplus \widetilde{k_3[2]}$	$k_3[3] = k_3[7] \oplus k_2[7]$
	$k_2[3] = k_3[3] \oplus \text{SB}(k_2[28])$	
5.	$w_2[0, 1], z_2[2, 3] = \text{MC}(z_2[0, 1], w_2[2, 3])$	$w_2[22, 23], z_2[23] = \text{MC}(z_2[20, 21, 22], w_2[20, 21]) ?$
	$k_3[0, 23] = (w_2 \oplus x_3)[0, 23]$	
6.	$k_2[4] = k_3[4] \oplus k_3[0]$	$k_3[27] = k_2[27] \oplus k_3[23]$
	$k_2[31] = k_3[31] \oplus k_3[27]$	$k_2[2] = k_3[2] \oplus \text{SB}(k_2[31])$
7.	$w_1[5], z_1[4, 5, 6] = \text{MC}(z_1[7], w_1[4, 6, 7])$	$k_2[5] = (w_1 \oplus x_2)[5]$
8.	$k_3[18] = \text{SB}(k_3[14]) \oplus \widetilde{k_2[18]}$	$k_2[20] = k_3[20] \oplus \widetilde{k_3[16]}$
	$k_3[1] = k_3[5] \oplus k_2[5]$	
9.	$w_1[16, 17, 19], z_1[16] = \text{MC}(z_1[17, 18, 19], w_1[18])$	$w_2[17, 19], z_2[16, 19] = \text{MC}(z_2[17, 18], w_2[16, 18])$
	$k_2[16, 17, 19] = (w_1 \oplus x_2)[16, 17, 19]$	$k_3[19] = (w_2 \oplus x_3)[19]$
10.	$k_3[13] = \widetilde{k_2[13]} \oplus k_3[9]$	$k_3[17] = k_2[17] \oplus k_3[13]$
	$k_2[21] = k_3[21] \oplus k_3[17]$	$k_3[12] = \text{SB}^{-1}(k_3[16] \oplus k_2[16])$
	$k_3[15] = \text{SB}^{-1}(k_3[19] \oplus k_2[19])$	$k_2[23] = k_3[23] \oplus k_3[19]$
11.	$w_1[12, 14, 15], z_1[12] = \text{MC}(z_1[13, 14, 15], w_1[13])$	$w_1[22], z_1[21, 22, 23] = \text{MC}(z_1[20], w_1[20, 21, 23])$
	$k_2[12, 14, 22] = (w_1 \oplus x_2)[12, 14, 22]$	
12.	$k_3[8, 10] = k_3[12, 14] \oplus k_2[12, 14]$	$k_2[8, 10] = k_3[8, 10] \oplus k_3[4, 6]$
	$k_3[22] = k_2[22] \oplus k_3[18]$	$k_3[26] = k_2[26] \oplus k_3[22]$
13.	$w_1[10, 11], z_1[8, 9] = \text{MC}(z_1[10, 11], w_1[8, 9])$	$k_2[11] = (w_1 \oplus x_2)[11]$
14.	$k_3[11] = k_2[11] \oplus k_3[7]$	$k_2[15] = k_3[15] \oplus k_3[11]$
	$w_2[28, 29, 30, 31] = \text{MC}(z_2[28, 29, 30, 31])$	$k_3[29, 30] = (w_2 \oplus x_3)[29, 30]$
15.	$k_2[29, 30] = k_3[29, 30] \oplus k_3[25, 26]$	$k_2[0] = k_3[0] \oplus \text{SB}(k_2[29]) \oplus \text{const}$
	$k_2[1] = k_3[1] \oplus \text{SB}(k_2[30])$	
16.	$z_1[0, 1, 2] = \text{MC}(z_1[3], w_1[0, 1, 2, 3]) ?$	$z_1[29, 30, 31] = \text{MC}(z_1[28], w_1[28, 29, 30, 31]) ?$

Table 17: Equations in the guess-and-determine steps for 6-round Rijndael-256-DM. The blue bytes are guessed. The red equations are conflicts.

1703 Degree of freedom and complexity.

- 1704 – There are totally 60 active Sboxes in the inbound phase, including $s_1 = 42$
1705 active Sboxes with probability 2^{-7} and $s_2 = 18$ active Sboxes with proba-
1706 bility 2^{-6} . Therefore, by accessing the DDT, there expect $2^{42+36}/2 = 2^{77}$
1707 combinations for the 60 active Sboxes, *i.e.*, there are 2^{77} choices for the bytes
1708 marked by 1.
- 1709 – Given one out of 2^{77} choices marked by 1, seven bytes $k_2[9, 13, 18, 24, 25], k_3[2, 16]$
1710 (marked by a wavy line) are guessed in steps 2, 4, 8 and 10. Since there are 3
1711 conflicts of Type III, there expect $2^{77+56-24} = 2^{109}$ starting points satisfying
1712 the inbound differential.
- 1713 – The probability of the outbound phase is $2^{-p_{out}} = 2^{-63}$. We have enough
1714 degrees of freedom to satisfy the outbound phase. Therefore, the total com-

plexity of the 6-round key-collision attack on Rijndael-256-DM is about $\mathcal{T} = 2^{63+24} = 2^{87}$.

9 Impacting on the Padding Fix with AES-GCM

9.1 Preliminaries

Committing Authenticated Encryption (AE). Authenticated encryption with associated data, which we call AE, consists of a symmetric encryption Enc and decryption Dec algorithms, where

$$\begin{aligned}\text{Enc} &: \mathcal{K} \times \mathcal{N} \times \mathcal{AD} \times \mathcal{P} \mapsto \mathcal{C}, \\ \text{Dec} &: \mathcal{K} \times \mathcal{N} \times \mathcal{AD} \times \mathcal{C} \mapsto \mathcal{P} \cup \{\perp\},\end{aligned}$$

\mathcal{K} , \mathcal{N} , \mathcal{AD} , \mathcal{P} , and \mathcal{C} refer to the key, nonce, associated data, plaintext/message, and ciphertext spaces, respectively. \perp is an error symbol not contained in \mathcal{P} . There are several notions of committing security framework proposed in [22,9,2].

- CMT-1: the adversary produces $((K_1, N_1, AD_1, P_1), (K_2, N_2, AD_2, P_2))$ such that $K_1 \neq K_2$ and $\text{Enc}(K_1, N_1, AD_1, P_1) = \text{Enc}(K_2, N_2, AD_2, P_2)$, where $K_i \in \mathcal{K}$, $N_i \in \mathcal{N}$, $AD_i \in \mathcal{AD}$, $P_i \in \mathcal{P}$.
- CMT-3: the adversary produces $((K_1, N_1, AD_1, P_1), (K_2, N_2, AD_2, P_2))$ such that $(K_1, N_1, AD_1) \neq (K_2, N_2, AD_2)$ and $\text{Enc}(K_1, N_1, AD_1, P_1) = \text{Enc}(K_2, N_2, AD_2, P_2)$.
- CMT-4: the adversary produces $((K_1, N_1, AD_1, P_1), (K_2, N_2, AD_2, P_2))$ such that $(K_1, N_1, AD_1, P_1) \neq (K_2, N_2, AD_2, P_2)$ and $\text{Enc}(K_1, N_1, AD_1, P_1) = \text{Enc}(K_2, N_2, AD_2, P_2)$.
- FROB game [22,29]: the adversary produces $((K_1, N_1, AD_1, P_1), (K_2, N_2, AD_2, P_2))$ such that $N_1 = N_2$, $K_1 \neq K_2$, and $\text{Enc}(K_1, N_1, AD_1, P_1) = \text{Enc}(K_2, N_2, AD_2, P_2)$.

The conventional AE security notions do not imply key-committing security, and there are attacks on popular schemes, including GCM [29,17], GCM-SIV [41], CCM [43], and ChaCha20-Poly1305 [29]. These attacks even lead to application-level attacks, e.g., the multi-recipient integrity attack that targets a specific user and sends malicious content to them and the partitioning oracle attack that effectively performs password brute-force attacks [41]. Researchers are studying AE schemes with committing security to address the issue [29,17,41,1].

At USENIX Security 2022, Albertini et al. proposed the Padding Fix scheme [1], which appends zeroes to a plaintext and checks them after decryption. This scheme maintains compatibility with the original AE and can be more efficient, if the setting can tolerate a small amount of ciphertext expansion and does not need a compact commitment. However, The security after padding should be evaluated for each scheme. Based on our key-collision attacks on AES, we will introduce several key-committing attacks on the Padding Fix scheme of AES-GCM with reduced AES.

Description of AES-GCM. AES-GCM combines AES-CTR mode for the encryption, and the GHASH algorithm for the authentication. The GHASH function computes a 128-bit hash with a 128-bit hash key H and m 128-bit input blocks $(X^{(1)}, X^{(2)}, \dots, X^{(m)})$, *i.e.*,

$$\text{GHASH}_H(X^{(1)} \| X^{(2)} \| \dots \| X^{(m)}) = X^{(1)} \cdot H^m \oplus X^{(2)} \cdot H^{m-1} \oplus \dots \oplus X^{(m)} \cdot H, \quad (15)$$

where the \cdot operation on the 2^{128} possible blocks corresponds to the multiplication operation for the binary Galois (finite) field of 2^{128} elements.

Define $MSB_l(X)$ to be a function that returns the l most significant bits of a bit string X , and $LSB_l(X)$ to be a function that returns the l least significant bits of X . For a positive integer s and a bit string X such that $\text{len}(X) \geq s$, the incrementing function is defined as $\text{inc}_s(X) = MSB_{\text{len}(X)-s}(X) \| [\text{int}(LSB_s(X)) + 1 \bmod 2^s]_s$, where the left-most $(\text{len}(X) - s)$ -bit of X remains and the right-most s -bit of X is regarded as an integer to add 1 modulo 2^s . We describe the AES-GCM with 96-bit nonce in Algorithm 1.

Algorithm 1: AES-GCM $_K(N, AD, P)$

Input: Key K , Nonce N , Plaintext P , Associated data AD

Output: Ciphertext C , t -bit Tag T

1. $H \leftarrow \text{AES}_K(0^{128})$
 2. $P^{(1)} \| P^{(2)} \| \dots \| P^{(n-1)} \| P^{(n)*} \leftarrow P$, where $n = \lceil \text{len}(P)/128 \rceil$
 3. $J^{(0)} \leftarrow N \| 0^{31} \| 1$, $J^{(i)} \leftarrow \text{inc}_{32}(J^{(i-1)})$ ($i = 1, \dots, n$)
 4. $S^{(i)} \leftarrow \text{AES}_K(J^{(i)})$ ($i = 0, \dots, n$)
 5. $C^{(i)} \leftarrow P^{(i)} \oplus S^{(i)}$ ($i = 1, \dots, n-1$), $C^{(n)*} \leftarrow P^{(n)*} \oplus MSB_{\text{len}(P^{(n)*})}(S^{(n)})$
 6. $R \leftarrow AD \| 0^v \| C \| 0^u \| [\text{len}(AD)]_{64} \| [\text{len}(C)]_{64}$, where
 $u = 128 \lceil \text{len}(C)/128 \rceil - \text{len}(C)$, $v = 128 \lceil \text{len}(AD)/128 \rceil - \text{len}(AD)$
 7. $R^{(1)} \| R^{(2)} \| \dots \| R^{(m)} \leftarrow R$, where $m = \text{len}(R)/128$
 8. $T \leftarrow MSB_t \left(\bigoplus_{i=1}^m R^{(i)} \cdot H^{m+1-i} \oplus S^{(0)} \right)$
 9. Return (C, T)
-

Key committing attack and the padding fix on AES-GCM. We briefly describe the attack on AES-GCM in [17], which is generalized in [1]. To mount a successful key committing attack, we have to ensure that the ciphertext C and authentication tag T under two different keys K_1 and K_2 are valid to pass the authentication. Without loss of generality, assume that the length of C is divisible by 128.

1. For two keys K_1 and K_2 , derive $H_1 = \text{AES}_{K_1}(0^{128})$, $H_2 = \text{AES}_{K_2}(0^{128})$,
 $S_1^{(i)} = \text{AES}_{K_1}(J^{(i)})$ and $S_2^{(i)} = \text{AES}_{K_2}(J^{(i)})$.
2. Split the ciphertext to m blocks $C = C^{(1)} \| C^{(2)} \| \dots \| C^{(m)}$, where $m = \text{len}(C)/128$.

- 1773 3. The computation of tag should satisfy $T = \bigoplus_{i=1}^m C^{(i)} \cdot H_1^{m+1-i} \oplus S_1^{(0)} =$
 1774 $\bigoplus_{i=1}^m C^{(i)} \cdot H_2^{m+1-i} \oplus S_2^{(0)}$. (For simplicity, we ignore the associated data
 1775 AD and the block of length.)
 1776 4. Fixing all ciphertext blocks except for $C^{(j)}$, there is

$$C^{(j)} \cdot (H_1^{m+1-j} \oplus H_2^{m+1-j}) = \bigoplus_{i=1, i \neq j}^m (C^{(i)} \cdot H_1^{m+1-i} \oplus C^{(i)} \cdot H_2^{m+1-i}) \oplus S_1^{(0)} \oplus S_2^{(0)}$$

1777 Then, we can get

$$C^{(j)} = (H_1^{m+1-j} \oplus H_2^{m+1-j})^{-1} \cdot \left(\bigoplus_{i=1, i \neq j}^m (C^{(i)} \cdot H_1^{m+1-i} \oplus C^{(i)} \cdot H_2^{m+1-i}) \oplus S_1^{(0)} \oplus S_2^{(0)} \right),$$

1778 where C and T are fully determined. Then we can determine $P_1 = P_1^{(1)} \parallel$
 1779 $P_1^{(2)} \parallel \dots \parallel P_1^{(m)}$ and $P_2 = P_2^{(1)} \parallel P_2^{(2)} \parallel \dots \parallel P_2^{(m)}$ as $P_1^{(i)} = C^{(i)} \oplus S_1^{(i)}$ and
 1780 $P_2^{(i)} = C^{(i)} \oplus S_2^{(i)}$, which lead to same C and T under K_1 and K_2 .

1781 Albertini *et al.* [1] provided two solutions for the setting that a small amount
 1782 of ciphertext expansion can be tolerated. One solution is the padding fix:

1783 “... prepend 2κ zeros for κ bits of security against key commitment at-
 1784 tacks, e.g. 256 zeros for 128 bits of security. For short-lived ciphertexts,
 1785 or settings where the cost of executing 2^{64} computation outweighs the ben-
 1786 efit of performing the attack, it suffices to use a single block to achieve
 1787 only 64 bit key commitment security — this will not impact AE security.”

1788 9.2 Key Committing Attacks on Round-Reduced AES-GCM with a 1789 128-bit Padding Fix

1790 We target on AES-GCM with a 96-bit nonce and a 128-bit tag, which appends
 1791 128 zeros before the message to get 64 bits of security against key commit-
 1792 ment attacks. We aim to find a key-committing attack with $((K_1, N, AD, P_1),$
 1793 $(K_2, N, AD, P_2))$, where $K_1 \neq K_2$ and $\text{AES-GCM}_{K_1}(N, AD, P_1) = \text{AES-GCM}_{K_2}(N, AD, P_2)$.
 1794 Supposing the length of P_1 and P_2 is divisible by 128, let $P_1 = P_1^{(1)} \parallel \dots \parallel P_1^{(m)}$ and
 1795 $P_2 = P_2^{(1)} \parallel \dots \parallel P_2^{(m)}$ ($m = \text{len}(P_1)/128 = \text{len}(P_2)/128$). There is $P_1^{(0)} = P_2^{(0)} = 0$
 1796 due to the padding fix scheme. The steps of our key-committing attack are given
 1797 below:

- 1798 1. Choose a 96-bit nonce N and a 128-bit AD . Then we can get $J^{(0)} = N \parallel 0^{31} \parallel 1$
 1799 and $J^{(i)} = \text{inc}_{32}(J^{(i-1)})$ ($i = 1, \dots, m$).
- 1800 2. Find key collision attacks applying our GD rebound attack, to get K_1 and
 1801 K_2 satisfying $\text{AES}_{K_1}(J^{(1)}) = \text{AES}_{K_2}(J^{(1)})$.
- 1802 3. With K_1 and K_2 , derive $H_1 = \text{AES}_{K_1}(0^{128})$, $H_2 = \text{AES}_{K_2}(0^{128})$, $S_1^{(i)} =$
 1803 $\text{AES}_{K_1}(J^{(i)})$ and $S_2^{(i)} = \text{AES}_{K_2}(J^{(i)})$ ($i = 1, \dots, m$), where $S_1^{(1)} = S_2^{(1)}$.

1804 4. To launch a successful attack, there should be

$$\left\{ \begin{array}{l} C^{(i)} = P_1^{(i)} \oplus S_1^{(i)} = P_2^{(i)} \oplus S_2^{(i)}, \quad i = 1, \dots, m \\ T = \bigoplus_{i=1}^m C^{(i)} \cdot H_1^{m+2-i} \oplus AD \cdot H_1^{m+2} \oplus L \cdot H_1 \oplus S_1^{(0)} \\ \quad = \bigoplus_{i=1}^m C^{(i)} \cdot H_2^{m+2-i} \oplus AD \cdot H_2^{m+2} \oplus L \cdot H_2 \oplus S_2^{(0)} \end{array} \right. \quad (16)$$

1805 where L is the block $[len(AD)]_{64} \parallel [len(C)]_{64}$.

1806 5. Set $C^{(1)} = P_1^{(1)} \oplus S_1^{(1)} = P_2^{(1)} \oplus S_2^{(1)}$, since $P_1^{(1)} = P_2^{(1)} = 0$ and $S_1^{(1)} = S_2^{(1)}$.
1807 Then fix $C^{(3)} \parallel \dots \parallel C^{(m)}$, we can get

$$\left\{ \begin{array}{l} C^{(2)} = (H_1^m \oplus H_2^m)^{-1} \left(\bigoplus_{i=1, i \neq 2}^m (C^{(i)} \cdot H_1^{m+2-i} \oplus C^{(i)} \cdot H_2^{m+2-i}) \right) \\ \quad \oplus (H_1^m \oplus H_2^m)^{-1} (AD \cdot H_1^{m+2} \oplus L \cdot H_1 \oplus S_1^{(0)} \oplus AD \cdot H_2^{m+2} \oplus L \cdot H_2 \oplus S_2^{(0)}). \end{array} \right. \quad (17)$$

1808 Then the whole $C = C^{(1)} \parallel \dots \parallel C^{(m)}$ and T are determined. We can deduce

$$\left\{ \begin{array}{l} P_1^{(i)} = C^{(i)} \oplus S_1^{(i)}, \\ P_2^{(i)} = C^{(i)} \oplus S_2^{(i)}, \end{array} \quad i = 2, \dots, m. \right. \quad (18)$$

1809 The time complexity of the attack procedure is depending on the complexity
1810 of finding key collisions in step 2.

1811 9.3 The Practical Key Committing Attack on Padding fixed 1812 AES-GCM with 3-round AES-128

1813 For the key collision attack on 3-round AES-128 in Section 4.3, we restrict
1814 $\Delta x_0[15] = \Delta k_0[15] = 0\text{xcc}$, $\Delta \text{SB}(k_0[15]) = \Delta \text{SB}(x_0[15]) = 0\text{x28}$, and keep
1815 $x_0[15] = k_0[15]$ to make $P[15] = 0$ in the attack. However, in AES-GCM, the
1816 $P[12 - 15]$ is corresponding to the 32-bit counter, which can not be restricted
1817 to zeros. So we search a new related-key differential, where $\Delta k_0[15] = 0$. So we
1818 can generate key collision for $\text{AES}_{K_1}(J^{(1)}) = \text{AES}_{K_2}(J^{(1)})$. The new key collision
1819 attack is given as follows.

1820 **A new practical key collision attack on 3-round AES-128.** We give a new
1821 key collision attack on 3-round AES-128 based on a new related-key differential
1822 characteristic as shown in Fig. 37. There is one active $k_0[14]$ in the first round
1823 key, *i.e.*, $\Delta k_0[14] = 0\text{x30}$, which brings the same difference to $x_0[14]$. Applying
1824 the observation in Section 3.2, we set $\Delta \text{SB}(k_0[14]) = \Delta \text{SB}(x_0[14]) = 0\text{xda}$, and
1825 keep $x_0[14] = k_0[14]$ in the attack, which makes $P[14] = 0$. So when we choose
1826 the value of $x_0[14]$ satisfying the difference over the active Sbox in the EN path,
1827 the value of $k_0[14]$ satisfies the difference over the active Sbox in the KS with

1828 probability 1. Therefore, although there are 19 active Sboxes in the differential,
 1829 we only count the probability of 18 of them, which is 2^{-126} . We choose the first
 1830 two rounds of the EN and the whole KS as the inbound phase, with a probability
 1831 of 2^{-90} . The remaining parts are the outbound phase, with a probability of
 1832 $2^{-p_{out}} = 2^{-28}$. The steps of the GD for the inbound phase are marked in Fig. 38
 with equations listed in Table 18.

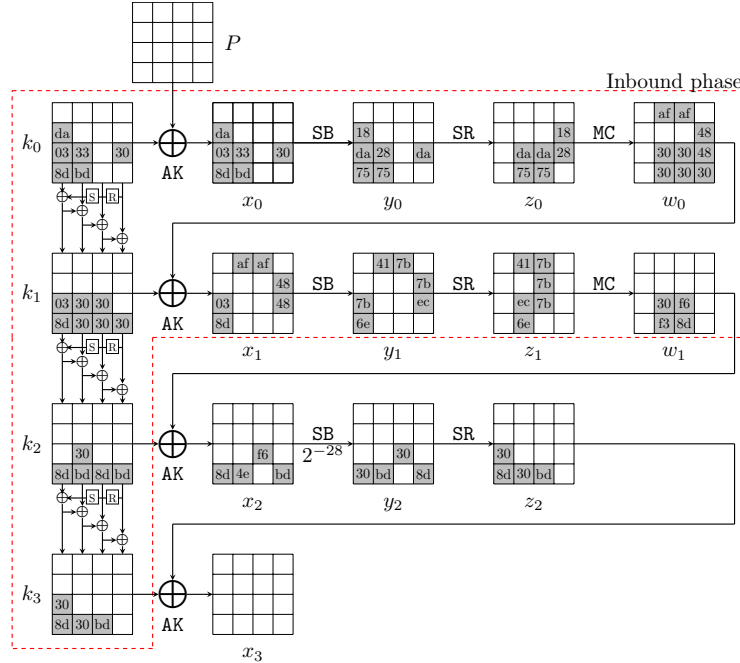


Fig. 37: The new related-key differential characteristic on 3-round AES-128

1833

1834 **Guess-and-determine procedures of the inbound phase in the new key** 1835 **collision attack.**

- 1836 1. With the fixed differences in the differential, deduce $x_0[1-3, 6, 7, 14]$, $y_0[1-3, 6, 7, 14]$, $x_1[2-4, 8, 13, 14]$ and $y_1[2-4, 8, 13, 14]$ (marked by 1 in Fig. 14) by accessing the DDT.
 - 1839 (a) In round 0, deduce $k_0[1-3, 6, 7, 14]$ (marked by ←1). Compute forward to $z_0[6, 7, 10, 11, 13, 14]$ (marked by →1).
 - 1841 (b) Since the differences $\Delta k_1[15]$, $k_2[15]$ and $\Delta SB(k_1[15])$, $\Delta SB(k_2[15])$ are known, deduce $k_1[15]$, $k_2[15]$ (marked by 1) by accessing the DDT.
 - 1843 2. Guess $k_0[12, 13, 15]$ (marked by 2). According to the key relations, deduce $k_0[11]$ and $k_1[1, 2, 3, 6, 7, 8, 11, 12]$ (marked by 2) as Table 18, where $k_2[15]$ is known since $\Delta k_2[15]$ and $\Delta SB(k_2[15])$ are fixed.
 - 1844
 - 1845

- 1846 (a) In round 0, compute forward to get $z_0[3, 9, 12, 15]$ (marked by $\overrightarrow{2}$).
- 1847 (b) In round 1, compute backward to get $w_0[2, 3, 8]$ (marked by $\overleftarrow{2}$).
- 1848 3. For columns 2,3 over the MC operation of round 0, deduce $w_0[9-15]$ and
- 1849 $z_0[8]$ (marked by $\overrightarrow{3}$) from $z_0[9-15]$ and $w_0[8]$.
- 1850 (a) Compute backward to get $k_0[8]$ (marked by $\overleftarrow{3}$).
- 1851 (b) Compute forward to get $k_1[13, 14]$ and $x_1[11, 12, 15]$ (marked by $\overrightarrow{3}$).
- 1852 4. According to the key relations, deduce $k_0[10]$ and $k_1[4, 9, 10]$ (marked by $\overrightarrow{4}$)
- 1853 as Table 18.
- 1854 (a) In round 0, compute forward to get $z_0[2]$ (marked by $\overrightarrow{4}$).
- 1855 (b) In round 1, compute backward to get $w_0[4]$ (marked by $\overleftarrow{4}$) and compute
- 1856 forward to get $x_1[9, 10]$ (marked by $\overrightarrow{4}$).
- 1857 5. For column 1 over the MC operation of round 0, deduce $w_0[0, 1]$ and $z_0[0, 1]$
- 1858 (marked by $\overrightarrow{5}$) from $z_0[2, 3]$ and $w_0[2, 3]$. Compute backward to get $k_0[0, 5]$
- 1859 (marked by $\overleftarrow{5}$).
- 1860 6. According to the key relations, deduce $k_0[4, 9]$ and $k_1[0, 5]$ (marked by $\overrightarrow{6}$).
- 1861 Compute forward to get $z_0[4, 5]$ (marked by $\overrightarrow{6}$).
- 1862 7. For column 1 over the MC operation of round 0, deduce $w_0[5, 6, 7]$ (marked by
- 1863 $\overrightarrow{7}$) from $z_0[4, 5, 6, 7]$ and $w_0[4]$. Since five values are known in the inputs/outputs over the MC operation, there is a conflict of Type III with a probability
- 1864 of 2^{-8} . Then we get all the states of the starting point.
- 1865

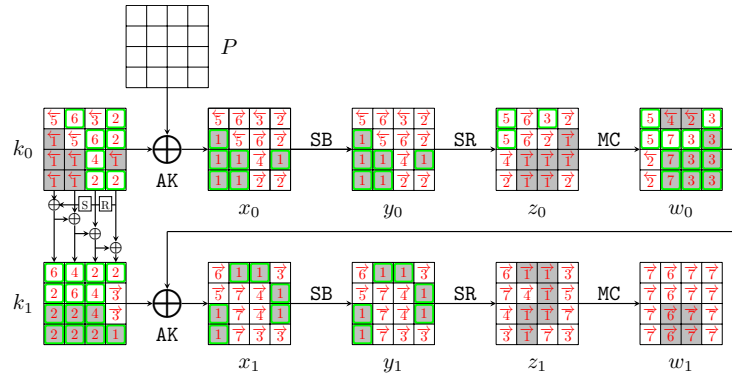


Fig. 38: Steps of the GD in the inbound phase for 3-round AES-128

Degree of freedom and complexity of the new key collision attack.

- In step 1, we deduce the values for active bytes from the input/output differences in the inbound phase. There are 14 active Sboxes with a total probability 2^{-98} , including $s_1 = 14$ active Sboxes with probability 2^{-7} . Therefore, there are $2^{14}/2 = 2^{13}$ combinations for the 14 active bytes, *i.e.*, there are 2^{13} choices for the bytes marked by $\overrightarrow{1}$ in Figure 38.

1.	$k_0[1 - 3, 6, 7, 14] = (x_0 \oplus P)[1 - 3, 6, 7, 14]$	
2.	$k_1[2, 3] = k_0[2, 3] \oplus \text{SB}(\underbrace{k_0[15, 12]})$	$z_0[9] = \text{SB}(P[13] \oplus \underbrace{k_0[13]})$
	$k_1[6, 7] = k_0[6, 7] \oplus k_1[2, 3]$	$k_1[11] = k_0[15] \oplus k_1[15]$
	$k_0[11] = k_1[11] \oplus k_1[7]$	$k_1[1] = k_0[1] \oplus \text{SB}(k_0[14])$
	$k_1[12] = \text{SB}^{-1}(k_2[15] \oplus k_1[15] \oplus k_1[11] \oplus k_1[7] \oplus k_1[3])$	
	$k_1[8] = k_0[12] \oplus k_1[12]$	
3.	$w_0[9, 10, 11], z_0[8] = \text{MC}(z_0[9, 10, 11], w_0[8])$	$w_0[12, 13, 14, 15] = \text{MC}(z_0[12, 13, 14, 15])$
	$k_0[8] = P[8] \oplus \text{SB}^{-1}(z_0[8])$	$k_1[13, 14] = (w_0 \oplus x_1)[13, 14]$
4.	$k_1[9, 10] = k_0[13, 14] \oplus k_1[13, 14]$	$k_0[10] = k_1[10] \oplus k_1[6]$
	$k_1[4] = k_1[8] \oplus k_0[8]$	
5.	$w_0[0, 1], z_0[0, 1] = \text{MC}(z_0[2, 3], w_0[2, 3])$	$k_0[0, 5] = P[0, 5] \oplus \text{SB}^{-1}(z_0[0, 1])$
6.	$k_1[0] = k_0[0] \oplus \text{SB}(k_0[13]) \oplus \text{const}$	$k_0[4] = k_1[4] \oplus k_1[0]$
	$k_1[5] = k_0[5] \oplus k_1[1]$	$k_0[9] = k_1[9] \oplus k_1[5]$
7.	$w_0[5, 6, 7] = \text{MC}(z_0[4, 5, 6, 7], w_0[4]) ?$	

Table 18: Equations in the GD steps for 3-round AES-128. The blue bytes are guessed. **The red equation is the conflict.**

- Given one out of 2^{13} choices marked by 1, three bytes $k_0[12, 13, 15]$ (marked by a wavy line) are guessed in step 2. In Step 7, there is a filter of 2^{-8} marked by underline. Therefore, there expect $2^{13+24-8} = 2^{29}$ states satisfying the inbound trial in total, which act as the starting points for the outbound phase.
- Since there is one conflict in the inbound phase, *i.e.*, $c_{in} = 1$, the time of the GD to find one starting point is $\mathcal{T}_{\text{GD}} = 2^8$. Since the probability of the outbound phase is $2^{-p_{out}} = 2^{-28}$, we need to collect 2^{28} starting points to expect one collision. The overall time complexity is $\mathcal{T} = 2^{28+8} = 2^{36}$ and the memory complexity is negligible, which is practical. We find key collisions in several hours on a desktop equipped with Intel Core i7-13700F @2.1 GHz and 16G RAM using one CPU core.

Key Committing Attack. Based on the practical key collision attack on 3-round AES-128, we conduct the key-committing attack on padding fix scheme of AES-GCM with 3-round AES-128. Following the attack procedure in Sect. 9.2, the time complexity is dominated by the key collision attack, which is 2^{36} . We have implemented the attack with two blocks of plaintext, while there is a 128-bit zero padding before message which results in three blocks of ciphertext. We give a pair of $((K_1, N, AD, P_1), (K_2, N, AD, P_2))$ with the same (C, T) in Table 4

9.4 The Practical Key Committing Attack on Padding Fixed AES-GCM with 5-round AES-192

We apply the practical key collision attack on 5-round AES-192 in Section 5.1 to conduct the key-committing attack on padding fix scheme of AES-GCM with 5-round AES-192 with the time complexity is 2^{21} , dominated by the time complexity of key collision attack on 5-round AES-192. We have practically implemented

the attack and give a pair of $((K_1, N, AD, P_1), (K_2, N, AD, P_2))$ with the same (C, T) in Table 4

9.5 The Practical Key Committing Attack on Padding Fixed AES-GCM with 6-round AES-256

We apply the practical key collision attack on 6-round AES-256 in Section 6.2 to conduct the key-committing attack on adding fix scheme of AES-GCM with 6-round AES-256. Following the attack procedure in Section 9.2, the time complexity is 2^{21} , dominated by the time of key collision attack on 6-round AES-256. We have practically implemented the attack and give a pair of $((K_1, N, AD, P_1), (K_2, N, AD, P_2))$ with the same (C, T) in Table 4

10 Discussion and Conclusion

Discussion. This paper combines the guess-and-determine approach [6] with the rebound attack [44] to propose a novel framework to build collision attacks. The GD approach [6] itself cannot build a collision attack on AES. Note that in [6, Section 3.2], the authors comment on their GD approach:

“The main limitation of this approach is that it completely fails to take into account the differential properties of the S-box. For instance, it cannot exploit the fact that when the input and output differences of the S-box are fixed and non-zero, then at most 4 possible input values are possible. Therefore, this approach alone does not bring useful result when more than one plaintext is available. However, it can be used as a sub-component in a more complex technique.”

The authors suggest their GD approach as a sub-component of a more complex technique when handling differentials. In our paper, we embed their GD approach into the rebound attack, called GD rebound, allowing the two tools to work together efficiently. Our GD rebound immediately and significantly improves Taiyama *et al.*’s key collision attack [53], demonstrating the power of combining these two cryptanalysis tools.

Conclusion. In this paper, we improve Dong *et al.*’s triangulating rebound attack by proposing the *guess-and-determine rebound* attack. Based on the new method, we significantly improve Taiyama *et al.*’s key collision attacks on AES and semi-free-start collision attacks on AES-DM. Most of our attacks are practical and the example collision pairs are given, including the 2-/3-round key collision attacks and 5-round semi-free-start collision attack on AES-128, 5-round key collision attack and 7-round semi-free-start collision attack on AES-192, 6-round key collision attack on AES-256, 3-round key collision attack on Rijndael-192-192, 3-round key collision attack and 5-round semi-free-start collision attack on Rijndael-256-256. Additionally, some quantum key collision attacks are proposed. Finally, some practical key committing attacks on padding fixed AES-GCM with round-reduced AES are given.

References

1. Ange Albertini, Thai Duong, Shay Gueron, Stefan Kölbl, Atul Luykx, and Sophie Schmieg. How to abuse and fix authenticated encryption without key commitment. In Kevin R. B. Butler and Kurt Thomas, editors, *31st USENIX Security Symposium, USENIX Security 2022, Boston, MA, USA, August 10-12, 2022*, pages 3291–3308. USENIX Association, 2022.
2. Mihir Bellare and Viet Tung Hoang. Efficient schemes for committing authenticated encryption. In Orr Dunkelman and Stefan Dziembowski, editors, *Advances in Cryptology - EUROCRYPT 2022 - 41st Annual International Conference on the Theory and Applications of Cryptographic Techniques, Trondheim, Norway, May 30 - June 3, 2022, Proceedings, Part II*, volume 13276 of *Lecture Notes in Computer Science*, pages 845–875. Springer, 2022.
3. Daniel J. Bernstein. Cost analysis of hash collisions: Will quantum computers make SHARCS obsolete. *SHARCS 2009* 9: 105.
4. Alex Biryukov, Orr Dunkelman, Nathan Keller, Dmitry Khovratovich, and Adi Shamir. Key recovery attacks of practical complexity on AES-256 variants with up to 10 rounds. In Henri Gilbert, editor, *Advances in Cryptology - EUROCRYPT 2010, 29th Annual International Conference on the Theory and Applications of Cryptographic Techniques, Monaco / French Riviera, May 30 - June 3, 2010. Proceedings*, volume 6110 of *Lecture Notes in Computer Science*, pages 299–319. Springer, 2010.
5. Xavier Bonnetain, Akinori Hosoyamada, María Naya-Plasencia, Yu Sasaki, and André Schrottenloher. Quantum attacks without superposition queries: The offline Simon’s algorithm. In *ASIACRYPT 2019, Proceedings, Part I*, pages 552–583.
6. Charles Bouillaguet, Patrick Derbez, and Pierre-Alain Fouque. Automatic search of attacks on round-reduced AES and applications. In Phillip Rogaway, editor, *Advances in Cryptology - CRYPTO 2011 - 31st Annual Cryptology Conference, Santa Barbara, CA, USA, August 14-18, 2011. Proceedings*, volume 6841 of *Lecture Notes in Computer Science*, pages 169–187. Springer, 2011.
7. Gilles Brassard, Peter Høyer, and Alain Tapp. Quantum cryptanalysis of hash and claw-free functions. In *LATIN ’98, Campinas, Brazil, April, 20-24, 1998, Proceedings*, pages 163–169, 1998.
8. André Chailloux, María Naya-Plasencia, and André Schrottenloher. An efficient quantum collision search algorithm and implications on symmetric cryptography. In *ASIACRYPT 2017, Proceedings, Part II*, pages 211–240, 2017.
9. John Chan and Phillip Rogaway. On committing authenticated-encryption. In Vijayalakshmi Atluri, Roberto Di Pietro, Christian Damsgaard Jensen, and Weizhi Meng, editors, *Computer Security - ESORICS 2022 - 27th European Symposium on Research in Computer Security, Copenhagen, Denmark, September 26-30, 2022, Proceedings, Part II*, volume 13555 of *Lecture Notes in Computer Science*, pages 275–294. Springer, 2022.
10. Shiyao Chen, Xiaoyang Dong, Jian Guo, and Tianyu Zhang. Chosen-prefix collisions on aes-like hashing. *IACR Trans. Symmetric Cryptol.*, 2024(4):64–96, 2024.
11. Yu Long Chen, Antonio Flórez-Gutiérrez, Akiko Inoue, Ryoma Ito, Tetsu Iwata, Kazuhiko Minematsu, Nicky Mouha, Yusuke Naito, Ferdinand Sibleyras, and Yosuke Todo. Key committing security of AEZ and more. *IACR Trans. Symmetric Cryptol.*, 2023(4):452–488, 2023.
12. Joan Daemen and Vincent Rijmen. Understanding two-round differentials in AES. In *SCN 2006, Proceedings*, volume 4116, pages 78–94. Springer.

13. Joan Daemen and Vincent Rijmen. *The Design of Rijndael: AES - The Advanced Encryption Standard*. Information Security and Cryptography. Springer, 2002.
14. Patrick Derbez, Pierre-Alain Fouque, Takanori Isobe, Mostafizar Rahman, and André Schrottenloher. Key committing attacks against aes-based AEAD schemes. *IACR Trans. Symmetric Cryptol.*, 2024(1):135–157, 2024.
15. Patrick Derbez, Paul Huynh, Virginie Lallemand, María Naya-Plasencia, Léo Perrin, and André Schrottenloher. Cryptanalysis results on Spook - bringing full-round Shadow-512 to the light. In *CRYPTO 2020, Proceedings, Part III*, volume 12172, pages 359–388.
16. Itai Dinur, Orr Dunkelman, Nathan Keller, and Adi Shamir. Efficient dissection of composite problems, with applications to cryptanalysis, knapsacks, and combinatorial search problems. In *CRYPTO 2012, Proceedings*, volume 7417, pages 719–740. Springer.
17. Yevgeniy Dodis, Paul Grubbs, Thomas Ristenpart, and Joanne Woodage. Fast message franking: From invisible salamanders to encryptment. In Hovav Shacham and Alexandra Boldyreva, editors, *Advances in Cryptology - CRYPTO 2018 - 38th Annual International Cryptology Conference, Santa Barbara, CA, USA, August 19-23, 2018, Proceedings, Part I*, volume 10991 of *Lecture Notes in Computer Science*, pages 155–186. Springer, 2018.
18. Xiaoyang Dong, Jian Guo, Shun Li, and Phuong Pham. Triangulating rebound attack on aes-like hashing. In Yevgeniy Dodis and Thomas Shrimpton, editors, *Advances in Cryptology - CRYPTO 2022 - 42nd Annual International Cryptology Conference, CRYPTO 2022, Santa Barbara, CA, USA, August 15-18, 2022, Proceedings, Part I*, volume 13507 of *Lecture Notes in Computer Science*, pages 94–124. Springer, 2022.
19. Xiaoyang Dong, Siwei Sun, Danping Shi, Fei Gao, Xiaoyun Wang, and Lei Hu. Quantum collision attacks on AES-like hashing with low quantum random access memories. In Shiho Moriai and Huaxiong Wang, editors, *ASIACRYPT 2020, Proceedings, Part II*, volume 12492, pages 727–757.
20. Xiaoyang Dong, Zhiyu Zhang, Siwei Sun, Congming Wei, Xiaoyun Wang, and Lei Hu. Automatic classical and quantum rebound attacks on AES-like hashing by exploiting related-key differentials. In Mehdi Tibouchi and Huaxiong Wang, editors, *ASIACRYPT 2021, Singapore, December 6-10, 2021, Proceedings, Part I*, volume 13090 of *Lecture Notes in Computer Science*, pages 241–271. Springer, 2021.
21. Alexandre Duc, Jian Guo, Thomas Peyrin, and Lei Wei. Unaligned rebound attack: Application to Keccak. In *FSE 2012, Revised Selected Papers*, volume 7549, pages 402–421.
22. Pooya Farshim, Claudio Orlandi, and Razvan Rosie. Security of symmetric primitives under incorrect usage of keys. *IACR Trans. Symmetric Cryptol.*, 2017(1):449–473, 2017.
23. Antonio Flórez-Gutiérrez, Gaëtan Leurent, María Naya-Plasencia, Léo Perrin, André Schrottenloher, and Ferdinand Sibleyras. New results on gimli: Full-permutation distinguishers and improved collisions. In Shiho Moriai and Huaxiong Wang, editors, *Advances in Cryptology - ASIACRYPT 2020 - 26th International Conference on the Theory and Application of Cryptology and Information Security, Daejeon, South Korea, December 7-11, 2020, Proceedings, Part I*, volume 12491 of *Lecture Notes in Computer Science*, pages 33–63. Springer, 2020.
24. Antonio Flórez-Gutiérrez, Gaëtan Leurent, María Naya-Plasencia, Léo Perrin, André Schrottenloher, and Ferdinand Sibleyras. Internal symmetries and linear

- properties: Full-permutation distinguishers and improved collisions on gimli. *J. Cryptol.*, 34(4):45, 2021.
25. Pierre-Alain Fouque, Jérémy Jean, and Thomas Peyrin. Structural evaluation of AES and chosen-key distinguisher of 9-round AES-128. In *CRYPTO 2013, Proceedings, Part I*, volume 8042, pages 183–203.
26. David Gérard, Pascal Lafourcade, Marine Minier, and Christine Solnon. Computing AES related-key differential characteristics with constraint programming. *Artif. Intell.*, 278, 2020.
27. Henri Gilbert and Thomas Peyrin. Super-Sbox cryptanalysis: Improved attacks for AES-like permutations. In *FSE 2010, Seoul, Korea, February 7-10, 2010*, pages 365–383, 2010.
28. Lov K. Grover. A fast quantum mechanical algorithm for database search. In *Proceedings of the Twenty-Eighth Annual ACM Symposium on the Theory of Computing, Philadelphia, Pennsylvania, USA, May 22-24, 1996*, pages 212–219, 1996.
29. Paul Grubbs, Jiahui Lu, and Thomas Ristenpart. Message franking via committing authenticated encryption. In Jonathan Katz and Hovav Shacham, editors, *Advances in Cryptology - CRYPTO 2017 - 37th Annual International Cryptology Conference, Santa Barbara, CA, USA, August 20-24, 2017, Proceedings, Part III*, volume 10403 of *Lecture Notes in Computer Science*, pages 66–97. Springer, 2017.
30. Jian Guo, Guozhen Liu, Ling Song, and Yi Tu. Exploring SAT for cryptanalysis: (quantum) collision attacks against 6-round SHA-3. In Shweta Agrawal and Dongdai Lin, editors, *Advances in Cryptology - ASIACRYPT 2022 - 28th International Conference on the Theory and Application of Cryptology and Information Security, Taipei, Taiwan, December 5-9, 2022, Proceedings, Part III*, volume 13793 of *Lecture Notes in Computer Science*, pages 645–674. Springer, 2022.
31. Akinori Hosoyamada and Yu Sasaki. Finding hash collisions with quantum computers by using differential trails with smaller probability than birthday bound. In Anne Canteaut and Yuval Ishai, editors, *EUROCRYPT 2020, Proceedings, Part II*, volume 12106, pages 249–279.
32. Akinori Hosoyamada and Yu Sasaki. Quantum collision attacks on reduced SHA-256 and SHA-512. In *CRYPTO 2021*, volume 12825, pages 616–646. Springer.
33. Jérémy Jean, María Naya-Plasencia, and Thomas Peyrin. Improved rebound attack on the finalist Grøstl. In *FSE 2012, Washington, DC, USA, March 19-21, 2012*, pages 110–126, 2012.
34. Jérémy Jean, María Naya-Plasencia, and Thomas Peyrin. Multiple limited-birthday distinguishers and applications. In *SAC 2013, Burnaby, BC, Canada, August 14-16, 2013*, pages 533–550, 2013.
35. Panos Kampanakis, Matt Campagna, Eric Crocket, Adam Petcher, and Shay Gueron. Practical challenges with AES-GCM and the need for a new cipher. In *The Third NIST Workshop on Block Cipher Modes of Operation*, 2023.
36. Marc Kaplan, Gaëtan Leurent, Anthony Leverrier, and María Naya-Plasencia. Breaking symmetric cryptosystems using quantum period finding. In *CRYPTO 2016, Santa Barbara, CA, USA, August 14-18, 2016, Proceedings, Part II*, pages 207–237, 2016.
37. Dmitry Khovratovich, Alex Biryukov, and Ivica Nikolic. Speeding up collision search for byte-oriented hash functions. In *CT-RSA 2009, Proceedings*, volume 5473, pages 164–181.
38. Dmitry Khovratovich, Ivica Nikolic, and Christian Rechberger. Rotational rebound attacks on reduced Skein. *J. Cryptol.*, 27(3):452–479, 2014.

- 2085 39. Mario Lamberger, Florian Mendel, Christian Rechberger, Vincent Rijmen, and
2086 Martin Schl  ffer. Rebound distinguishers: Results on the full Whirlpool com-
2087 pression function. In *ASIACRYPT 2009, Tokyo, Japan, December 6-10, 2009.*
2088 *Proceedings*, pages 126–143, 2009.
- 2089 40. Gregor Leander and Alexander May. Grover Meets Simon - quantumly attacking
2090 the FX-construction. In *ASIACRYPT 2017, Hong Kong, China, December 3-7,*
2091 *2017, Proceedings, Part II*, pages 161–178, 2017.
- 2092 41. Julia Len, Paul Grubbs, and Thomas Ristenpart. Partitioning oracle attacks. In
2093 Michael D. Bailey and Rachel Greenstadt, editors, *30th USENIX Security Sympo-*
2094 *sium, USENIX Security 2021, August 11-13, 2021*, pages 195–212. USENIX Asso-
2095 ciation, 2021.
- 2096 42. Krystian Matusiewicz, Mar  a Naya-Plasencia, Ivica Nikolic, Yu Sasaki, and Martin
2097 Schl  ffer. Rebound attack on the full LANE compression function. In *ASIACRYPT*
2098 *2009, Proceedings*, volume 5912, pages 106–125.
- 2099 43. Sanketh Menda, Julia Len, Paul Grubbs, and Thomas Ristenpart. Context discov-
2100 ery and commitment attacks - how to break ccm, eax, siv, and more. In Carmit
2101 Hazay and Martijn Stam, editors, *Advances in Cryptology - EUROCRYPT 2023 -*
2102 *42nd Annual International Conference on the Theory and Applications of Crypto-*
2103 *graphic Techniques, Lyon, France, April 23-27, 2023, Proceedings, Part IV*, volume
2104 14007 of *Lecture Notes in Computer Science*, pages 379–407. Springer, 2023.
- 2105 44. Florian Mendel, Christian Rechberger, Martin Schl  ffer, and S  ren S. Thomsen.
2106 The rebound attack: Cryptanalysis of reduced Whirlpool and Gr  stl. In *FSE 2009,*
2107 *Leuven, Belgium, February 22-25, 2009*, pages 260–276, 2009.
- 2108 45. Florian Mendel, Vincent Rijmen, and Martin Schl  ffer. Collision attack on 5 rounds
2109 of Gr  stl. In *FSE 2014, London, UK, March 3-5, 2014*, pages 509–521, 2014.
- 2110 46. Marcel Nageler, Felix Pallua, and Maria Eichlseder. Finding collisions for round-
2111 reduced romulus-h. *IACR Trans. Symmetric Cryptol.*, 2023(1):67–88, 2023.
- 2112 47. Yusuke Naito, Yu Sasaki, and Takeshi Sugawara. Committing security of ascon:
2113 Cryptanalysis on primitive and proof on mode. *IACR Trans. Symmetric Cryptol.*,
2114 2023(4):420–451, 2023.
- 2115 48. Mar  a Naya-Plasencia. How to improve rebound attacks. In *CRYPTO 2011, Santa*
2116 *Barbara, CA, USA, August 14-18, 2011. Proceedings*, pages 188–205, 2011.
- 2117 49. Jianqiang Ni, Yingxin Li, Fukang Liu, and Gaoli Wang. Practical key collision on
2118 AES and kiasu-bc. *IACR Cryptol. ePrint Arch.*, page 462, 2025.
- 2119 50. Yu Sasaki. Meet-in-the-middle preimage attacks on AES hashing modes and an
2120 application to Whirlpool. In *FSE 2011, Revised Selected Papers*, pages 378–396.
- 2121 51. Yu Sasaki, Yang Li, Lei Wang, Kazuo Sakiyama, and Kazuo Ohta. Non-full-active
2122 Super-Sbox analysis: Applications to ECHO and gr  stl. In *ASIACRYPT 2010,*
2123 *Singapore, December 5-9, 2010. Proceedings*, pages 38–55, 2010.
- 2124 52. Andr   Schrottenloher. Quantum linear key-recovery attacks using the QFT.
2125 In Helena Handschuh and Anna Lysyanskaya, editors, *Advances in Cryptology*
2126 *- CRYPTO 2023 - 43rd Annual International Cryptology Conference, CRYPTO*
2127 *2023, Santa Barbara, CA, USA, August 20-24, 2023, Proceedings, Part V*, volume
2128 14085 of *Lecture Notes in Computer Science*, pages 258–291. Springer, 2023.
- 2129 53. Kodai Taiyama, Kosei Sakamoto, Ryoma Ito, Kazuma Taka, and Takanori Isobe.
2130 Key collisions on AES and its applications. In Kai-Min Chung and Yu Sasaki, edi-
2131 tors, *Advances in Cryptology - ASIACRYPT 2024 - 30th International Conference*
2132 *on the Theory and Application of Cryptology and Information Security, Kolkata,*
2133 *India, December 9-13, 2024, Proceedings, Part VII*, volume 15490 of *Lecture Notes*
2134 *in Computer Science*, pages 267–300. Springer, 2024.

- 2135 54. Kodai Taiyama, Kosei Sakamoto, Ryoma Ito, Kazuma Taka, and Takanori Isobe.
2136 Key collisions on AES and its applications. *IACR Cryptol. ePrint Arch.*, page
2137 1508, 2024.
- 2138 55. Ryunouchi Takeuchi, Yosuke Todo, and Tetsu Iwata. Key recovery, universal
2139 forgery, and committing attacks against revised rocca: How finalization affects
2140 security. *IACR Trans. Symmetric Cryptol.*, 2024(2):85–117, 2024.
- 2141 56. Paul C. van Oorschot and Michael J. Wiener. Parallel collision search with crypt-
2142 analytic applications. *J. Cryptol.*, 12(1):1–28, 1999.